REPORT DOCUMENTATION PAGE

0579

1. AGENCY USE ONLY (Leave blank)	2. REPORT DATE July 1994	3. REPORT TYPE AND DATES COVERED Final Technical Report

4. TITLE AND SUBTITLE (U) Modeling Study to Evaluate the Ionic Mechanism of Soot Formation	5. FUNDING NUMBERS PE - 61102F PR - 2308 SA - BS G - AFOSR F49620-91-C-0021
6. AUTHOR(S) H.F. Calcote, D.G. Keil, R.J. Gill and C.H. Berman	

7. PERFORMING ORGANIZATION NAME(S) AND ADDRESS(ES) AeroChem Research Laboratories, Inc. P.O. Box 12 Princeton, NJ 08542-0012	8. PERFORMING ORGANIZATION REPORT NUMBER TP-531

9. SPONSORING/MONITORING AGENCY NAME(S) AND ADDRESS(ES) AFOSR/NA 110 Duncan Avenue, Suite B115 Bolling AFB DC 20332-0001	10. SPONSORING/MONITORING AGENCY REPORT NUMBER

DTIC SELECTED OCT 0 4 1995 S G

11. SUPPLEMENTARY NOTES

12a. DISTRIBUTION/AVAILABILITY STATEMENT Approved for public release; distribution is unlimited	12b. DISTRIBUTION CODE

13. ABSTRACT (Maximum 200 words)

To evaluate the ionic mechanism of soot formation, calculated ion profiles are compared with experimental profiles. The Sandia Flame Code has been modified to accommodate ions. The thermochemical data base on ions has been expanded to accommodate larger ions and additional isomers. Thermochemistry plays a greater role than expected. Good agreement between calculated and experiment is obtained up to ion mass 165, perinaphthalene, by reducing the maximum flame temperature by 10%. However, when the calculations are extended to ion mass 301, coronene, it is necessary to reduce the maximum flame temperature to 1700 K to obtain agreement. This indicates a serious problem. One possibility being tested, previously suggested by S. Stein, is that the flame ions add a hydrogen atom in the sampling cone of the mass spectrometer so that the observed ion is not the ion in the flame. Additional evidence for the ionic mechanism has been developed: (1) the rate of carbon growth is faster for an ionic mechanism than for a free radical mechanism; (2) the thermochemical driving force toward large ions is greater than toward large neutrals; and (3) the only change in flame property at the threshold soot index is a dramatic change in ion concentration and an increase in ion size.

14. SUBJECT TERMS Soot Formation; Ionic Mechanism; Thermodynamics; Ion-Molecule Reactions; Computer Modeling	15. NUMBER OF PAGES 95
	16. PRICE CODE

17. SECURITY CLASSIFICATION OF REPORT Unclassified	18. SECURITY CLASSIFICATION OF THIS PAGE Unclassified	19. SECURITY CLASSIFICATION OF ABSTRACT Unclassified	20. LIMITATION OF ABSTRACT UL

19951002 001

DTIC QUALITY INSPECTED 5

AeroChem TP-531

MODELING STUDY TO EVALUATE THE IONIC MECHANISM OF SOOT FORMATION

H.F. Calcote, D.G. Keil, R.J. Gill and C.H. Berman

AEROCHEM RESEARCH LABORATORIES, INC.
P.O. Box 12
Princeton, New Jersey 08542

July 1994

Annual Report for Period 15 December 1990 to 14 January 1994

Accesion For	
NTIS CRA&I	☒
DTIC TAB	☐
Unannounced	☐
Justification	
By	
Distribution /	
Availability Codes	
Dist	Avail and / or Special
A-1	

Prepared for

**AIR FORCE OFFICE OF SCIENTIFIC RESEARCH
Bolling Air Force Base
Washington, DC 20332**

TP-531

TABLE OF CONTENTS

LIST OF TABLES

LIST OF FIGURES

TP-531

<u>APPENDICES</u>

A.   "A DETAILED MODEL OF CATION GROWTH IN FLAMES" - RESPONSE TO REVIEWERS' COMMENTS

B.   "THERMODYNAMIC CONSIDERATIONS OF SOOT FORMATION" - RESPONSE TO REVIEWERS' COMMENTS

C.   "SIMULATION OF ELECTRIC FIELD EFFECTS IN PREMIXED METHANE FLAMES" - T. PEDERSEN AND R.C. BROWN, IOWA STATE UNIVERSITY

I. INTRODUCTION

This is the final report on a program to develop and evaluate a model for an ionic mechanism of soot formation. The nucleation steps in soot formation remain unknown, while the subsequent steps are reasonably well understood. The nucleation steps refers to the formation of an incipient soot particle from a gas phase precursor. In the ionic mechanism the gas phase precursor is assumed to be the chemiion, HCO^+; in the free radical mechanism it is benzene. The mechanism of forming HCO^+ is well established; the mechanism of forming benzene is still subject to study. In the ionic mechanism, a series of ion molecule reactions starting with the precursor produce larger and larger ions on the way to soot. Many large soot-like ions have been observed in sooting flames. Our immediate concern is to account for these large ions by using a reaction mechanism involving a series of likely ion-molecule reactions. A major task has been the development of adequate data bases for: (1) ion thermochemistry; (2) ion-molecule reaction rate coefficients; (3) cation-electron recombination coefficients; and (4) diffusion coefficients. While thermochemical data were available on some large ions with even numbers of carbon atoms, there were no such data for large, odd carbon number ions. The thermochemical data base proved to be the most difficult to develop and it also proved to be the most important. The rate coefficients for the reverse reactions were calculated from the thermochemistry of the species involved, and hence depends on the development of the thermochemical data base. For the forward (no energy barrier) reactions the Langevin theory of ion-molecule reaction rates is consistent with experimental data at ambient temperatures and for small ions but inadequate at flame temperatures and for large ions. We thus extended this theory to cover large ions and found that a slightly positive temperature coefficient was introduced into the calculated rate coefficients. However, use of the extended theory made very little difference in the final results. The other two data bases are less critical and were easier to prepare. The data bases are continually being updated as new data appear in the literature or as our modeling effort requires data which are unavailable and we estimate it. The model predictions were compared with experimental data to confirm its validity.

In another task the Sandia Flame Code was modified to handle ions. Modifications were made in the code to incorporate: (1) ion chemistry; (2) ambipolar diffusion; (3) the ability to input neutral and ion profiles; and (4) the ability to employ a modified Arrhenius form for ion-molecule reaction (necessary for handling equilibrium reverse reactions without exceeding the Langevin reaction rate).

The ionic mechanism of soot formation was applied to experimental acetylene/oxygen flame data and compared with a free radical mechanism used to model the same data. The resultant models were compared by calculating the times to add a carbon atom to the growing species [1,2] (the ionic mechanism appears to be faster); and by determining the thermodynamic driving force between the two mechanisms (the driving force for the ionic mechanism is much greater). The experimental measurements made on benzene/oxygen flames under a previous contract [3] have been organized [4] to form the experimental data base for comparing with a computer model of the benzene/oxygen flame. This flame is much different from the acetylene/oxygen flame, contains different large ions, and will require additional thermochemical and reaction kinetic estimates. We initiated an effort to understand the relationship of observed soot formation and the thermochemistry of soot formation in flames involving a variety of fuels. Experimental data in the

literature on soot threshold equivalence ratios, soot yields, and acetylene concentrations are compared with thermochemical equilibrium calculations of these quantities. (Appendix B)

Two papers summarizing the work of this program were submitted for consideration for presentation at the Twenty-Fifth Combustion Symposium; both were rejected. The reasons for the rejections are interesting, and require a response, so we use this report as a medium to record and respond to them. The two papers with reviewers' comments and our responses are thus included as Appendices A and B.

II. STATEMENT OF WORK

The ionic mechanism of soot formation in flames will be further evaluated and compared with the neutral mechanism by pursuing the following phases:

A. PHASE I - EXTEND THE IONIC MECHANISM TO BENZENE-OXYGEN FLAMES

1.   Extend the thermodynamic and reaction rate coefficient data base to include those species found in benzene/oxygen flames which are not present in acetylene/oxygen flames.

2.   Organize the experimental data available on the benzene flame including both neutral and ionic species.

3.   Develop a detailed ionic mechanism for the formation of soot in benzene flames and submit this to others to run on a large computer to compare its agreement with experimental data and to compare its simulation of soot formation with the neutral mechanism.

4.   Compare the computer modeling results with experimental data and interpret the results in terms of the major chemical pathway to soot in the benzene flame.

B. PHASE II - MODEL COAGULATION AND AGGLOMERATION

1.   Extend the detailed mechanism of soot nucleation to include coagulation of large ions and neutrals, and charged with charged and neutral incipient particles.

2.   Program a desktop computer to test the model developed in Task 1 (in a limited fashion) against experimental data. If warranted, submit this model to others to test on a mainframe computer.

3.   Interpret the results from Task 2 in terms of a simplified mechanism.

C. PHASE III - DEVELOP A THEORY FOR LARGE ION-MOLECULE REACTIONS

1.   Extend the Langevin theory of ion-molecule reactions to include large ions by removing the restriction of a point charge on the ion.

D. PHASE IV - COMPARE THERMODYNAMIC PREDICTIONS OF SOOT FORMATION WITH EXPERIMENTAL OBSERVATIONS

1.   Collect and organize the literature data on soot yield and acetylene concentrations as a function of equivalence ratio.

2.   Calculate the thermodynamic equilibrium concentration of acetylene and soot as a function of equivalence ratio for the literature systems identified in Task 1.

3.   Compare the experimental and calculated values and interpret them in terms of generalizations relevant to the mechanisms of soot formation.

III. THERMOCHEMISTRY

The thermochemistry of cations continues to be a major source of uncertainty in the kinetics model. The thermochemistries of several cations have been revised according to the most recent literature, and we have added a few larger cations to the original data base. As before, we prefer evaluated literature values for enthalpies of formation [5,6]; however, when they are not available, we estimate the enthalpies of formation from proton affinities, ionization potentials, or theoretical calculations. Heat capacities and entropies are calculated by either rigid-rotor-harmonic oscillator statistical mechanics (SM) formulae [7], hindered rotor harmonic oscillator SM formulae [8] or Benson's group additivity scheme [9] using the most recent group values [10]. SM formulae are preferred over Benson's method when reliable, experimental or high level QM, structural and vibrational frequency information are available for an ion. This data is being assembled for a major publication which will be submitted when the data base is complete.

IV. REACTION MECHANISM AND REACTION COEFFICIENTS

The reaction mechanism has remained essentially the same as developed in the previous program, with some changes in isomers used and with the deletion of others. The only changes in ion-molecule reaction rate coefficients resulted from use of the extended Langevin theory or from the effect of new thermochemistry on the reverse ratio coefficient.

To apply the extended Langevin theory to our set of reactions, we used the conducting sphere model of the extended Langevin theory [11]. For acetylene and diacetylene, the two major neutral species reacting with ions, we calculated rate coefficients as a function of temperature for a series

of ion diameters. The polarizabilities of acetylene and diacetylene (important parameters in the calculations) are: 3.33×10^{-24} and 5.99×10^{-24} cm^3, respectively. To incorporate the calculated rate coefficients into the kinetic model, we cast the temperature dependence in terms of the classical Arrhenius equation, (i.e., $k(T) = A\,T^n e^{\frac{-E_{act}}{RT}}$). We assumed that E_{act} is small (~ 0) for exothermic ion-molecule reactions. The calculated rate coefficients for each ion diameter were then fit by regression analysis to the equation:

$$\log k = \log A + n \log T \tag{1}$$

This gave a table of A's and n's as a function of ion diameter. These were then each fit to simple equations giving the dependence of A and n on ion diameter (d) for both acetylene and diacetylene. The resultant coefficients are given below.

Acetylene:

$$A \quad = \quad (3.37 + 12\ d) \times 10^{13},\ cm^3/mol/s$$

$$n \quad = \quad 0.292 + 0.0397 \times d,\ d\ in\ nm$$

Diacetylene:

$$A \quad = \quad (2.96 + 9.93 \times d) \times 10^{13},\ cm^3/mol/s$$

$$n \quad = \quad 0.298 + 0.033 \times d,\ d\ in\ nm$$

For all of the fits, the correlation coefficients (r^2) were 0.98 or greater, for $d \geq 0.7$ nm; there were large changes in values below this ion diameter which is where the extended Langevin theory breaks down.

The ion diameters were deduced from experimental ion mobility (κ) data for PAH molecules in nitrogen gas [12]. From the mobility data and the hard sphere diameter of the nitrogen molecule ($= 0.375$ nm, Ref. 13), using Langevin's ion mobility equation [14],

$$\kappa = \frac{A}{\sqrt{\rho_g(\kappa - 1)}} \left(1 + \frac{M}{m}\right)^{\frac{1}{2}} \tag{2}$$

we back calculated the equivalent ion diameters of the PAH ions in nitrogen gas. Here, M is the MW of nitrogen and m is the MW of the ion, κ is the dielectric constant of nitrogen and ρ_g is the gas density. A is a complicated function of a parameter (λ - not mean free path), gas pressure, p, κ, and the sum of the neutral and ion collision radii (D_{12}). The λ parameter is given by:

$$\lambda^2 = \frac{8\pi p\, D_{12}^4}{(\kappa - 1)\, e^2} \tag{3}$$

4

where e is the electron charge. Fitting these data to various empirical functions, we found the following relationship between the deduced ion size and the PAH ion mass:

$$\ln(d, \mathring{A}) = -1.375 + 2.154 \ln(\ln(m)) \tag{4}$$

The correlation coefficient (r^2) for this fitting equation was 0.999--almost a perfect fit to the ion diameters.

For comparison, we plot ion diameters deduced from ion mobility data against ion diameters calculated for homogeneous spheres having densities, ρ, of 1.5 or 2.0 g/cm^3 -- the density range for soots. The results are plotted in Fig. 1 and they show close agreement. This agreement indicates that the effective ion diameters derived from mobility data are fairly reliable. The fitting function, Eq. (4), is routinely used to calculate PAH ion diameters for all ions in our modeling work.

Table I includes a comparison of the rate coefficients by the two theories for this present mechanism. There is little difference in the calculated ion concentration profiles when the rate coefficients from the extended Langevin theory are substituted for the original Langevin coefficients.

In modeling experimental flame results using the kinetic scheme presented in Table I, we input experimental profiles for $C_3H_3^+$ and $H_5C_6^+$ (phenyl cation) because we do not have good experimental profiles for the HCO$^+$ ion, the initial ion produced by chemiionization, from which all other ions are derived. This ion is not observed in fuel rich flames because it reacts extremely fast, transferring a proton to many neutral species including water. When we calculated the concentration of HCO$^+$, using the basic neutral reaction scheme of Frenklach, et.al. [15] for soot formation with the addition of chemiionization reactions to form HCO$^+$ and experimental electron recombination rates, the calculated value was too high compared to the maximum possible value based on experimental measurements.

The question arises as how to handle $C_3H_3^+$. The ion is identified as a flame ion by mass spectrometry which, unfortunately, provides no direct information on the ion structure. Two isomeric structures for $C_3H_3^+$ have been considered as potentially important [16]. (These are the linear propargylium cation, denoted as $C_3H_3(l)^+$, and the cyclic cyclopropenium cation, $C_3H_3(c)^+$). In the mechanism we have chosen to identify the $C_3H_3(l)^+$ ion with the experimentally observed ion. Recent calculations [17] show that the cyclic cation is more stable than the linear cation by 116 kJ/mol; the experimental difference is 105 kJ/mol [18]. The effect of this difference in stability decreases with increasing temperature; on the basis of the derived thermochemistry, at 300 K the equilibrium ratio of linear to cyclic is 5 $\times$ 10^{-18} but at 2000 K the ratio is 0.03, Fig. 2.

It has been determined experimentally that at low temperatures the cyclic isomer is not reactive with acetylene or diacetylene, but that the linear isomer is reactive with acetylene and diacetylene [19]. There is no evidence that the cyclopropenium cation isomerizes to the propargylium cation in the absence of encounter complexes with neutral molecules, e.g., acetylene [17]. Yet Cameron, et.al. [17] suggest that in sooting flames the cyclic form may not be the most abundant. This assumes that the linear ion is formed and does not rapidly isomerize to the more stable cyclic ion. In the flame, the $C_3H_3^+$ cation is assumed to be formed in a number of elementary reactions involving HCO$^+$[20].

5

V. COMPUTER CODE

In our earliest work, the model was run on an IBM 3090 computer by M. Frenklach and Hai Wang at Penn State [21]. There was a long turnaround time and their code was not adaptable to ions or some of the computer tests which we wanted to run. We subcontracted for one summer to Prof. Robert Brown at Iowa State University, who had a code in which ion/electron diffusion was treated with Poissons equation [22], which treats ion transport more exactly than ambipolar diffusion, an approximation we eventually used. There was again a problem with long turnaround time, and the program not being as flexible as we required. We thus hired Fokian Egolfopoulos at Princeton University (now at University of Southern California) as a consultant to modify the flame code package, based on Sandia's CHEMKIN and Flame Codes. Modifications were made in the code to incorporate: (1) ion chemistry; (2) ambipolar diffusion; (3) the ability to input neutral and ion profiles; and (4) the ability to employ a modified Arrhenius form for handling rate coefficients calculated by equilibrium constants.

These changes and the means of using the modified program are described in the Symposium paper, Appendix A. To decrease run times, AeroChem purchased a Silicon Graphics IRIS workstation. Run times have been relatively short, from 20 minutes to a few hours. Part of the ability to run on a work station in reasonable times, rather than requiring a computer with the power of an IBM 3090, is due to using selected experimental mole fraction profiles as inputs. Thus we were able to eliminate a large number of neutral species reactions. We note that the neutral part of the mechanism gave results which did not agree with experimental profiles. Clearly when we obtain satisfactory agreement with experimental ion concentrations we will have to consider a modified neutral mechanism in order to model the chemiionization steps.

VI. COMPARISON OF CALCULATED AND EXPERIMENTAL ION CONCENTRATION PROFILES

The availability of the modified Sandia Flame Code to handle ions and the availability of a workstation have greatly accelerated the rate of progress on this program. Thermodynamic equilibrium has a much greater effect on the ion-molecule association reactions than expected (the reverse reaction rate constants are calculated from the forward rate and the equilibrium constants); this shows up as a stronger temperature dependence than anticipated. At higher temperatures the ion-molecule reverse reactions become more important as entropy effects become more important:

$$\Delta_f G \;=\; \Delta_f H \,-\, T\Delta_f S \tag{5}$$

This same effect, of course, controls neutral reactions and may very well explain why the rate of soot formation peaks in the temperature range of 1400 to 1900 K (see, e.g., Ref. 23). The usual explanation involves a competition between the rate of soot formation and the rate of soot oxidation.

The strong temperature effect on ion growth reactions has shown up on several occasions. In some of our first computer runs with Frenklach and Wang, a table with the experimental flame temperature vs. distance, in which one point was in error, was inadvertently used as input. This showed up in the calculation of ion profiles as a dip in the concentration profiles. In the early ion profile calculations made by Frenklach and Wang, the ions always peaked much closer to the burner than the experimental data, occurring close to the burner where the flame temperature is low.

Our findings, submitted to the 25th Combustion Symposium and presented in Appendix A, can be summarized briefly. First, we find that our calculated ion concentrations are very sensitive to the ion Gibb's free energies of formation used. Second, the calculated ion concentrations are almost always low compared with experimental concentrations. Third, electron-ion recombination rates can be lowered by a factor of 100 with little effect on the profiles. This means that the model predictions would be relatively unaffected by the inclusion of other negatively charged species, which have been reported in sooting flames, and could result in higher positive ion concentrations.

We ask why the thermodynamics, which controls the reverse reaction rates, plays such an important role. We also ask why the calculated concentrations are so much smaller than the measured concentrations. It could, of course, be that ion growth is not the source of larger ions in flames, but we have eliminated many other possible mechanisms [1,24]. Earlier Homann was critical of an ion growth mechanism. Homann and associates [25] now seem to believe that the source of large ions is ion growth, as we proposed years ago! [26] Another possibility is that the experimental measurements are off. It is difficult to see how they could be off by this much. Equivalent experimental results have been obtained by Homann and associates in Germany [27,28] and by Delfau and associates in France [29]. An attempt to bring the model into agreement with experimental through incorporation of the modified Langevin theory was ineffective.

Several rather "brutal" modifications were made in an attempt to determine what has to be done to obtain agreement. The best agreement was found by reducing the flame temperature profile by 10 % at the maximum temperature, and linearly decreasing the extent of reduction to zero at the burner surface. The results for modeling the profiles of ions up to the perinaphthenyl ion, $C_{13}H_6H3^+$ in Table I, looked acceptable. The data and discussion are in one of the rejected Symposium papers, Appendix A.

Subsequent to submitting the Symposium paper, we extended the model to the protonated coronene ion, $C_{24}H_{13}^+$. The temperature effect became even more evident. If a reduced temperature maximum of 1700 K is assumed and the temperature profile closer to the burner is modified to extrapolate to the experimental burner surface temperature, then the ratios of the maximum experimental to the maximum calculated ion concentrations are obtained as shown in Fig. 3. Negative log values (left of zero) imply the observed concentrations are low compared with the model and are acceptable because reaction rate coefficients involved in the production of such species can be decreased. Log ratios to the right of zero are of greater concern. In addition to reducing the maximum temperature, the $\Delta H_f(C_{11}H_8H^+)$ was reduced by about 3%. The apparent requirements to adjust the experimental temperature will be our major consideration in continuing this work. It would be premature to abandon the concept of ion growth and the ionic mechanism of soot formation because there is so much evidence in favor of both concepts [see e.g, references 1,2,30 and below]. It is also difficult to explain the rather good agreement between experimental

7

and calculated ion concentrations just by scaling the temperature profile, even by the large amount required.

VII. COMPARISON OF THE RATE OF CARBON SPECIES GROWTH FOR THE FREE RADICAL AND IONIC MECHANISMS

In the final report on the last contract [31], we compared the rates of increase in carbon content by a free radical and the ionic mechanism, using experimentally measured neutral and ion species and the appropriate rate coefficients. That comparison has been further refined and has been accepted for publication [1]. The more relevant experimental neutral species data of Bittner and Howard [32] are used rather than the data of Vovelle [33] (our burner and conditions were designed to match those of Bittner and Howard so such comparisons could be made). The experimental data on which this analysis was made are presented in Fig. 4. To the extent that the Bittner and Howard data can be smoothly extrapolated, beyond 250 u the ion and neutral concentrations become equal and the difference in growth rate will be determined by: the reaction rate coefficients in the neutral and ion mechanisms; the concentration of the other reactants (hydrogen atoms and acetylene for the free radical mechanism, and acetylene for the ionic mechanism); and the number of reaction steps to account for the same number of carbon atoms added, ratio 2:1 for the free radical mechanism over the ionic mechanism. On this basis, the ionic mechanism is faster; compare 6.7 μs for the ionic mechanism with 25 μs for the free radical mechanism. This is still not a conclusive comparison, recognizing the inaccuracies in the data and in the rate coefficients, but it certainly suggests that the commonly promoted radical mechanism is not necessarily the dominant path to soot formation.

VIII. COMPARISON OF THE THERMOCHEMICAL DRIVING FORCE FOR THE IONIC AND FREE RADICAL MECHANISMS

The ultimate driving force for any sequence of chemical reactions, such as must occur for soot formation, is thermochemistry. As water flows downhill, reactions proceed in the direction of a negative gradient in free energy. To compare this driving force for ions, free radicals, and neutral molecules, we compare the free energy of formation of these three components of the ionic and free radical mechanism of soot formation in Figs. 5 and 6 for the respective temperatures, 1000 and 2000 K.

Several features are obvious on inspection. First, the driving force (the negative slope of the curve) for ions is distinctly greater than for free radicals or neutral molecules in the initial stages of growth. Second, the free energy per carbon atom of any of the species (free radical, neutral molecule, or ion) rapidly levels off as the molecules become larger. Third, the ion and neutral species free energies of formation converge when the species contain about 30 carbon atoms, i.e., a molecular weight of about 350 to 400 u.

TP-531

The conclusion to be drawn is clear. There is very little thermochemical driving force for the growth of free radicals (or neutral molecules) compared to the corresponding driving force for ions.

IX. IONS IN BENZENE/OXYGEN FLAMES

The above kinetic scheme has been applied to modeling acetylene/oxygen flames. In a previous program [3], we measured ion spectra of benzene/oxygen flames in the same flames and on the same burner as used by Bittner and Howard [32] to measure neutral species profiles. This was done to have a data base available for modeling a different flame. We are currently analyzing that data in preparation for modeling the benzene/oxygen flame.

The ion structures of these flames are quite different. As in acetylene flames, $C_3H_3^+$ is assumed to be the primary ion, yet its concentration profile is different in benzene flames. In both nonsooting ($\phi = 1.8$) and sooting ($\phi = 2.0$) benzene/oxygen flames, this ion exhibits two peaks, a small one near the burner and a relatively large second peak downstream. It slowly decays further from the burner. Another unique feature of the benzene flame is that a large number of oxygenated ions, e.g., $C_6H_7O^+$, are observed which are not observed in acetylene/oxygen flames. Additionally, of the ions observed in acetylene/oxygen flames are also observed in the benzene/oxygen flame.

The apparent stability of the $C_3H_3^+$ ion in the benzene flame contrasts with its behavior in the C_2H_2/O_2 flame. In the benzene flame its concentration is an order of magnitude greater than the concentration of other ion species; in the sooting acetylene flame its concentration is similar to those of other ions. In the benzene flames its concentration decays with distance more slowly than in the acetylene flame. The difference can probably be explained by the equilibrium between the linear reactive ion and the stable cyclic nonreactive ion favoring the nonreactive form at the lower temperature 1900 K (maximum) in the benzene flame compared to 2020 K (maximum) in the acetylene flame. Some of the differences may be due to the fact that the sooting acetylene flame is more fuel rich, relative to the critical equivalence ratio for soot formation, than the benzene flames. There are other great differences (see Section X and Appendix B) between the two flames. Soot formation in the benzene flame is greatly in excess of equilibrium and occurs at an equivalence ratio less that the equilibrium equivalence ratio for soot formation. In contrast, soot formation in the acetylene flame is less than equilibrium and occurs at an equivalence ratio greater than the equilibrium equivalence ratio. Further, since the total ion concentrations in the benzene flames are greater than in the acetylene flame, compare about 10^{11} with 7×10^9 ions cm^{-3}, the greater stability of $C_3H_3^+$ (cyclic) compared to $C_3H_3^+$ (linear) apparently does not limit the formation of large ions, but may spread their formation over a greater distance. These differences between the two flames will be explained by successful models.

Recently Löffler and Homann [34,35] reported ion profile measurements in sooting benzene/oxygen flames. The conditions in their experiments and in ours are compared in Table II. In Table III we compare the ions observed in acetylene/oxygen and benzene/oxygen flames at both AeroChem and at Darmstadt. In their paper, Löffler and Homann concentrate [34] on oxygenated ions, but observed ion mass spectra are reported in Löffler's thesis [35]. We have therefore used these spectra to determine other ions observed in their flames.

9

In any such comparison of mass spectrometer data, one should be aware that the reporting of the appearance of an ion involves a somewhat subjective factor in the choice of which peaks are identified as important, and an objective factor that is dependent upon the sensitivity and resolution of the mass spectrometer. The list used here for acetylene/oxygen flames at Darmstadt was kindly furnished by Homann [36] to supplement those given in the paper [27]. Many other ions were identified by Homann; we used only those identified as "prominent peaks". Some of these ions, e.g., 71, 83, and 85 u are identified by Löffler and Homann in the acetylene flame as an oxygen molecule attached to an ion. This indicates reactions in the sampling cone of their instrument; these ions would not be expected to be stable in a flame. Our experience has been that the attachment of water, sometimes more than one water molecule, to an ion indicates sampling problems. Such ion signals can be eliminated by changing the sampling cone geometries, temperature, bias voltage, or the pressure behind the cone. Some of the oxygenated species observed by Gerhardt and Homann, may in fact be water clustered to a hydrocarbon ion, e.g. in Table III, for ion masses: 47, 67, 69, 73, 81, 85, 95, 105, 109, and 119. This could also be the case for some of the oxygenated species observed in both laboratories in benzene flames.

The above consideration raises again [37] the problem of sampling ions which have very high reaction rate coefficients. Are the identified ions the true flame ions or ions that have been produced in the sampling system, by e.g., reacting with a species in large concentration, e.g., H_2O, as discussed above, H_2, $H \cdot$, or C_2H_2? This would muddle an already complicated problem. It would mean that some of the observed ions are not flame ions, but are produced in the sampling cone. To model the flame chemistry, one would first have to deduce, from the observed ions, the actual ions in the flame.

In general, for the benzene flame, Table II, the agreement in observed ions between Löffler and Homann and AeroChem are consistent, except for $C_{13}H_9^+$. We observe this ion in benzene flames but they do not. This is a very stable ion and we both observe it in large concentrations in acetylene flames. Instead of this ion, they observe $C_{12}H_9O^+$, 4 u greater than $C_{13}H_9^+$, an ion we observe only in very small concentrations. Because we had previously reported $C_{13}H_9^+$ in benzene flames [38], Löffler and Homann were very careful to confirm the fact that it was not observed [39]. Their instrumentation is better than ours, but it is difficult to see how we could be off in our calibration by 4 u. If we shift our mass scale by 4 u to force a match at 169 u, then our agreement with identifying larger ions falls from 80 ions to 54 ions. Further, we would identify 40 ions which they do not observe and are not observed in the acetylene flame.

One possibility is that the two ions, $C_{13}H_9^+$ and $C_{12}H_9O^+$, have similar thermodynamic stabilities, so that the differences in our two experiments, Table II, are sufficient to switch the stability from one to the other ion. To determine the feasibility of this would require estimating the thermodynamics for other ions of mass 169 u, which we will do. This ion may derive from an ion of mass 152 u with H_2O replacing a H atom or 151 u with H_2O added. The question remains, why does Darmstadt not observe mass 165? The differences in the two flames, Table II, do not explain this observation difference. Hopefully, the difference will become clear when we model this flame.

The next step in analyzing the benzene/oxygen flame will be to calibrate our mass spectrometer comparing the mass spectral data with our Langmuir probe data, as we did for the acetylene flame [40].

10

TP-531

X. THERMODYNAMIC CONSIDERATIONS OF SOOT FORMATION

Data in the literature on soot and acetylene concentration variation through the threshold equivalence ratio for soot formation were compared with thermodynamic equilibrium concentrations. One of the reasons for exploring this is that at soot threshold, the only other observed property of the flame which changes dramatically with equivalence ratio is the ion concentration and size of the ions, Fig. 7.

It was found that in most flames soot is observed at C/O ratios very much lower than where soot is predicted to form by equilibrium, and the concentrations of soot, acetylene and other hydrocarbons are in great excess of equilibrium. However in the well studied acetylene/oxygen flame, the "standard flame", the opposite is true. For the acetylene/oxygen flame, acetylene is in excess of equilibrium concentrations, and soot concentrations are less than equilibrium. To our knowledge, this is the first time this has been noted. This work is presented in one of the papers rejected for the Combustion Symposium, see Appendix B. We will expand the manuscript, explaining the implications for the ionic mechanism of soot formation, and submit it for publication in *Combustion and Flame*.

XI. PRESENTATIONS and PUBLICATIONS

Calcote, H.F., "Mechanisms of Soot Formation", Air Products International Combustion Symposium, Air Products and Chemical Company Inc. Allentown, PA, 25-26 March 1991.

Calcote, H.F., "Modeling Study to Evaluate the Ionic Mechanism of Soot Formation," presented at AFOSR Contractors Meeting on Propulsion Research, La Jolla, CA, 15-19 June 1992.

Calcote, H.F. and Gill, R.J., "A Detailed Computer Model of Ion Growth in a Fuel Rich Acetylene/Oxygen Flame," presented at Joint Meeting of the British and German Sections of the Combustion Institute, Queens College, Cambridge, England, 29 March to 2 April 1993.

Calcote, H.F. and Gill, R.J., "A Model of Ion Growth in a Fuel Rich Acetylene/Oxygen Flame," presented at Eastern States Section/The Combustion Institute Fall Meeting, Princeton, NJ, 25-27 October 1993.

Calcote, H.F. and Keil, D.G., "Thermodynamic Considerations of Soot Formation," presented at Western States Section/The Combustion Institute, 1993 Fall Meeting, October 1993.

Pedersen, T. and Brown, R.C., "Simulation of Electric Field Effects in Premixed Methane Flames", *Comb. and Flame* 94: 433-448 (1993). Professor Brown was under subcontract to AeroChem in the summer of 1990; the work reported herein was partially funded by that subcontract. Paper in Appendix C.

TP-531

Calcote, H.F., "The Role of Ions in Soot Formation," presented at International Workshop, Mechanisms and Models of Soot Formation, Ruprecht-Karls-Universitat, Heidelberg, Germany, 29 September - 2 October 1991.

Calcote, H.F. and Gill, R.G., "Comparison of the Ionic Mechanism of Soot Formation with a Free Radical Mechanism," to be published in Proceedings International Workshop, Mechanisms and Models of Soot Formation, Springer-Verlag.

XII. PROFESSIONAL PARTICIPATION

The Principal Investigator for this program was Dr. H.F. Calcote. Dr. C.H. Berman extended the Langevin theory to large molecular ions. Dr. Fokian Egolfopoulos, University of California in Los Angeles, modified the Sandia Flame Code to handle ions. Dr. R.J. Gill has been responsible for collecting and calculating the thermodynamics data and for running the modified Sandia Flame Code. Dr. David G. Keil worked on the thermodynamics of soot formation. Leslie Van Hoose has assisted with detailed calculations and graphics and in final editing.

We would also like to acknowledge Drs. Vovelles (Orleans) and Dr. Homann (Darmstadt) sending us unpublished experimental profiles on neutral and ions, respectively. Dr. Steve Stein sent us unpublished thermochemistry on ions and discussed thermochemical problems with us.

XIII. INVENTIONS

None.

XIV. REFERENCES

1.   Calcote, H.F., "The Role of Ions in Soot Formation," presented at International Workshop, Mechanisms and Models of Soot Formation, Ruprecht-Karls-Universitat, Heidelberg, Germany, 29 September-2 October 1991; Calcote, H.F. and Gill, R.G., "Comparison of the Ionic Mechanism of Soot Formation with a Free Radical Mechanism," to be published in Proceedings International Workshop, Mechanisms and Models of Soot Formation, Springer-Verlag.

2.   Calcote, H.F. and Keil, D.G., "The Role of Ions in Soot Formation," *Pure & Appl. Chem.* 62, 815-824 (1990).

3.   Calcote, H.F. and Keil, D.G., "Ionic Mechanisms of Soot Formation in Flames," Final Report, AeroChem TP-465, June 1987.

4. Keil, D.G. and Calcote, H.F., "Large Ion Formation in a Sooting and Near Sooting Benzene/Oxygen Flame," Fall Technical Meeting, Eastern Section: The Combustion Institute, Orlando, FL, 3-5 December 1990.

5. Lias, S.G., Bartmess, J.E., Liebman, J.F., Holmes, J.L., Levin, R.D., Mallard, W.G., "Gas-Phase Ion and Neutral Thermochemistry," *J. Phys. Chem. Ref. Data* 17, Suppl. 1 (1988).

6. Lias, S.G., Liebman, J.F., Levin, R.D., Kedef, S.A. and Stein, S., "NIST Standard Reference Database 19A, Positive Ion Energetics, Version 2.01, distributed by The Standard Reference Data Program, NIST, Gaithersburg, MD, January 1994.

7. Rock, P.A., Chemical Thermodynamics, (University Science Books, Mill Valley, CA, 1983), Chap. 14.

8. Hui-yun, P., "The Modified Pitzer-Gwinn Method for Partition Function of Restricted Internal Rotation of a Molecule," *J. Chem. Phys.* 87, 4846 (1987).

9. Benson, S.W., Thermochemical Kinetics, 2nd ed. (Wiley, New York, 1976).

10. Stein, S.E. and Fahr, A., "High Temperature Stabilities of Hydrocarbons," *J. Phys. Chem.* 89, 3714 (1985).

11. Berman, C.H. and Calcote, H.F., "Langevin Theory for Large Ions," in preparation.

12. Lin, S.N., Griffin, G.W., Horning, E.C., and Wentworth, W.E., "Dependence of Polyatomic Ion Mobilities and Ionic Size," *J. Chem. Phys.* 60, 4994 (1974).

13. Kennard, E.H., Kinetic Theory of Gases, (McGraw-Hill, New York, 1938) p. 149.

14. McDaniels, E.W., Collision Phenomena in Ionized Gases (Wiley, New York, 1964) pp. 432-433.

15. Frenklach, M. and Warnatz, J., *Combust. Sci. Technol.* 51, 265-283 (1987).

16. Eyler, J.R., Oddershede, J., Sabin, J.R., Diercksen, G.H.F. and Grüner, N.E., *J. Phys. Chem.* 88, 3121-3123 (1984).

17. Cameron, A., Leszczynski, J., Zerner, M.C., and Weiner, B., "Structure and Properties of $C_3H_3^+$ Cations," *J. Phys. Chem.* 93, 139 (1989).

18. Lossing, F.P., "Free Radicals by Mass Spectrometry. XLV. Ionization Potentials and Heats of Formation of C_3H_3, C_3H_5, and C_4H_7 Radicals and Ions," *Can. J. Chem.* 50, 3973 (1972).

19. Ozturk, F., Baykut, G., Moini, M. and Eyler, J.R., "Reactions of $C_3H_3^+$ with Acetylene and Diacetylene in the Gas Phase," *J. Phys. Chem.* 91, 4360 (1987).

20. Calcote, H.F., "Ions in Flames," in Ion-Molecule Reactions, Vol. 2, J.L. Franklin, Ed. (Plenum Press, New York, 1972) p. 673.

21. Frenklach, M. and Wang, H., "Computer Modeling of Soot Formation Comparing Free Radical and Ionic Mechanisms," Final Report, January 1991.

22. Eraslan, A.N. and Brown, R.C., "Chemiionization and Ion-Molecule Reactions in Fuel-Rich Acetylene Flames," *Combust. Flame* 74, 19 (1988).

23.   "Soot Formation in Combustion," An International Round Table Discussion, Section IV, "Comparison of Soot Formation in Pyrolysis, Premixed and Diffusion Flames," led by I. Glassman and Discussion, Vandenhoeck and Ruprecht in Göttingen, July 1990, pp. 67-119.

24.   Calcote, H.F., "Ionic Mechanisms of Soot Formation," in Soot in Combustion Systems and Its Toxic Properties, J. Lahaye and G. Prado, Eds. (Plenum Press, New York, 1983) pp. 197-215.

25.   Homann, K.H., International Workshop, Mechanisms and Models of Soot Formation, Ruprecht-Karls-Universitat, Heidelberg, Germany, 29 September-2 October 1991.

26.   Calcote, H.F., "Mechanisms of Soot Nucleation in Flames - A Critical Review," *Combust. Flame* 42, 215-242 (1981).

27.   Gerhardt, P.H. and Homann, K.H., "Ions and Charged Soot Particles in Hydrocarbon Flames. 2. Positive Aliphatic and Aromatic Ions in Ethyne/Oxygen Flames," *J. Phys. Chem.* 94, 5381 (1990).

28.   Gerhardt, P.H.,"Massenspektrometrie Positiver und Negativer Ionen in Brennstofffreichen Ethin-Sauerstoff-Flammen," Dissertation, Technischen Hochschule Darmstadt, 1988.

29.   Michaud, P., Delfau, J.L., and Barrassin, A., "The Positive Ion Chemistry in the Post Combustion Zone of Sooting Premixed Acetylene Low Pressure Flat Flames," Eighteenth Symposium (International) on Combustion (The Combustion Institute, Pittsburgh, 1981) p. 443.

30.   Calcote, H.F., Olson, D.B., and Keil, D.G., "Are Ions Important in Soot Formation?", *Energy & Fuels* 2, 494 (1988).

31.   Calcote, H.F. and Gill, R.J., "Computer Modeling of Soot Formation Comparing Free Radical and Ionic Mechanisms," Final Report, AeroChem TP-495, February 1991.

32.   Bittner, J.D. and Howard, J.B., "Pre-particle Chemistry in Soot Formation," in Particulate Carbon: Formation During Combustion, D.G. Siegla and G.W. Smith, eds. (Plenum, New York, 1981) p. 109.

33.   Vovelle, C., personal communications, December 1989 and July 1990.

34.   Löffler, S. and Homann, K.H., "Large Ions in Premixed Benzene-Oxygen Flames," Twenty-Third Symposium (International) on Combustion (The Combustion Institute, Pittsburgh, 1991) p. 355.

35.   Löffler, S., "Polyeder-Kohlerstaff-und Andere Interessante Ionen in Benzolsauerstaft Flammen," Dissertation, Technischen Hochschule Darmstadt, 1990.

36.   Homann, K.H., personal communication, September 1991.

37.   Stein, S.E., "Structure and Equilibria of Polyaromatic Flame Ions," *Combust. Flame* 51, 357 (1983).

38.   Olson, D.B. and Calcote, H.F., "Ions in Fuel-Rich and Sooting Acetylene and Benzene Flames," Eighteenth Symposium (International) on Combustion (The Combustion Institute, Pittsburgh, 1981) p. 453.

39. Homann, K.H., personal communication, March 1991.

40. Calcote, H.F. and Keil, D.G., "Ion-Molecule Reactions in Sooting Acetylene-Oxygen Flames," *Combust. Flame* 74, 131 (1988).

41. Calcote, H.F., Gill, R.G. and Berman, C.H., "Modeling Study to Evaluate the Ionic Mechanism of Soot Formation," Final Report, AeroChem TP-508, April 1992.

TABLE I

REACTIONS AND RATE COEFFICIENTS (LANGEVIN AND EXTENDED LANGEVIN) FOR
IONIC MECHANISM OF SOOT FORMATION

$$k(T) = A\,T^n \exp(-E_{act}/RT)$$
units J, cm^3 mole, s

REACTIONS	Langevin Rate Parameters			Extended Langevin Rate Parameters		
	A	n	E_{act}	A	n	E_{act}
$C_3H_3^+ + C_2H_2 = C_5H_2H^+ + H_2$	6.50e+14	0	0	8.60e+13	0.3	0
$C_3H_3^+ + C_2H_2 = C_5H_5^+$	6.50e+14	0	0	8.60e+13	0.3	0
$C_3H_3^+ + C_4H_2 = C_5H_2H^+ + C_2H_2$	7.40e+14	0	0	7.28e+13	0.3	0
$C_3H_3^+ + C_4H_2 = C_7H_4H^+$	7.40e+14	0	0	7.28e+13	0.3	0
$C_4H_5^+ + C_2H_2 = H_5C_6^+ + H_2$	6.20e+14	0	0	9.17e+13	0.3	0
$C_5H_2H^+ + H_2 = C_5H_5^+$	9.00e+14	0	0	8.97e+14	0.0	0
$C_5H_2H^+ + C_2H_2 = C_7H_4H^+$	6.00e+14	0	0	9.51e+13	0.3	0
$C_5H_2H^+ + C_3H_4 = H_5C_6^+ + C_2H_2$	6.50e+14	0	0	9.51e+13	0.3	0
$C_5H_5^+ + C_2H_2 = C_7H_4H^+ + H_2$	6.00e+14	0	0	9.58e+13	0.3	0
$C_5H_5^+ + C_2H_2 = C_7H_5^+ + H_2$	2.40e+14	0	-319	9.58e+13	0.3	0
$C_5H_5^+ + C_4H_2 = C_9H_7^+$	6.50e+14	0	0	9.58e+13	0.3	0
$C_5H_5^+ + C_4H_2 = H_7C_9^+$	6.50e+14	0	0	8.09e+13	0.3	0
$C_5H_5^+ + C_2H_2 = C_7H_7^+$	6.50e+14	0	0	8.09e+13	0.3	0
$H_5C_6^+ + C_2H_2 = C_8H_7^+$	5.80e+14	0	0	9.94e+13	0.3	0
$C_7H_4H^+ + H_2 = C_7H_7^+$	8.90e+14	0	0	8.93e+14	0.0	0
$C_7H_4H^+ + H_2 = H_7C_7^+$	8.90e+14	0	0	8.93e+14	0.0	0
$C_7H_5^+ + C_2H_2 = C_9H_7^+$	5.70e+14	0	0	1.03e+14	0.3	0
$C_7H_5^+ + C_2H_2 = H_7C_9^+$	5.70e+14	0	0	1.03e+14	0.3	0
$C_7H_5^+ + M = C_7H_4H^+ + M$	4.60e+14	0	0	1.03e+14	0.3	0
$C_7H_5^+ + C_3H_4 = C_8H_7^+ + C_2H_2$	6.15e+14	0	0	1.03e+14	0.3	0
$C_7H_5^+ + C_3H_4 = C_{10}H_9^+$	6.15e+14	0	0	1.03e+14	0.3	0
$C_7H_4H^+ + C_2H_2 = H_7C_9^+$	5.70e+14	0	0	1.03e+14	0.3	0

REACTIONS					Langevin Rate Parameters			Extended Langevin Rate Parameters		
					A	n	E_{act}	A	n	E_{act}
$C_3H_3^+$	+	C_2H_2	= $C_5H_2H^+$	+ H_2	6.50e+14	0	0	8.60e+13	0.3	0
$C_7H_4H^+$	+	C_2H_2	= $C_9H_7^+$		5.70e+14	0	0	1.03e+14	0.3	0
$C_7H_7^+$	+	M	= $H_7C_7^+$	+ M	4.60e+14	0	0	1.03e+14	0.3	0
$C_7H_7^+$	+	C_2H_2	= $H_7C_9^+$	+ H_2	5.70e+14	0	0	1.03e+14	0.3	0
$H_7C_7^+$	+	C_2H_2	= $H_7C_9^+$	+ H_2	5.70e+14	0	0	1.03e+14	0.3	0
$C_7H_7^+$	+	C_4H_2	= $C_{11}H_8H^+$		6.10e+14	0	0	8.69e+13	0.3	0
$H_7C_7^+$	+	C_4H_2	= $C_{11}H_8H^+$		6.10e+14	0	0	8.69e+13	0.3	0
$C_8H_7^+$	+	C_2H_2	= $C_{10}H_9^+$		5.64e+14	0	0	1.06e+14	0.3	0
$C_8H_7^+$	+	C_2H_2	= $H_9C_{10}^+$		5.64e+14	0	0	1.06e+14	0.3	0
$C_8H_7^+$	+	C_3H_4	= $C_{11}H_8H^+$	+ H_2	6.02e+14	0	0	1.06e+14	0.3	0
$C_8H_7^+$	+	C_4H_2	= $C_{12}H_9^+$		5.95e+14	0	0	8.94e+13	0.3	0
$C_9H_7^+$	+	M	= $H_7C_9^+$	+ M	4.50e+14	0	0	1.09e+14	0.3	0
$C_9H_7^+$	+	C_2H_2	= $C_{11}H_8H^+$		5.60e+14	0	0	1.09e+14	0.3	0
$H_7C_9^+$	+	C_2H_2	= $C_{11}H_8H^+$		5.60e+14	0	0	1.09e+14	0.3	0
$C_9H_7^+$	+	C_4H_2	= $C_{13}H_6H_3^+$		5.80e+14	0	0	9.16e+13	0.3	0
$H_7C_9^+$	+	C_4H_2	= $C_{13}H_6H_3^+$		5.80e+14	0	0	9.16e+13	0.3	0
$H_9C_{10}^+$	+	M	= $C_{10}H_9^+$	+ M	4.50e+14	0	0	1.12e+14	0.3	0
$C_{10}H_9^+$	+	C_2H_2	= $C_{12}H_9^+$	+ H_2	5.53e+14	0	0	1.12e+14	0.3	0
$H_9C_{10}^+$	+	C_2H_2	= $C_{12}H_9^+$	+ H_2	5.53e+14	0	0	1.12e+14	0.3	0
$H_9C_{10}^+$	+	C_2H_2	= $H_9C_{12}^+$	+ H_2	5.53e+14	0	0	1.12e+14	0.3	0
$C_{10}H_9^+$	+	C_3H_4	= $C_{13}H_6H_3^+$	+ $2H_2$	5.85e+14	0	0	1.12e+14	0.3	0
$C_{10}H_9^+$	+	C_4H_2	= $C_{12}H_9^+$	+ C_2H_2	5.75e+14	0	0	9.40e+13	0.3	0
$H_9C_{10}^+$	+	C_4H_2	= $C_{12}H_9^+$	+ C_2H_2	5.75e+14	0	0	9.40e+13	0.3	0
$H_9C_{10}^+$	+	C_4H_2	= $H_9C_{12}^+$	+ C_2H_2	5.75e+14	0	0	9.40e+13	0.3	0
$C_{11}H_8H^+$	+	C_2H_2	= $C_{13}H_6H_3^+$	+ H_2	5.50e+14	0	0	1.14e+14	0.3	0
$C_{11}H_9^+$	+	C_2H_2	= $C_{13}H_6H_3^+$	+ H_2	5.50e+14	0	0	1.14e+14	0.3	0
$H_9C_{11}^+$	+	M	= $C_{11}H_8H^+$	+ M	4.50e+14	0	0	1.14e+14	0.3	0

17

REACTIONS					Langevin Rate Parameters			Extended Langevin Rate Parameters		
					A	n	E_{act}	A	n	E_{act}
$C_3H_3^+$	+	C_2H_2	$= C_5H_2H^+$	+ H_2	6.50e+14	0	0	8.60e+13	0.3	0
$H_9C_{11}^+$	+	M	$= C_{11}H_9^+$	+ M	4.50e+14	0	0	1.14e+14	0.3	0
$C_{11}H_9^+$	+	M	$= C_{11}H_8H^+$	+ M	4.50e+14	0	0	1.14e+14	0.3	0
$H_9C_{12}^+$	+	M	$= C_{12}H_9^+$	+ M	4.47e+14	0	0	1.16e+14	0.3	0
$C_3H_3^+$	+	E	$\rightarrow C_2H_2$	+ CH	1.05e+19	-0.5	0	1.05e+19	-0.5	0
$C_4H_5^+$	+	E	$\rightarrow C_2H_2$	+ C_2H_3	1.20e+19	-0.5	0	1.20e+19	-0.5	0
$C_5H_2H^+$	+	E	$\rightarrow C_3H_3$	+ C_2	1.33e+19	-0.5	0	1.33e+19	-0.5	0
$C_5H_5^+$	+	E	$\rightarrow C_3H_3$	+ C_2H_2	1.40e+19	-0.5	0	1.40e+19	-0.5	0
$H_5C_6^+$	+	E	$\rightarrow C_4H_4$	+ C_2H	1.42e+19	-0.5	0	1.42e+19	-0.5	0
$C_7H_4H^+$	+	E	$\rightarrow C_4H_2$	+ C_3H_3	1.50e+19	-0.5	0	1.50e+19	-0.5	0
$H_7C_7^+$	+	E	$\rightarrow C_6H_4$	+ CH_3	1.52e+19	-0.5	0	1.52e+19	-0.5	0
$C_8H_7^+$	+	E	$\rightarrow C_6H_6$	+ C_2H	1.61e+19	-0.5	0	1.61e+19	-0.5	0
$H_7C_9^+$	+	E	$\rightarrow C_8H_6$	+ CH	1.70e+19	-0.5	0	1.70e+19	-0.5	0
$C_{10}H_9^+$	+	E	$\rightarrow C_{10}H_8$	+ H	1.79e+19	-0.5	0	1.79e+19	-0.5	0
$C_{11}H_8H^+$	+	E	$\rightarrow C_{10}H_8$	+ CH	1.86e+19	-0.5	0	1.86e+19	-0.5	0
$C_{12}H_9^+$	+	E	$\rightarrow C_{12}H_8$	+ H	1.93e+19	-0.5	0	1.93e+19	-0.5	0
$C_{13}H_6H_3^+$	+	E	$\rightarrow C_{13}H_9$		1.99e+19	-0.5	0	1.99e+19	-0.5	0

TABLE II

COMPARISON OF BENZENE/OXYGEN FLAMES OBSERVED
AT AEROCHEM AND AT DARMSTADT

	AeroChem	Darmstadt
EQUIVALENCE RATIO	1.8, 2.0	1.9, 2.0
	+30 mol% argon	
UNBURNED GAS VELOCITY, cm s^{-1}	50	42
PRESSURE, kPa	2.67	2.67
THRESHOLD SOOT FORMATION, Φ	1.90	1.83
TEMPERATURE PEAK, K:	1900	2094
- at mm above burner	12.9	11.6
- for equivalence ratio	1.80	1.95

TABLE III

COMPARISON OF IONS OBSERVED IN ACETYLENE/OXYGEN AND
BENZENE/OXYGEN FLAMES AND IONS OBSERVED AT AEROCHEM
AND AT HOMANN'S LABORATORY IN DARMSTADT, GERMANY

ION MASS	ION FORMULA	ACETYLENE/OXYGEN		BENZENE/OXYGEN	
		AERO[a]	DARMS[b]	AERO[c]	DARMS[d]
19	H_3O^+			X	
24	C_2^+			X	X
31	CH_3O^+		X		
33	CH_5O^+		X		
39	$C_3H_3^+$	X	X	X	X
41	C_2HO			X	X
43	$C_2H_3O^+$		X	X	X
47	$C_2H_7O^+$		X		
49	C_4H^+				X
51	$C_4H_3^+$		X	X	X
53	$C_4H_5^+$	X	X	X	X
55	$C_3H_3O^+$		X		
57	$C_4H_9^+, C_3H_5O^+$			X	X
63	$C_5H_3^+$	X	X	X	X
65	$C_5H_5^+$		X	X	
67	$C_4H_3O^+$		X	X	X
69	$C_4H_5O^+$		X		
71	$C_3H_3^+ \cdot O_2$		X		
73	$C_6H^+, C_4H_9O^+$		X		X
75	$C_6H_3^+$		X	X	X
77	$C_6H_5^+$	X	X	X	

ION MASS	ION FORMULA	ACETYLENE/OXYGEN		BENZENE/OXYGEN	
		AERO[a]	DARMS[b]	AERO[c]	DARMS[d]
79	$C_6H_7^+$		X	X	X
81	$C_5H_5O^+$		X	X	X
83	$C_4H_3^+ \cdot O_2$		X		
85	$C_4H_5^+ \cdot O_2$		X		
87	$C_7H_3^+$		X	X	X
89	$C_7H_5^+$	X	X	X	
91	$C_7H_7^+$	X	X	X	X
95	$C_6H_7O^+, C_5H_3^+ \cdot O_2$		X	X	X
97	$C_8H^+, C_5H_5^+ \cdot O_2$		X		X
99	$C_8H_3^+$		X	X	X
103	$C_8H_7^+$	X	X	X	X
105	$C_7H_5O^+$		X	X	X
109	$C_7H_9O^+$		X	X	X
111	$C_9H_3^+, C_6H_7^+ \cdot O_2$		X	X	X
115	$C_9H_7^+$	X	X	X	X
117	$C_9H_9^+$			X	X
119	$C_8H_7O^+$		X	X	X
121	$C_8H_9O^+$			X	X
123	$C_8H_{11}O^+$		X	X	X
124	$C_8H_{12}O^+$			X	X
126	$C_{10}H_6^+$			X	X
129	$C_{10}H_9^+$	X	X	X	X
131	$C_9H_7O^+, C_{10}H_{11}^+$		X	X	X
133	$C_9H_9O^+$			X	X
135	$C_{11}H_3^+$		X		
139	$C_{11}H_7^+$		X	X	
141	$C_{11}H_9^+$	X	X	X	X

TP-531

ION MASS	ION FORMULA	ACETYLENE/OXYGEN		BENZENE/OXYGEN	
		AERO[a]	DARMS[b]	AERO[c]	DARMS[d]
143	$C_{10}H_7O^+$		X	X	X
145	$C_{10}H_9O^+$		X	X	X
147	$C_{12}H_3^+$		X		
152	$C_{12}H_8^+$			X	X
153	$C_{12}H_9^+$	X	X	X	
155	$C_{11}H_7O^+, C_{12}H_{11}^+$			X	X
157	$C_{11}H_9O^+$			X	X
159	$C_{13}H_3^+$		X		
165	$C_{13}H_9^+$	X	X	X	
169	$C_{12}H_9O^+$				X
170	$C_{12}H_{10}O^+$			X	X
171	$C_{14}H_3^+$		X		
177	$C_{14}H_9^+$		X	X	X
179	$C_{14}H_{11}^+$	X		X	
181	$C_{13}H_9O^+$			X	X
183	$C_{15}H_3^+$		X		
189	$C_{15}H_9^+$		X	X	X
191	$C_{15}H_{11}^+$	X	X	X	
192	$C_{14}H_8O^+$			X	X
193	$C_{14}H_9O^+$			X	X
203	$C_{16}H_{11}^+$	X	X	X	
204	$C_{15}H_8O^+$			X	X
205	$C_{15}H_9O^+$			X	X
215	$C_{17}H_{11}^+$	X	X	X	X
217	$C_{16}H_9O^+$			X	X
219	$C_{16}H_{11}O^+$			X	X
227	$C_{18}H_{11}^+$	X	X	X	X

22

ION MASS	ION FORMULA	ACETYLENE/OXYGEN		BENZENE/OXYGEN	
		AERO[a]	DARMS[b]	AERO[c]	DARMS[d]
228	$C_{17}H_8O^+$			X	X
231	$C_{17}H_{11}O^+$			X	X
239	$C_{19}H_{11}^+$	X	X	X	X
240	$C_{18}H_8O^+$			X	X
241	$C_{18}H_9O^+$			X	
243	$C_{18}H_{11}O^+$			X	X
250	$C_{20}H_{10}^+$		X		
251	$C_{20}H_{11}^+$	X	X	X	
253	$C_{19}H_9O^+$			X	X
255	$C_{19}H_{11}O^+$				X
263	$C_{21}H_{11}^+$	X	X	X	X
265	$C_{20}H_9O^+$, $C_{21}H_{13}^+$			X	X
267	$C_{20}H_{11}O^+$, $C_{21}H_{15}^+$				X
276	$C_{22}H_{12}^+$		X		
277	$C_{22}H_{13}^+$	X	X	X	
279	$C_{21}H_{11}O^+$, $C_{22}H_{15}^+$			X	X
287	$C_{23}H_{11}^+$		X		
289	$C_{23}H_{13}^+$	X		X	X
293	$C_{22}H_{13}O^+$			X	X
300	$C_{24}H_{12}^+$		X		
301	$C_{24}H_{13}^+$	X	X	X	X
303	$C_{23}H_{11}O^+$			X	X
313	$C_{25}H_{13}^+$	X	X	X	
317	$C_{24}H_{13}O^+$				X
324	$C_{26}H_{12}^+$		X		
325	$C_{26}H_{13}^+$	X	X	X	
329	$C_{25}H_{13}O^+$				X

ION MASS	ION FORMULA	ACETYLENE/OXYGEN		BENZENE/OXYGEN	
		AERO[a]	DARMS[b]	AERO[c]	DARMS[d]
337	$C_{27}H_{13}^+$	X	X	X	
341	$C_{26}H_{13}O^+$				X
348	$C_{28}H_{12}^+$		X		
349	$C_{28}H_{13}^+$		X		
350	$C_{28}H_{14}^+$		X		
351	$C_{28}H_{15}^+$		X	X	X
353	$C_{27}H_{13}O^+$				X
361	$C_{29}H_{13}^+$	X	X	X	X
363	$C_{28}H_{11}O^+$		X	X	X
365	$C_{28}H_{13}O^+$			X	X
374	$C_{30}H_{14}^+$		X		
375	$C_{30}H_{15}^+$	X		X	
377	$C_{29}H_{13}O^+$		X		X
385	$C_{31}H_{13}^+$		X		
386	$C_{31}H_{14}^+$			X	X
387	$C_{31}H_{15}^+$	X		X	
391	$C_{30}H_{15}O^+$				X
398	$C_{32}H_{14}^+$		X		
399	$C_{32}H_{15}^+$	X	X	X	
403	$C_{31}H_{15}O^+$				X
411	$C_{33}H_{15}^+$	X	X	X	X
415	$C_{32}H_{15}O^+$				X
422	$C_{34}H_{14}^+$		X		
423	$C_{34}H_{15}^+$	X	X	X	X
427	$C_{33}H_{15}O^+$				X
435	$C_{35}H_{15}^+$	X	X	X	X
439	$C_{34}H_{15}O^+$				X

ION MASS	ION FORMULA	ACETYLENE/OXYGEN		BENZENE/OXYGEN	
		AERO[a]	DARMS[b]	AERO[c]	DARMS[d]
446	$C_{36}H_{14}^{+}$		X		
447	$C_{36}H_{15}^{+}$	X	X	X	X
459	$C_{37}H_{15}^{+}$	X	X	X	X
470	$C_{38}H_{14}^{+}$		X		
471	$C_{38}H_{15}^{+}$	X	X	X	
472	$C_{38}H_{16}^{+}$		X		
473	$C_{38}H_{17}^{+}$			X	X
483	$C_{39}H_{15}^{+}$	X	X	X	X
495	$C_{40}H_{15}^{+}$		X	X	
497	$C_{40}H_{17}^{+}$	X			
506	$C_{41}H_{14}^{+}$			X	X
507	$C_{41}H_{15}^{+}$		X		
508	$C_{41}H_{16}^{+}$			X	X
509	$C_{41}H_{17}^{+}$	X		X	X
520	$C_{42}H_{16}^{+}$		X		
521	$C_{42}H_{17}^{+}$	X		X	X
533	$C_{43}H_{17}^{+}$	X	X	X	X
544	$C_{44}H_{16}^{+}$		X		
545	$C_{44}H_{17}^{+}$	X	X	X	X
557	$C_{45}H_{17}^{+}$	X	X	X	X
568	$C_{46}H_{16}^{+}$		X		
569	$C_{46}H_{17}^{+}$		X		
581	$C_{47}H_{17}^{+}$		X		

[a]AeroChem, Ref. 38, 40.
[b]Darmstadt, Refs. 27, 28, 39.
[c]Refs. 4, 41.
[d]Refs. 34, 35.

FIGURE 1 PAH ION DIAMETERS

PAH ion diameters calculated from experimental ion mobility (Langevin),
and spheres of density 1.5 cm^3 ($\rho=1.5$) and 2.0 cm^3 ($\rho=2.0$).

FIGURE 2 LOG$_{10}$ OF EQUILIBRIUM CONSTANT FOR SYSTEM
$C_3H_3^+(l) = C_3H_3^+(c)$.

94-34

FIGURE 3 COMPARISON OF EXPERIMENTAL $(EXP)_{maximum}$ AND CALCULATED $(CALC)_{maximum}$ CATION CONCENTRATIONS.

FIGURE 4 RATE OF DECAY OF NEUTRAL AND IONIC SPECIES CONCENTRATIONS IN ACETYLENE/OXYGEN FLAMES AT 2.67 kPa AND AN EQUIVALENCE RATIO OF 3.0

FIGURE 5 FREE ENERGY OF FORMATION PER CARBON ATOM FOR IONS,
FREE RADICALS AND MOLECULES AT 1000 K.

FIGURE 6 FREE ENERGY OF FORMATION PER CARBON ATOM FOR IONS,
FREE RADICALS AND MOLECULES AT 2000 K.

ION PROFILES THROUGH AN
ACETYLENE-OXYGEN FLAME AT 2.7 kPa

NEUTRAL PROFILES THROUGH A PROPANE-
OXYGEN FLAME at 15 kPa

from Bockhorn, Fetting and Wenz, Ber. Bunsenges.
Phys. Chem. 87:1067 (1983).

FIGURE 7 COMPARISON OF CHANGES IN CONCENTRATIONS OF IONS AND
NEUTRALS FOR TWO FLAMES NEAR SOOT THRESHOLD.

APPENDIX A

A DETAILED MODEL OF CATION GROWTH IN FLAMES[*]

H. F. Calcote, R. J. Gill
AeroChem Research Laboratories, Inc.
Princeton, NJ 08542-0012, USA

and

F. N. Egolfopoulos
Department of Mechanical Engineering
University of Southern California
Los Angeles, CA 90089-1453, USA

ABSTRACT

A detailed model of ion growth in the standard acetylene-oxygen premixed flat flame (equivalence ratio = 3.0, P = 2.67 kPa, u = 50 cm/s) was developed to model cation growth from $C_3H_3^+$ (mass 39 u) to $C_{13}H_9^+$ (165 u). The model included all observed ions and no ions were included which have not been measured. The reaction scheme included ion-molecule association reactions with neutral reactants (ie, H_2, C_2H_2, C_4H_2 and C_3H_4), ion-electron dissociative recombination, isomerization reactions and ambipolar diffusion. The Sandia Flame Code was modified to accommodate ionic reactions and non-Arrhenius rate coefficients for ion-molecule reactions. The calculated ion profiles were compared with the experimental ion profiles measured for the standard flame. In general, the calculated ion profiles were in good agreement with both the shape and the number density when compared to the experimental measurements.

INTRODUCTION

Very large ions have been observed in flames [1-4] and these have been associated with soot formation [5-6]. The source of these large ions has been debated by the combustion community and many schemes have been invented to explain their origin. These schemes range from thermal ionization of large polycyclic aromatic hydrocarbons [7] to thermal ionization of soot particles [8] and a kind of chemiionization of large PCAH [9,10]. All of these require that the charge be transferred from a larger moiety to a small moiety by charge transfer or ion-molecule reactions. This is contrary to thermodynamic expectations because the larger moiety is more stable than the smaller [11-14] so the reactions would be expected to progress from the smaller to the larger moiety. We have proposed that the large ions are derived from smaller ions by a series of ion-molecule reactions and that this growth of ions is an important mechanism in incipient soot formation [15,16]. The

---

[*]submitted to 25th International Symposium on Combustion, University of California, Irvine, CA, July 31 - August 5, 1994, November 1993.

A-1

initial ion is produced by chemiionization which is recognized as the source of highly non-equilibrium concentrations of small ions eg HCO^+ and $C_3H_3^+$ [6] and the $C_3H_3^+$ ion grows by rapid ion-molecule reactions to produce larger ions. Homann, in a recent paper [10] seems to have accepted the growth of ions as responsible for the large ions in flames.

The challenge was to develop a detailed quantitative mechanism which would account for the observed ions. This was not a straight forward problem because the necessary data bases were unavailable. Thus, for large ions at flame temperatures, the thermochemistry, ion-molecule reaction rate coefficients, ion-electron recombination coefficients, and ion and electron transport properties all had to be developed [11,17,18]. An additional complication was that a computer code to handle ions and to do some of the other tasks required to model an ionic mechanism was unavailable. Eraslan and Brown [19] had developed a code to handle ions but it lacked some of the capabilities which we needed for this study. The Sandia Flame Code was thus modified to include ionic reactions and to satisfy other requirements. When these components were developed, a reaction scheme was assembled to simulate ion growth from small chemiions to perinaphthenyl, $C_{13}H_6H_3^+$, mass 165 u in the standard acetylene/oxygen flame (ϕ=3.0, p=2.67 kPa, unburnt flow velocity=50 cm/s).

Clearly, where so much had to be done to compare experiment and theory, there remains much more to be done in terms of refinement (eg, Ref. 20). The objective of this work was to determine if it is feasible to model ion growth with a reasonable set of assumptions. If it is, then those assumptions will be refined to increase their scientific precision. If it is not possible to account for the large ions by the proposed mechanism, the challenge becomes greater because other mechanisms for large ion formation in flames have been rejected [6].

In this paper, the development of the necessary data bases, development of a detailed mechanism, modifications to the Sandia Flame Code, and a comparison of the mechanism with experimental data are briefly summarized. The details will be reported elsewhere [11,17,18].

THERMODYNAMICS

The major source of uncertainty in the kinetics model was the thermodynamics of cations. These uncertainties were manifest in the flame simulations where rates for reverse reactions were calculated from thermodynamics and forward reaction rate coefficients. The required thermodynamic data for the ions were either collected from the literature or calculated [11]. Available compilations of data for ions, e.g. Refs. 13, 21, 22, contained very few odd number carbon atom ions; experimentally these species dominate in the flame. The compilations included only a few isomers of which there can be many for each ion mass. Isomerization was included in the model as an elementary reaction step.

There were several neutral molecules for which the thermodynamic data are uncertain; for example, diacetylene. The available heats of formation for diacetylene at 298 K range from 439 to 473 kJ/mol. [24-28] We used 440 kJ/mol [24] because this value has been used previously in several thermochemical calculations with large ions. For a few cases, such as for the cyclopropenyl ion, there was sufficient experimental information to employ the more accurate statistical mechanical

methods to calculate C_p° and S°. It is difficult to assess the accuracy of the thermodynamic data for ions (or neutrals!) because experimental data on heat capacities and entropies, or equilibrium measurements, at flame temperatures are unavailable. The estimated errors in these quantities can be as large as 10% at 1500 K [29].
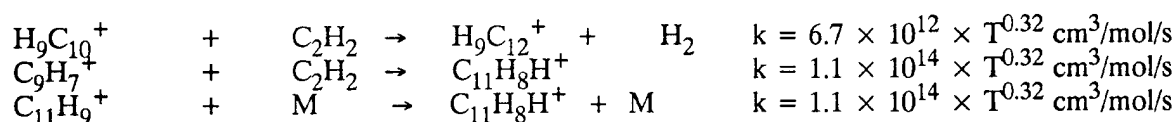
REACTION RATE COEFFICIENTS

Experimental rate coefficients for ion-molecule and ion-electron recombination reactions were available only for small ions near room temperature. It was thus necessary to estimate most of these coefficients.

A.   ION-MOLECULE REACTIONS

In general, experimental reaction rate coefficients are very close to the rate calculated by Langevin theory [30] which does not have a temperature coefficient for non-dipole molecules. Langevin theory accounts only for ion-molecule collisions and assumes all collisions lead to reaction. Langevin theory is substantiated by it's agreement with experiment. In the Langevin theory, the ion is treated as a point charge. This is certainly not true for large ions; even when the charge is localized, an approaching reactant will be shielded by the rest of the ion. We have thus extended the Langevin theory to include large ions, and this leads to a small positive temperature coefficient [18]. Inclusion of the extended Langevin theory made a negligible difference in the calculated ion profiles.

Ion-molecule reactions in our reaction scheme were written toward increasing molecular size; thus as the temperature is increases the free energy of reaction becomes more positive, due to entropy effects. To avoid excessively fast reverse reactions, forward reaction rate coefficients were adjusted so that the reverse reaction rate did not exceed the extended Langevin rate. One of the major problems in modeling large ion formation was structure identification; mass spectrometry gives mass only. The number of carbon and hydrogen atoms was determined by the use of isotopes [4] so the molecular formulas are well known. However, for a given molecular formula there can be several isomeric structures. Each of these was considered as a separate reactant/product entity. To avoid an overly complex mechanism, only the most stable structures were considered. To account for the fact that a Langevin ion complex may lead to several reaction products it was assumed, as a first order correction, that product branching was determined by the reaction free energy of that path. The set of 64 ion-molecule reactions used in this paper were chosen from a set of 192 reactions leading to $C_{13}H_6H_3^+$.

Typical reactions with their rate coefficients are:

$$H_9C_{10}^+ \quad + \quad C_2H_2 \rightarrow H_9C_{12}^+ + \quad H_2 \qquad k = 6.7 \times 10^{12} \times T^{0.32} \text{ cm}^3/\text{mol/s}$$
$$C_9H_7^+ \quad + \quad C_2H_2 \rightarrow C_{11}H_8H^+ \qquad\qquad k = 1.1 \times 10^{14} \times T^{0.32} \text{ cm}^3/\text{mol/s}$$
$$C_{11}H_9^+ \quad + \quad M \quad \rightarrow C_{11}H_8H^+ + M \qquad k = 1.1 \times 10^{14} \times T^{0.32} \text{ cm}^3/\text{mol/s}$$

The order of "C" and "H" in the ions was used to distinguish among the isomers in the model.

B. ION-ELECTRON RECOMBINATION

Ions disappear by either cation-electron or cation-anion recombination. Cation-anion recombination rate coefficients are about two orders of magnitude slower than cation-electron recombination rate coefficients. There are no good measurements of anion concentrations in sooting flames but there is evidence for their presence [32-34]. They have not been included in this mechanism; their inclusion could increase the cation concentrations but calculations indicated that they have little effect on the calculated ion profiles. In choosing product channels for large cation-electron dissociative recombination reactions, only molecules observed by Bockhorn et al.[35] were considered as products.

We estimate the rate of ion recombination, α, by the equation for the rate of collision of electrons with particles [36]:

$$\alpha \;=\; \frac{\pi d^2}{4} \left(\frac{8kT}{\pi m_e}\right)^{1/2} \left(1 + \frac{e^2}{(2\pi\epsilon_0 d)kT}\right) \tag{1}$$

in which d = ion diameter, m_e = electron mass, and ϵ_0 = dielectric constant of free space. Ion diameters were calculated from experimental ion mobilities by use of the Langevin equation for ion mobilities. Equation (1) gives a $T^{-1/2}$ temperature dependence which compares favorably with experiments of Ogram et al.[37] for H_3O^+. The values calculated by Eq. (1) were about twice the measured values of Ogram, so the calculated values were divided by 2. From Eq. 1, reaction rate coefficients increase with the size of the ion.

A typical dissociative recombination reaction and rate coefficient is:

$$C_{12}H_9^+ \;+\; e \;\rightarrow\; C_{12}H_8 \;+\; H \qquad \alpha = 1.0 \times 10^{20} \times T^{-0.5} \; cm^3/mol/s$$

REACTION MECHANISM

The ionic path starts with the chemiionization reaction:

$$CH^* \;+\; O \;\rightarrow\; HCO^+ \;+\; e$$

The chemiion HCO^+ (formyl cation) reacts in a series of ion-molecule reactions to produce $C_3H_3^+$, an ion observed in large concentrations in fuel rich flames. To minimize the number of reactions, only H_2, C_2H_2, C_4H_2 and C_3H_4 were considered as reactants with ions in the ion growth scheme. As ions grew, they were neutralized through ion-electron recombination reactions at rates which increase with increasing ion mass, producing neutral by-product polycyclic aromatic hydrocarbons.

In the kinetic scheme, experimental profiles for $C_3H_3^+$ (propargylium) and $H_5C_6^+$ (phenyl cation) were used because good experimental profiles for the HCO^+ ion were unavailable in fuel rich flames. When the concentration of $C_3H_3^+$ was calculated, using the neutral mechanism for soot

formation of Frenklach and Wang [20], chemiionization reactions to form HCO^+ and reactions to produce $C_3H_3^+$ from HCO^+, the calculated concentration was excessively greater than the experimental value.

How to handle $C_3H_3^+$ isomers was not clear. The ion has been identified in flames by mass spectrometry which provides no direct information on structure. Two isomers, the linear propargylium cation, $C_3H_3^+$, and the cyclic cyclopropenium cation, $H_3C_3^+$, have been considered as potentially important [38]. Calculations [39] show that the cyclic cation is more stable ($\Delta_f H$) than the linear cation by 116 kJ/mol; the experimental difference is 105 kJ/mol [40-41]. The difference in stability decreases with increasing temperature; based on experimental $\Delta_f H$'s, we estimate at 300K that ΔG(isomerization) = +99.4 kJ/mol, giving an equilibrium ratio of [linear]/[cyclic] = 5×10^{-18}, but at 2000 K the ratio is 0.03. It has been determined experimentally that at low temperatures the cyclic isomer is not reactive with acetylene or diacetylene, but the linear isomer is very reactive [42]. There is no evidence that the cyclopropenium cation isomerizes to the propargylium cation in the absence of encounter complexes with neutral molecules, e.g., acetylene.[39] Cameron et al.[39] have suggested that in sooting flames the linear isomer may be the most abundant. We have chosen in the mechanism to identify the linear $C_3H_3^+$ ion with the experimentally observed ion in the absence of evidence to the contrary.

In developing this mechanism only ionic species which have been observed in sooting flames have been included and all observed ions have been accounted for. This is a more stringent constraint than has been imposed on the free radical mechanism [20,43].

NUMERICAL METHODOLOGY

The numerical codes developed at Sandia National Laboratories by Kee and coworkers [44-46] were used as a starting point for modeling the ion growth. The one-dimensional flame code [44] was chosen because it has a very accurate and efficient integration routine, using a hybrid time-integration/Newton-iteration technique to solve the steady-state equations of mass and energy. For the kinetics calculations, the CHEMKIN-II code [45] was used, because it has capabilities for a variety of calculations during and after the solution of the problem, and it can be integrated very efficiently into the flame code. For transport property calculations, the code of Ref. 46 was used, because its validity has been tested by a variety of investigators and can be integrated efficiently into the flame code. Major modifications, however, were implemented into all three codes to allow for non-Arrhenius behavior of the ion kinetics, ambipolar diffusion coefficients, and to allow the user to input of species profiles obtained from experiments.

In the original flame code [44] there was provision for inputing the experimental temperature profile. This approach facilitates the calculations greatly because the need to model heat losses in the flat flame burner experiment is eliminated. The code was further modified to allow for the input of any number of species concentration profiles for which the code does not solve but simply sets their values to the input (experimental) values. This modification allows for the "isolation" of any part of the kinetic scheme so that uncertainties related to the chemistry of certain species do not affect conclusions about the chemistry of the species of interest. In the present study the purpose was to eliminate uncertainties related to the neutrals and selected ions. For the electrons, no

conservation equation was solved; their concentration was determined by balancing the electric charge between the electrons and ions. This is consistent with the assumption of ambipolar diffusion. The more exact method of solving ion diffusion (Poisson's equations) has been used by Eraslan and Brown [19].

The original CHEMKIN-II code [45] was modified to accept a three-parameter Arrhenius type expression for the elementary reactions:

$$k = AT^\beta \exp(-E_a/RT) + B \tag{2}$$

where B is a constant. This rate expression was used to fit rate data for ionic reactions which were non-Arrhenius.

The molecular transport code [46] was modified to use ambipolar diffusion coefficients for the ions. Specifically, the diffusion coefficient D_i of ion i in a gas is given by Einstein's relationship:

$$D_i = 2kT\mu_i/e \tag{3}$$

where k is the Boltzmann's constant, T is the temperature, μ_i is the ion mobility and e is the elementary charge. The ionic mobility, μ_j, at P_o = 2.67 kPa and T_o = 273 K was calculated [48] for each of the dominant neutral flame gases (j = neutral gas index) by first determining the coefficients, a_j and b_j, for each gas in the Langevin equation:

$$\mu_{ij}(P_o, T_o) = a_j \times MW_i^{b_j} \quad cm^2 V^{-1} s^{-1} \tag{4}$$

by fitting this to experimental values of PCAH ion diffusion [49-51] MW_i is the mass of the ith ion. The coefficients are:

Gas	a	b	r^2
H_2	3472	-0.499	0.998
O_2	743	-0.487	0.998
CO_2	493	-0.464	0.998
C_2H_2	473	-0.434	0.999
CO	688	-0.472	0.998
H_2O	761	-0.465	0.998

where r^2 is the coefficient of determination of the fit to the actual data.

The ion mobilities calculated above, were corrected to flame pressures and temperatures, by the following formula (except for water), where P is the flame pressure (kPa) and T is the local temperature:

$$\mu_{ij}(P,T) = (P_o/P) \times (T_o/T)^{0.72} \times \mu_{ij}(P_o,T_o) \tag{5}$$

For water vapor:

$$\mu_{i,H_2O}(P,T) = (P_o/P) \times (T/T_o)^{1.16} \times \mu_{i,H_2O}(P_o,T_o) \tag{6}$$

The ion mobility in the gas mixture was calculated by:

$$\mu_i^{-1} = \sum X_j/\mu_{ij} \tag{7}$$

where X_j is the mole fraction of gas j in the flame.

RESULTS AND COMPARISON WITH EXPERIMENTS

A comparison of the calculated with the experimental ion concentration profiles [4] for the standard acetylene/oxygen flame (equivalence ratio = 3.0, P = 2.67 kPa, unburned gas velocity = U_o = 50 cm/s) is shown in Fig. 1, and a comparison between the maximum calculated and experimental ion concentrations is shown in Fig. 2. The experimental profile of the propargylium and phenyl cations and all neutral species involved in the ionic mechanism (ie, acetylene, diacetylene, allene and hydrogen) were input profiles. Because the ion growth paths seemed to run parallel for even and odd numbers of carbon atoms, and generally independent of one another, it was necessary to use both an odd and an even numbered carbon cation as input ions. Cation reactions with C_3H_4 couple the odd and even ion growth pathways; but there were few such reactions in this model.

The experimental temperature profile was input to the model to avoid the necessity of heat transfer calculations. Temperature was an unexpectedly important parameter and to obtain reasonable results, the experimental temperature profile was reduced linearly by 0% at the burner surface to 10% at the temperature maxima. The reduced maximum flame temperature was 1818 K. Thermodynamic equilibrium had a much greater effect on the ion-molecule reactions than expected (the reverse reaction rates were calculated from forward rates and equilibrium constants); this showed up as a very strong temperature dependence for ion concentrations. At higher temperatures ion-molecule reverse reactions became more important because entropy effects increase with increasing temperature. This same effect, of course, controls neutral mechanisms as well and may very well explain the high temperature portion of the bell shaped curve for soot formation between about 1400 and 1900 K. The entropy effect is a more probable explanation of the bell shaped curve than the explanation based on the increased rate of soot oxidation with temperature [52]. A number of isomers were included in the calculations, but only the most abundant calculated cation isomer for any ion mass is plotted in Figs 1 and 2; the mass spectrometer is blind to isomeric structure. It is, of course, conceivable that the most thermodynamically stable isomer is not formed because of reaction kinetic restrictions. This may increase or decrease the agreement with experiment.

For most of the ions the calculated and experimental profiles were in agreement within the accuracy of the data. The ion most out of agreement in the initial calculation was $C_{11}H_8H^+$

(isomers are distinguished by the order of C and H) which led to large discrepancies for $C_{12}H_9^+$ and $C_{13}H_6H_3^+$. The measured value for $C_{11}H_8H^+$ exceeded the calculated value by three orders of magnitude. Reduction in the heat of formation of $C_{11}H_8H^+$ by 10% gave the agreement reported in Figs. 1 and 2.

Of concern is the fact that some of the calculated concentration profiles show an increase as the burner is approached. Double cation peaks have been observed experimentally and it is not clear whether these are related or not. The calculated ion concentration increase toward the burner is due to too a large temperature effect and the use of a flame temperature profile that is not accurate near the burner surface. This situation could be corrected by modifying the input temperature profile even more than we have already done.

To better evaluate the agreement between experimental and calculated concentrations, the maximum concentration ratios, $\log_{10}$ (experimental concentration/calculated concentration) are presented in Fig. 2. The isomer which had the highest calculated concentration is compared with the experimental data. In general, calculated concentrations are within a decade of the experimental data. The source of the original disagreement with the $C_{11}H_8H^+$ cation has been considered by carefully reviewing the thermodynamics, including the possibility of other more stable isomers, without arriving at a better solution than reducing the Δ_fH by 10%. It appears that there is little latitude for adjusting the rate coefficients. The experimental results could be called into question, but the major error is probably in the thermodynamics. This will be pursued further as we extend the model to larger ions; development of the thermodynamics and reaction kinetics for larger ions has already been completed.

The major ion growth paths (Fig. 3) were identified by integrating ion fluxes over the distance grid. This flow diagram shows the weak coupling between the odd and even ion growth paths in this model.

Oxidation of ions has yet to be added to the mechanism. Unlike the neutral mechanism, wherein oxidation removes the neutral growth species from the growth chain, for ions, oxidation simply removes carbon atoms from the ion, making a smaller ion, or removes hydrogen from the growing ion at a greater rate. Removal of hydrogen may in fact contribute to ion growth toward soot which has a C/H ratio of about 10, while for the largest ion treated here the ratio is only 1.4. Since the ions considered in the model have a decreasing free energy per carbon atom with increasing size [53], it is assumed that the charge will remain on the larger hydrocarbon products, thus e.g.:

$$C_{13}H_9^+ \; + \; OH \; \rightarrow \; C_{13}H_8^+ \; + \; H_2O$$

would be expected to occur, rather than:

$$C_{13}H_9^+ \; + \; OH \; \rightarrow \; C_{13}H_7 \; + \; H_3O^+$$

This of course requires further consideration with other oxidizers and other products.

SUMMARY AND CONCLUSIONS

The current model of ion-growth correctly predicts both the shape of the ion profiles and the magnitude of the ion concentrations. Although, adjustments in the temperature profile (10%) and the enthalpy of formation of the $C_{11}H_8H^+$ ion (10%) were used to obtain closer agreement with experiment, the results were very encouraging for such a simple model. The changes in the mechanism are physically reasonable, considering the uncertainties in the thermodynamics and temperature measurements.

ACKNOWLEDGEMENTS

REFERENCES

1. Michaud, P., Delfau, J.L., and Barassin, A., Eighteenth Symposium (International) on Combustion (The Combustion Institute, Pittsburgh, 1981), pp. 443-451.

2. Gerhardt, Ph., and Homann, K.H., J. Phys. Chem. 94, 5381-5391 (1990).

3. Olson, D.B., and Calcote, H.F., Eighteenth Symposium (International) on Combustion (The Combustion Institute, Pittsburgh, 1981), pp. 453-464.

4. Calcote, H.F., and Keil, D.G., Combust. Flame 74, 131-146(1988).

5. Prado, G.P., and Howard, J.B., "Formation of Large Hydrocarbon Ions in Sooting Flames," Chap. 10 in Evaporation - Combustion of Fuels, Ed. Joseph T. Zung (Advances in Chemistry Series No. 166, American Chemical Society, Washington, D.C. 1978).

6. Calcote, H.F., Olson, D.B., and Kiel, D.G., Energy & Fuels 2, 494-504 (1988).

7. Delfau, J.L., Michaud, P., and Barassin, A., Combust. Sci. Technol. 20, 165-177 (1979).

8. Homann, K.H., Ber. Bunsenges. Phys. Chem. 83, 738 (1979).

9. Homann, K.H., and Ströfer, E., "Charged Soot Particles in Unseeded and Seeded Flames," in Soot in Combustion Systems and its Toxic Properties, ed. J. Lahaye and G. Prado (Plenum

Press, NY, 1983).

10.   Wegert, R., Wiese, W., and Homann, K.H., Comb. Flame 95, 61 (1993).

11.   Gill, R.J., and Calcote, H.F., "Thermodynamic Properties of Organic Cations," submitted to J. Phys. Chem. Ref. Data.

12.   Stein, S.E., and Kafafi, S.A., <u>Abstracts of the Eastern Section, Twentieth Fall Technical Meeting of The Combustion Institute</u> (The Combustion Institute, Pittsburgh, Nov. 2-5, 1987) pg. A-1.

13.   Lias, S.G., Bartmess, J.E., Liebman, J.F., Holmes, J.L., Levin, R.D. and Mallard, W.G., J. Phys. Chem. Ref. Data 17, Suppl. 1 (1988).

14.   Stein, S.E., Combust. Flame 51, 357-364 (1983).

15.   Calcote, H.F., Combust. Flame 42, 215-242 (1981).

16.   Calcote, H.F., and Keil, D.G., Pure Appl. Chem. 62, 815-824 (1990).

17.   Calcote, H.F., and Gill, R.J. "Ion-Molecule Kinetic Modeling of Soot Formation," in preparation.

18.   Berman, C.H., and Calcote, H.F. "Extended Langevin Theory," in preparation.

19.   Eraslan, A.N. and Brown, R.C., Combust. Flame 74, 19-37 (1988).

20.   Wang, H., Weiner, B., and Frenklach, M., J. Phys. Chem. 97, 10364-10371 (1993).

21.   Rosenstock, H.M., Draxl, K., Steiner, B.W., and Herron, J.T., J. Phys. Chem. Ref. Data 6, Suppl. 1 (1977).

22.   Levin R.D. and Lias, S.G., "Ionization Potential and Appearance Measurements, 1971-1981," NSRDS-NBS 71 (1982).

24.   Stein, S.E., and Fahr, A., J. Phys. Chem. 89, 3714-3725 (1985).

25.   Benson, S.W., and Garland, L.J., J. Phys. Chem. 95, 4915-4918 (1991).

26.   Bittner, J.D., and Howard, J.B., <u>Nineteenth Symposium (International) on Combustion</u> (The Combustion Institute, Pittsburgh, 1982), p. 211-

27.   Deakyne, C.A., Meot-Ner, M., Buckley, T.J., and Metz, R., J. Chem. Phys. 86, 2334- (1987).

28.   Stull, D.R., Westrum, E.F., and Sinke, G.C., <u>The Chemical Thermodynamics of Organic</u>

Compounds (Wiley, New York, 1969).

29.   Conversation with Dr. R.C. Wilhoit of The Thermodynamic Research Center (College Station, TX) July 1, 1993.

30.   Gioumousis, G. and Stevenson, D.P., J. Chem. Phys. 29, 294 (1958).

32.   Keil, D.G., Gill, R.J., Olson, D.B., and Calcote, H.F., Twentieth Symposium (International) on Combustion (The Combustion Institute, Pittsburgh, 1984) p. 1129-1137.

33.   Homann, K.H. and Stroefer, E., "Charged Soot Particles in Unseeded and Seeded Flames," in Soot in Combustion Systems, J. Lahaye and G. Prado, Eds. (Plenum Press, New York, 1981) p. 217.

34.   Gerhardt, P. and Homann, K.H., Combust. Flame 81, 289-303 (1990).

35.   Bockhorn, H., Fettig, F., and Wenz, H.W., Ber. Bunsenges. Phys. Chem. 87, 1067 (1983).

36.   Sodha, M.S., and Guha, S., Adv. Plasma Phys. 4, 219 (1971).

37.   Ogram, G.L., Chang, J.-S., and Hobson, R.M., Phys. rev. 21, 982 (1980).

38.   for example see; Eyler, J.R., Oddershede, J., Sabin, J.R., Diercksen, G.H.F. and Grüner, N.E., J. Phys. Chem. 88, 3121-3123 (1984).

39.   Cameron, A., Leszczynski, J., Zerner, M.C., and Weiner, B., J. Phys. Chem. 93, 139 (1989).

40.   Lossing, F.P., Can. J. Chem. 50, 3973 (1972).

41.   Sen Sharma, D.K. and Franklin, J.L., J. Amer. Che. Soc. 95, 6562-6566 (1973).

42.   Ozturk, F., Baykut, G., Moini, M. and Eyler, J.R., J. Phys. Chem. 91, 4360 (1987).

43.   Frenklach, M. and Warnatz, J., Combust. Sci. Technol. 51, 265-283 (1987).

44.   Kee, R.J., Grear, J.F., Smooke, M.D., and Miller, J.A., "A Fortran Program for Modeling Steady Laminar One-Dimensional Premixed Flames," Sandia Report, SAND85-8240, 1985.

45.   Kee, R.J., Rupley, F.M., and Miller, J.A., "Chemkin-II: A Fortran Chemical Kinetics Package for the Analysis of Gas-Phase Chemical Kinetics," Sandia Report SAND89-8009, 1989.

46.   Kee, R.J., Warnatz, J., and Miller, J.A., "A FORTRAN Computer Code Package for the Evaluation of Gas-Phase Viscosities, Conductivities, and Diffusion Coefficients," Sandia Report SAND83-8209, 1983.

47. Harmony, M.D., Laurie, V.W., Kuczkowski, R.L., Schwendeman, R.H., Ramsay, D.A., Lovas, F.J., Lafferty, W.L., and Maki, A.G., J. Phys. Chem. Ref. Data $\underline{8}$, 619 (1979).

48. McDaniels, E.W., Collision Phenomena in Ionized Gases (Wiley, New York, 1964) pp. 432-433.

49. Lin, S.N., Griffin, G.W., Horning, E.C., and Wentworth, W.E., J. Chem. Phys. $\underline{60}$, 4994 (1974).

50. Griffin, G.W., Dzidic, I., Carroll, D.I., Stillwell, R.N., and Horning, E.C., Anal. Chem. $\underline{45}$, 1204 (1973).

51. Hagen, D.F., Anal. Chem. $\underline{51}$, 870 (1980).

52. Glassman, I., Twenty-Second Symposium (International) on Combustion (The Combustion Institute, Pittsburgh, 1988) pp. 295-311.

53. Calcote, H.F., "The Role of Ions in Soot Formation," presented at International Workshop, Mechanisms and Models of Soot Formation, Ruprecht-Karls-Universitat, Heidelberg, Germany, 29 September–2 October 1991. To be published by Springer-Verlag.

FIGURE CAPTIONS

Fig. 1.   Calculated (solid lines) and Experimental (dashed lines) Ion Concentration Profiles for Ions up to Mass 165 u.

Fig. 2.   Horizontal Bar Graph of Log_{10} (Maximum Experimental Concentration / Maximum Calculated Concentration) for Cation Isomers having the Highest Calculated Concentration.

Fig. 3.   Ion Flow Diagram Based on Integrated Flux (over Calculation Distance Grid) for Even and Odd Cations.

Fig 1

A-14

93-23b

$C_5H_2H^+$
$C_7H_4H^+$
$C_7H_7^+$
$C_8H_7^+$
$H_7C_9^+$
$C_{10}H_9^+$
$C_{11}H_8H^+$
$C_{12}H_9^+$
$C_{13}H_6H_3^+$

-1   0   1   2

LOG_{10} (EXPTL. CONC./CALC. CONC.)

Fig 2

A-15

-C4H2

C3H3+   H5C6+

C5H2H+ ← C5H5+   C8H7+

-H2

C7H4H+   C7H7+   C10H9+

-C4H2

H7C7+   C12H9+

H7C9+

LARGER EVEN
CARBON IONS

C11H8H+

C13H6H3+

LARGER ODD
CARBON IONS

Fig 3

A-16

APPENDIX A

REVIEWER A, No. 362

There is much of interest in this paper but, overall, not enough new or definitive material for me to be sure that the paper should be accepted for the Symposium. The authors have something of a dilemma in trying to describe their approach to the reaction-kinetic modelling, as well as presenting a meaningful analysis of the results, within the constraints of a Symposium submission - unfortunately, on neither front does the paper succeed in reaching the standard required. **1**

Successes in the modelling of neutral chemistry in combustion systems have relied heavily on the use of sensitivity analysis, in order that the overall model can be see in terms of its most crucial parameters. It is one of the deficiencies of this paper that there is no coherent approach to parameter evaluation, with parameters being adjusted on a more or less *ad hoc* basis to achieve desired results. A case in point is the adjustment of the ΔH°_f for $C_{11}H_8H^-$. The enormous sensitivity of ion concentrations to heats of formation was shown previously by Eraslan and Brown (Ref. 19) and one can expect a more quantitative assessment here. **2**

Thermochemistry also appears in some other issues. Forward rate constants have apparently been adjusted so that the reverse rate calculated from the equilibrium constant is not "too fast" to be consistent with calculated rates, but the same theory has been used to estimate the forward rates in the first place. The alternative of adjusting the thermochemical data is not discussed. A clear hierarchy needs to be established here because it is not clear that the estimation of the thermochemical data is in effect any more reliable than the estimation of rate constants in this system. **3**

A substantial part of the text is devoted to describing how ambipolar diffusion coefficients have been estimated. Eraslan and Brown (Ref. 19) argued that it was not necessay to allow for ambipolar diffusion and the authors' earlier work (Ref 4.) shows no evidence to the contrary. At the very least, the present Discussion should include some comments and results from the present modelling on this issue. **4**

The input temperature profile is another (distributed) parameter which needs to be assessed more rigorously. The authors have adjusted the profile in one part of the flame in order to obtain a better fit with the chosen data set. Without a more detailed evaluation of the sensitivity coefficients for important factors such as thermochemical and kinetic parameters, it is possible to evaluate what is actually being achieved by this manipulation other than curve-fitting. This is particularly so when one considers that the maximum temperature reported for the Aerochem burner was already 100K lower than others had obtained (see Ref. 4) and further downward adjustment seems contrary to the weight of experimental evidence. **5** **5a**

There is no way that anyone reading this paper could ever duplicate the modelling which has been reported as mechanism and thermochemistry are not reported in full. Nor is there any comparison with the modelling undertaken by Eraslan and Brown (Ref. 19) in terms of the mathematical procedures, the reaction mechanism, or the results. While I look forward to future work by the authors, the present paper really only whets the appetite. **6** **7**

This work deals with the question whether one can characterize soot formation as a non-equilibrium process, with respect to the equilibrium concentrations of acetylene (a potential reactant) and of soot (the product), as compared to the experimental C_2H_2 and soot concentrations. Although one knows that soot formation is kinetically controlled and not thermodynamically, it is useful to learn from the figures how large the discrepancies are.

However, the paper suffers from the fact that the results of complicated quantitative equilibrium calculations, which cannot be reproduced by the reader, are mixed with very qualitative concepts such as 'driving force'. Deviations from equilibrium for characteristic reactions could have been expressed in terms of thermodynamic affinities, so that the reader gets a more quantitative idea, how far from equilibrium some important reactions are. From the figures, one only gets the impression, that the real 'flame world' and the equilibrium state occupy areas in the diagrams, which are at quite a distance from each other. The authors speak of 'driving force' through supra-equilibrium concentrations of H and ions. In chemical thermodynamics 'driving force' can be quantified by *affinity* (de Donder) which is defined for one stoichiometric equation as $-\Sigma v_i \mu_i$. In an ideal system $\mu_i = \mu_i^c + RT \ln c_i$. Through this the 'driving force' is coupled to concentrations. Now, the concentration of H is many orders of magnitude greater than that of ions. Would the authors comment on the absolute values of these driving forces ?

1
2
3
4

Extended equilibrium calculations have been performed. However, the equilibrated reactions considered are not given, only a number of species. It does not become clear, what reaction is considered, for example, for circumcoronene. Is it 9 H_2 + 54 C(Graphite) or + 54 C(Soot) = $C_{54}H_{18}$? The same applies for other species.

5

There are other shortcomings and non-adequate formulations which the authors might consider, in order not to convey the impression that they are going to oversimplify things. For example:

They say that the only flame property that changes at the soot threshold is the ionic character. This statement is far too simple and because of its simplicity it is not correct. There are a great number of properties concerning flame structure and composition that change, although gradually.

6

Introduction, line 5 from below: The presence of anions is not only indicated by a change in the measured ion recombination coefficient. From mass spectrometry of flame ions one knows exactly what kinds of negative ions are present for different fuels when soot formation starts in a premixed flame.

7

It should not only be justified by quotations (36, 37) but discussed by the authors why they hold a super-equilibrium concentration of H to be a 'driving force' for soot formation. There are a number of observations of a presumed influence of H on the formation of benzene, PAH and soot. But the results are not conclusive and there seems to be a strong influence of temperature.

8

P. 11, line 11. What is the meaning of the statement 'Only one ion is required per soot particle'. Required for what ? If it shall be expressed that one positive charge is required on the soot particle for its existence as a charged species, it is trivial. But I presume that the authors do not have this in mind.

9

Some further comments and recommendations:

Introduction, p.4, line 6: What is meant by the statement, that charge is 'transferred from a larger moiety to a small moiety by charge transfer or ion-molecule reactions' ? What is the exact meaning of 'moiety' in this context ?   **10**

Homann is not correctly quoted by reference [10], since that paper deals with the growth of charged soot particles and not with the growth of small molecular ions to larger ions.   **11**

The name perinaphthenyl is not a IUPAC name for any $C_{13}H_9^{\cdot}$. There are several possible structures for this molecular formular. What structure is indicated by the formula $C_{13}H_6H_3^{\cdot}$?   **12**

P. 7, line 14: In which way were isomers distinguished by the order of "C" and "H" in the formulas ?   **13**

The experimental profiles of $C_3H_3^+$ and of the phenyl ion, which have been put into the calculations, should also be given in fig. 1.   **14**

REVIEWER C, No. 331

3. The abstract should mention that ion profiles were computed with temperature and other species profiles imposed from the experiment. It should qualify that the temperature profile was also reduced to improve the comparison, since by the authors' admission this was unexpected.   **1**

5. The model is new and its verification is limited; it may be prudent to delay this paper's publication. The modifications to Sandia's flame code seem reasonable, yet critical reviews of the extensions of thermodynamic properties and Langevin theory have not been completed; they are referenced as "submitted" or "in preparation." The accuracy of the predictions of ion profiles in this one flame may be promising, but many questions remain.   **2**   **3**   **4**

The proposed mechanism starts with chemiionization to form HCO+, eventually producing C3H3+ by a series of reactions; further cation growth proceeds by the mechanism in fig. 3. However, the present results skip this initiation, using the experimental profile of C3H3+ directly, because HCO+ data were not available, and including the proposed initiation steps produced "excessive" concentrations. This leaves the initiation of the proposed mechanism in doubt. It seems that several adjustments were involved in producing the agreement in fig. 1. It is not obvious why a factor of 2 is necessary in the electron collision rate. In addition, the experimental temperature profile and the enthalpy of formation of one ion were adjusted by 10% to improve the agreement. The need to reduce the flame temperature was "unexpected" and is a concern, yet there is no real discussion of why this is reasonable (experimental accuracy?) or how sensitive the predictions are to the temperature profile.   **5**   **6**   **7**   **8**

Given these concerns, I hesitate to judge the predictions accurate, or the proposed mechanism ready for acceptance.

9

9. The authors should be able to address the questions regarding some of their parameter adjustments. However, justification of skipping the initiation steps will take more effort. In any case, this work is relevant, and further effort will surely make this a fine paper.

10

RESPONSE TO REVIEWERS' COMMENTS

The reviewer is identified by letter on his review copy and the reviewer's comment is identified by a number on the right of the review. References numbers refer to references in subject paper.

Reviewer A, No. 362

1. This material has not been previously published.

2. Sensitivity analysis takes many forms, from formal mathematical treatments to inspection of how specific changes affect the result. We used the latter. That is the means by which we determined the desirability of adjusting the temperature profile and $\Delta_f H$ for one ion. Paper length limitations do not allow presentation of the many versions of the model tested in arriving at the mechanism.

3. Equilibrium is determined by the relative forward and reverse rates. The exothermic ion-molecule reactions are assumed to have no activation energies, consistent with experimental data on small ions. The adjustment is a means of determining the rate for the forward reaction when the reverse reaction has a negative ΔG at flame temperatures. It is standard procedure to calculate a rate coefficient from the reverse rate coefficient and the equilibrium constant. It is treated a little differently for ion-molecule reactions where the temperature effect is non-Arrhenius. If this were not done some rates would exceed collision rates. The question of hierarchy does not arise, this correction must be done - it is not arbitrary as assumed by the reviewer.

4. Eraslan and Brown do not argue against the need for ambipolar diffusion, they treat it in a more exact way, by the use of Poisson's equations. Ambipolar diffusion, or a more exact treatment as used by Eraslan and Brown, must be included for a neutral plasma made up of cations and electrons. It accounts for the difference in diffusion coefficients of electrons and cations and the interaction of the electric field produced by the diffusion of the two charges (positive and negative). It makes a small difference whether one uses the treatment of Eraslan and Brown or ambipolar diffusion, and neither makes a significant difference in this particular modeling result. The authors earlier work shows the importance of ambipolar diffusion in flames [Eighth Symposium on Combustion, 1962, pg 184].

5. Adjustment of the temperature profile was made only after consideration of the sensitivity to thermodynamic and reaction kinetics. The need for this adjustment is of some concern to the authors. See the Introduction for the philosophy of our approach. The maximum temperature for the data under discussion was the temperature AeroChem measured on the MIT burner and is not already 100 K lower than reported by others [see Ref. 4 of the paper]. The reason for the differences in temperatures reported in Ref. 4 are well known - see Ref. 4.

5a. Modeling often reduces to curve fitting, it is a very powerful analytical tool.

6. Symposium restrictions do not permit reporting thermochemistry in full (this is an extensive paper which stands alone), nor is it normal practice to report complete thermochemistry data with kinetic mechanisms. The equations, with a condensed mechanism, is equivalent to reporting the complete mechanism.

7. Symposium restrictions do not permit the paper length which would be required to compare the modeling and mathematical procedures used here with those of Eraslan and Brown for non-sooting flames, nor would it be appropriate, or useful.

Reviewer B, No. 428

1. The Sandia flame code is a well established code for this kind of work. The question of "how the rate constants describe the neutral structure is not germane because we start with two known ion profiles to avoid the complexity of the neutral chemistry. As pointed out, page 4, the neutral chemistry as used by Frenklach over-estimates the neutral radical concentrations and thus the initial chemiion, HCO^+, concentration. That is one of the reasons we start with experimental cation profiles. When the ionic mechanism is demonstrated to be adequate for a number of different flames, we will consider a neutral mechanism to produce chemiions. Brown and associates have done it for non-sooting flames.

2. There is an extensive set of experimental data on this flame obtained in a number of different laboratories. We know of no other such well documented flame.

3. H_2, C_2H_2, C_4H_2, and C_3H_4, see text, page 4 bottom.

4. Some examples are given on page 3, space limitation prevents presentation of the complete reaction scheme, but the equations should permit one to calculate them and compare them with the examples given. The thermochemistry is of course required, our program uses the complete JANNAF tables plus a very

large number of ions for which we developed the data. We will be delighted to furnish a copy to anyone interested prior to publication.

5. All observed ions in the flame under study are in the mechanism and protonated polyynes have been handled the same as any other ion, we have not checked to see if they are in equilibrium or not. We are not as sure as the reviewer that their equilibrium is "well established". Michaud, et.al. (1981) assumed equilibrium to calculate equilibrium constants, and I am not aware that Homann, et.al. (e.g., 1990), who observe more polyynes than we do, ever demonstrated they are in equilibrium - they also assumed equilibrium. The calculated concentration profile for $C_5H_3^+$ is about 10^9 times in excess of the equilibrium value. This is typical of all flame ions, and is explained by the now well established phenomenon of chemiionization.

6. Proton transfer reactions have not been included in this kinetic scheme to date. Their contribution appears to be small because of the low concentration of large neutral species.

7. The source of all ions is the initial chemiionization step which produces an electron for each cation. Dissociative recombination eliminates one of each unless the electron is attached to an entity to produce an anion and then recombination removes both a cation and an anion from the system. As a simplification, the program assumes an equal number of electrons as cations. This is a programmers means of producing an electron every time a cation is produced and removing an electron every time a cation is removed. This procedure maintains internal consistency.

8. In our flux analyses, we have not concentrated on answering this question. Obviously, if we travel with a gas volume leaving the burner surface and moving through the flame front, ion concentration will rise and fall as the net rate of production of an ion increases and then declines.

9. This is not an extended abstract of a paper published or to be published elsewhere, but is obviously a condensation of a large amount of work. Separate papers will be published on the thermochemistry, kinetics, and extension of Langevin theory, as is appropriate.

10. Moiety is misused in this text and can be replaced by "species". This statement describes how one would have to interpret Homann's thesis that the observed (small) ions are produced from the ionization of particles or large molecules. The meaning is that, for a large ion to produce a small ion, either simple charge transfer (an elementary ion-molecule reaction) or transfer of a charged fragment (moiety) by an ion-molecule reaction must occur between the large ion or charged particle and a small neutral species.

11. The processes are related in terms of the source of the charge on particles. Homann, in the past, has rejected conventional chemiionization processes as the source of this charge, although he has proposed different chemiionization processes for which there is absolutely no evidence (see e.g., Ref. 10, page 72, last left column paragraph). The first reference, Ref. 9, to Homann is for this paragraph and the second reference is to demonstrate Homann's recognition of the importance of chemiions, "- - - it is approached from the ionic rather than the neutral side." The reviewer might appreciate this point more by reading Ref. 6 of the submission, especially page 497, left column. Reference could be left out, it may be too subtle.

12. Perinaphthenyl is the name used by Stein, U.S. NIST, and other U.S. authorities, e.g., Kebarle. It is a reference to the three fused six- membered aromatic rings. A number of isomers of this ion have been considered.

13. Arbitrary, what else would be possible? It turns out in practice that the simplest relationships e.g., $C_{13}H_9$, H_9C_{13} to more complex relationships $C_{13}H_7H_2$ are determined by the order in which we identified the isomer. We will help the reader by naming them on the figure. We use this relationship to communicate with the computer program. For our data base we use a number in parenthesis following the usual order of symbols; the computer program does not recognize this.

14. Reasonable suggestion. We were trying to simplify what is an already complex figure.

Reviewer C, No. 331

1. We agree.

2. It is the nature of all new works to require further testing.

3. Correct, but we believe that this work stands sufficiently alone to be published, and is of sufficient importance.

4. A very large number of questions remain, which should not be surprising since this represents a major step toward the solution of a problem for which the thermochemistry and reaction kinetics were all missing when we started. Many questions still remain in the neutral proposed mechanisms of soot formation, after considerably more effort by a far larger number of people. As an example, it is still debated in the literature how benzene is formed in the neutral/free radical models.

5. The proposed mechanism that is in doubt is that part of the neutral mechanism required to produce the reactants for chemiionization, these were taken from Frenklach's neutral mechanism of soot formation. The indication is that the

reactions in the neutral mechanism are too fast. Our objective is to examine the ionic growth mechanism unencumbered by idiosyncrasies in the neutral mechanisms, so we modified the Sandia program to avoid involvement in the same mechanism everyone else is working on. Hopefully, by the time we need the neutral mechanism to complete our model, the folks working on it will have reached some kind of consensus.

6. It is valid procedure to make reasonable adjustments, see e.g., Gardiner, *J. Phys. Chem.* <u>83</u>, 37 (1979).

7. As stated, to reconcile theory with experiment. This was not an adjustment to fit the model to experiment, as the reviewer seems to think, but a means of developing a reliable data base. Incidentally our sensitivity analysis showed very little sensitivity to the recombination rate of ions with electrons.

8. Modeling is a process by which one adjusts parameters within reason to fit experiments in order to better understand the phenomena. Fitting only two parameters to obtain such good agreement is very encouraging. It should be rated as "excellent" when compared to the agreement reported for neutral models of soot nucleation where it is common practice to include species in the mechanism that are not observed in the flame and where some of the major products which are observed are not predicted. We are concerned about the temperature correction and are trying to understand why it was necessary, or whether it is really necessary.

9. Neither would we propose the mechanism as "ready for acceptance". It would be inappropriate to propose any current mechanism of soot formation as "ready for acceptance" while there is so much disagreement on some of the most elementary aspects of the problem. Presumably we will continue to improve the model as we extend it to large ions and to other flames. How much of the published work on combustion does the reviewer rate as "ready for acceptance"?

10. The initial steps are a problem all to themselves as we described above and will be addressed in a separate paper; they have no relevance to the growth process, so long as there is a starting point for the growth process - which we have taken as $C_3H_3^+$ and $H_5C_6^+$ profiles.

APPENDIX B

THERMODYNAMIC CONSIDERATIONS OF SOOT FORMATION[*]

H. F. CALCOTE AND D. G. KEIL

AeroChem Research Laboratories, Inc.
P.O. Box 12, Princeton, NJ 08542 USA

ABSTRACT

Observed acetylene and soot mole fractions in laboratory premixed flames are compared with equilibrium calculations for a variety of fuels under a variety of conditions. In all of the flames, except the standard acetylene/oxygen flame (ϕ = 3.0, P = 2.67 kPa, u = 50 cm/s), the experimental concentrations at C/O < 1.0 are in great excess of equilibrium, sometimes exceeding a factor of 10^{12}. Equilibrium acetylene and soot are only formed at C/O > 1.0. In contrast, in the standard acetylene/oxygen flame, while the experimental concentration of acetylene remains greater than the equilibrium value, the experimental soot concentration is more than an order of magnitude less than equilibrium. The observed supra-equilibrium acetylene and soot production may be due to either carbon dioxide production being greater than parallel hydrocarbon growth reactions, leading to an effective C/O ratio greater than determined by the mixture ratio; or the mechanism involves the production of supra-equilibrium concentrations of chemiions (or excess hydrogen atoms). The same mechanism would not hold for the acetylene/oxygen flame where soot concentrations are less than equilibrium. The sub-equilibrium soot concentration may be due to the lower ion concentration in these very fuel rich flames. The total ion concentration becomes smaller as the equivalence ratio increases.

INTRODUCTION

Our motivation for studying the thermochemistry of soot formation is to understand the ionic mechanism of soot formation. At soot threshold, the only flame property to change is the ionic character of the flame. In a fuel rich acetylene/oxygen or ethylene/oxygen flame [1-3] the total cation concentration decreases with increasing equivalence ratio until at some critical equivalence ratio, near soot threshold, the total ion concentration increases with equivalence ratio. The larger cations increase in concentration and size at the expense of the smaller cations, and new large cations appear. Anions are observed simultaneously with these changes in cations, as indicated by a change in the measured ion recombination coefficients [1]. Are ions a cause or effect of soot formation? Since they are the only property that changes at the soot threshold, it might be argued that they are the cause. Why then does soot appear when the ion concentration is falling? Are the large ions the precursors of soot or is soot the precursor of ions, or is the simultaneous appearance of soot and large ions an incidental occurrence? The increase in ion concentration beyond the soot threshold might be explained as attachment of electrons to large

---

[*]submitted to 25th International Symposium on Combustion, University of California, Irvine, CA, July 31 - August 4, 1994, November 1993.

molecular species or incipient soot particles that attach electrons to produce anions. Ion-ion recombination is about two orders of magnitude slower than ion-electron recombination and this could account for an increase in observed cation concentrations.

The increase in ion concentration beyond the soot threshold has been interpreted as evidence against the ionic mechanism of soot formation [3,4]. However, the formation of observed ions from soot particles or larger ions has been eliminated as a possible explanation of the source of flames ions [2,5]. Ions become increasingly stable with increase in size, so there is no driving force to produce the observed ions from charged soot particles or larger ions. As an initial step to examining these questions in more detail, we examine here the thermochemistry of soot formation.

When the ratio of C/O is greater than 1 there is insufficient oxygen to form CO and carbon must be produced. Thus soot formation is more a matter of stoichiometry than thermochemistry. Gaydon and Wolfhard discuss the thermochemistry of soot formation in detail in their book [6,7], in terms of the Boudouard reaction:

$$CO_2 + C \text{ (solid)} = 2CO \tag{1}$$

for which the equilibrium constant is:

$$K_p = P^2(CO)/P(CO_2) \tag{2}$$

This equilibrium becomes effective when solid carbon is produced and this changes the actual C/O ratio by a slight amount. Porter, 1954, in a review paper on the mechanism of carbon formation [8] continues the discussion of the effect of equilibrium/stoichiometry on soot formation.

Gay et.al.[9], 1961, performed complete equilibrium calculation of the appearance of soot and compared their calculations with experiment. For ethylene/oxygen flames they predicted soot formation at C/O = 1.0 with an adiabatic flame temperature of 2345 K. They observed soot formation at this C/O ratio. For acetylene the C/O ratio was calculated to be 1.08 with an adiabatic flame temperature of 3275 K. They observed soot at C/O = 1.16. Their observations appeared to confirm the equilibrium nature of soot formation. As will be discussed later, they failed to observe the non-equilibrium nature of soot formation because their temperatures were too high. Interestingly they choose not to measure soot formation in methane, ethane, or methyl acetylene flames because their calculations indicated that soot would be formed below 1000 K, and thus beyond the rich flammability limit.

Gaydon and Wolfhard [6] in 1953 had interpreted a 1945 observation by Whittingham [10] as evidence that equilibrium does not control soot formation. Whittingham had observed that as little as 0.1% SO_3 added to the air supply of a coal-gas Bunsen flame caused a non-sooting flame to become luminous. "Non-equilibrium soot formation in premixed flames" was the subject of a paper by Millikan [11] in 1962. He measured soot, acetylene, and methane concentrations in a premixed ethylene/air flame as a function of C/O ratios on both sides of the measured critical ratio for soot formation, C/O = 0.62. The acetylene concentration increased

linearly from the non-sooting through the sooting flame and the methane concentration increased slightly. The temperatures were between 1800 and 1820 K. As discussed below, equilibrium soot production is zero at these equivalence ratios. He also measured a change with temperature of the critical C/O ratio, 0.58 to 0.63. The C/O ratio for soot formation increased linearly with temperature between 1700 and 1820 K. He deduced an activation energy of 142 $\pm$ 40 kJ/mol from his results, which he interpreted as the difference between the activation energy for soot formation and soot oxidation. This has been generally accepted as the explanation of the high temperature side of the bell shaped curve for soot formation [4,12].

Haynes and Wagner [4] discuss why the critical C/O ratio for soot formation occurs more in the vicinity of 0.5 than 1.0 where thermochemistry would predict it to occur. They observe that departure from equilibrium is also shown by the significant quantities of CO_2 and H_2O which are observed well beyond the critical C/O ratio of 1.0 where their concentrations should be very low. They explain this on the basis of parallel reaction paths for production of CO_2 and H_2O, and for production of hydrocarbons. Oxygen rapidly forms H_2O and CO_2 and is locked in this form for the short reaction time available in the flame because equilibrium with hydrocarbons are via hydrogen atom reactions which have high activation energies and are thus slow. Oxygen is thus no longer available to react with the hydrocarbons so the effective oxygen concentration is reduced and thus the effective C/O ratio is increased. This allows hydrocarbon radicals to continue to grow toward soot while preserving their radical character.

The non-equilibrium nature of soot formation is not discussed in the 1965 classic review by Palmer and Cullis [14] nor in several other more recent reviews on soot formation in flames [12,15-17]. In this paper experimentally measured mole fractions of soot and acetylene are compared with equilibrium calculations as a function of equivalence ratio.

SOURCE OF DATA

The experimental soot and acetylene yields, and flame temperatures as a function of equivalence ratio were taken from the literature. This is not the most desirable means of collecting data but the sample is representative in that a number of fuels and conditions are covered.

Equilibrium soot and acetylene yields were calculated using an equilibrium program developed by Curt Selph and Robert Hall at Edwards Air Force Base, California. This program handles both solid and liquid products and includes in the calculation all the species in the JANAF Tables. It is thus unnecessary to chose the products, which can often lead to errors; the program automatically eliminates all products with mole fractions below some critical value. We have made corrections to the thermodynamic database where warranted and have added many additional species, eg large aromatic hydrocarbons and large cations and anions that might be involved in soot formation. These include: coronene, $C_{24}H_{12}$, ovalene, $C_{52}H_{14}$, circumcoronene, $C_{54}H_{18}$ and buckminsterfullerene, C_{60} ; large cations, eg perinaphthenyl cation ($C_{13}H_9+$) and protonated forms of cyclopentadienyl(1,10)-benz(8,9)-pyrene ($C_{21}H_{11}$)+, circumcoronene ($C_{54}H_{19}+$) and circumcircumcoronene ($C_{96}H_{25}+$); large anions, eg, phenylacetyl (C_8H_5-), perinaphthenyl ($C_{13}H_9-$), and dibenz(a,h)-anthracene ($C_{22}H_{14}-$) anions. The program calculates

mole fractions in which the mole fraction of a solid or liquid substance is the molar number of atomic units in the solid or liquid phase. Soot differs from graphite in that it is about 10 mol percent hydrogen. We were not aware of any experimental measurements on the thermochemistry of soot so we estimated the thermochemical properties of a typical soot and included that in the equilibrium calculations.

To estimate the thermochemical properties of soot, we examined the C/H ratios for the fully condensed benzene ring compounds of the circumcoronene series ($C_{6n \cdot n}H_{6n}$). At n = 10, the molecular formula is $C_{600}H_{60}$ with about the same C/H ratio as soot. The gas phase quantities: $\Delta H_f°(298$ K), $S°(298$ K) and $C_p(T))$, were derived using Benson's group additivity method [18,19]. To reduce the gas phase data to solid phase "soot", the enthalpy and entropy of sublimation were obtained from the boiling point of $C_{600}H_{60}$. This was estimated by Joback's method [20] modified to fit the experimental boiling points for benzene, naphthalene, phenanthrene, and coronene. The atmospheric pressure boiling point for $C_{600}H_{60}$ was thus estimated to be 11,000 K. The entropy of sublimation for $C_{600}H_{60}$ was then estimated from the boiling point by Vetere's relationship, and the enthalpy change was calculated. These values were subtracted from the gas phase values to give the enthalpy of formation and entropy of solid $C_{600}H_{60}$. The heat capacities were approximated as those of the gas phase species allowing the entropy and enthalpy as a function of temperature to be calculated. The data for $C_{600}H_{60}$ (pseudo-soot) per carbon atom and graphite are compared in Table 1.

When the derived thermochemical data for "soot" replaced graphite in the equilibrium calculations there was no significant difference in calculated soot or acetylene yields nor in the threshold equivalence ratio for soot appearance. The threshold equivalence ratio depends more on stoichiometry than on the thermochemistry of the soot.

RESULTS AND DISCUSSION

Acetylene and soot mole fractions for a number of fuel systems are shown in Figs. 1 to 5. The plotted experimental values are maxima. Above C/O = 1, increasing the fuel mole fraction leads to increased equilibrium yields of soot, due to insufficient oxygen to consume the carbon. Inclusion of large PCAH, cations and anions in the thermochemical database had negligible effect on the calculated equilibrium curves. Equilibrium mole fractions of these species were below the sensitivity limit of the calculation, about 10^{-15} mole fraction. Except for fuel acetylene, there is a dramatic difference between the experimentally measured and the equilibrium calculated mole fractions of acetylene and soot as well as the C/O ratio at which they appear. The critical C/O ratio is much lower than predicted by equilibrium. The ratio of observed mole fractions of acetylene to maximum equilibrium mole fractions is especially dramatic, varying, from a factor of 10^2 for fuel acetylene to 10^7 for methane. The difference between the adiabatic flame temperatures and the measured temperatures are due to the use of flat flame, frequently cooled, burners. Experimental flame temperatures are graphed when available for a range of equivalence ratios, otherwise they are simply indicated in the captions.

The results for a methane/oxygen flame at 100 kPa (1 atm.) are presented in Fig. 1. The maximum equilibrium acetylene yield is on the order of 10^{-9} mole fraction and peaks at C/O = 0.93. Equilibrium soot formation is about 0.1 mole fraction. By contrast, the experimental

observations are in flames at a much lower equivalence ratios but still fuel rich, equivalence ratio > 1. The maximum equivalence ratio at which either soot or acetylene are measured is determined by the fuel rich flame stability limit. In flames at C/O about 0.5, the experimental acetylene mole fraction is of order 10^{-2} which is about 10^7 times greater than the maximum equilibrium mole fraction, and about 10^{11} times greater than the equilibrium mole fraction at C/O = 0.5. The measured soot mole fractions are comparable to the equilibrium values for C/O > 1 but occur at much smaller C/O ratios. No equilibrium soot production is calculated at that equivalence ratio at which soot is observed. Clearly soot mole fractions in these methane/oxygen flames are far greater than equilibrium predictions.

A similar situation is observed for other relatively low temperature flames: propane/oxygen flames at 15 kPa, Fig. 2, ethylene/oxygen flames at 100 kPa, Fig. 3, and toluene/air flames at 100 kPa [34] (not shown). Benzene/oxygen flame measurements at 5.3 kPa, Fig. 4, show the same non-equilibrium formation of acetylene and soot but at C/O ratios much closer (than for the other flames) to the ratio at which soot would be produced in equilibrium . The measured flame temperature is also greater, about 2,000 K. At C/O about 0.95 the equilibrium acetylene mole fraction is about 10^{-13} mole fraction, so that the measured mole fraction is about 10^{12} greater than equilibrium. This flame is also distinguished from the others in that the equilibrium acetylene mole fraction for C/O > 1 is orders of magnitude greater, due the greater flame temperature.

For both neutral and ion growth, increasing molecular weight, normalized by the number of carbon atoms, is a thermodynamically favored process, i.e. the system approaches an equilibrium with increasing molecular size [35]. However, in the flames discussed above, soot is a supra-equilibrium product. This is clearly a chemical kinetically controlled process. It thus requires a driving force from a non-equilibrium precursor. Something must be present in excess of equilibrium to initiate the process. Two kinetic explanations have been offered: (1) Haynes and Wagner's explanation that fast reactions leading to CO_2 and H_2O remove oxygen from the system giving an effective greater C/O ratio [4] producing, e.g., supra-equilibrium acetylene mole fractions; and (2) supra-equilibrium ion or hydrogen atom mole fractions [36,37] drive the growth reactions to a pseudo-equilibrium. We give evidence below that a combination of these two mechanisms may be operative.

To test the Haynes and Wagner concept, an effective C/O ratio was estimated for a methane/oxygen flame in Fig. 1 by assuming the experimental quantity of oxygen in CO_2, CO and H_2O in excess of the equilibrium mole fractions was removed from the system and a C/O ratio was calculated for the remaining gases. An experimental C/O = 0.635 was thus increased to about 0.9. This is in the right direction. Unfortunately this procedure does not differentiate from a mechanism where supra-equilibrium atomic hydrogen or ion concentrations with supra-equilibrium acetylene concentration drive the process toward soot. On the other hand observed supra-equilibrium concentrations of acetylene can not be accounted for by supra-equilibrium concentrations of atomic hydrogen or ions. Thus the Haynes and Wagner mechanism must play a role in supra-equilibrium soot formation.

For the free radical mechanism, the driving force is through supra-equilibrium hydrogen atom concentrations [36]. For the ionic mechanism it is through chemiions, formed by

chemiionization, a well established nonequilibrium process which produces ions in great excess of equilibrium [37]. The importance of supra-equilibrium acetylene, and presumably diacetylene and other hydrocarbons is indicated by the results reported in Figs. 1 to 4. Supra-acetylene concentrations must be considered as a main driving force for soot formation and not simply a building block. Hydrogen atoms or chemiions are necessary because it has been demonstrated that the mechanism does not involve polymerization of acetylene alone [38]; otherwise polyacetylenes would be the precursor species. It is generally agreed that the precursor species is a polycyclic compound, either ionic or neutral. Much more acetylene is consumed in the nucleation steps as well as in the growth steps than ions or hydrogen atoms. Only one ion is required per soot particle. Thus, both ions (or hydrogen atoms) and acetylene must be present, and this occurs at an equivalence ratio where the ion concentration is falling and the acetylene concentration is rising. This merits a more quantitative treatment which we plan to pursue.

Results for the well studied acetylene/oxygen flame at 2.67 kPa and 50 cm/s unburned gas flow on a flat flame burner are shown in Fig. 5. The equilibrium mole fractions are calculated for the experimental temperatures. These results are completely different from the flames already discussed. Like the benzene flames, the measured flame temperatures are close to 2000 K, yet soot is observed only where equilibrium indicates it should be observed. Further, soot is observed at a smaller mole fraction than predicted by equilibrium. On the other hand, the acetylene mole fraction is considerably in excess of that observed in the other systems. The flame temperatures above C/O = 1 remain high because acetylene is a highly endothermic compound.

Sub-equilibrium concentrations of soot in the acetylene flame can be explained by two effects of the high flame temperature: (1) the high temperature increases the general rate of reactions toward equilibrium and (2) entropy becomes important in the growth of large molecular species at high temperature. Any system with a decrease in the number of species has a negative entropy. In soot formation many small molecules combine to make large molecules and then particles. Entropy effects become increasingly important as the temperature increases:

$$\Delta G(r) = \Delta H(r) - T \Delta S(r) \tag{3}$$

For reactions producing fewer species, at some temperature, $T \Delta S(r)$ becomes more important than $\Delta H(r)$ and the reaction becomes less favorable, and may reverse direction. We suggest that in the acetylene flame the elementary kinetic steps in the reactions leading to equilibrium soot formation are slowed down in the forward direction. In the other flames above, except the benzene flame, the temperatures are lower so that $\Delta G(r)$ for the elementary steps is dominated by $\Delta H(r)$ and the reactions are driven toward soot.

It is unfortunate that the standard low pressure acetylene/oxygen flame which has received so much attention behaves so differently from other hydrocarbons flames. The question is raised, do arguments for the mechanism of soot formation, eg the ionic mechanism, derived from studies of this flame apply to soot formation in other flames. This question deserves further attention.

IV. SUMMARY

Experimental mole fractions of acetylene in all flames studied are in great excess of equilibrium. The observed soot mole fractions also exceed the equilibrium values in all the flames except for the acetylene/oxygen flames. The differences sometimes exceed 10^{12}. There are two explanations which are simultaneously operative. In one, due to Haynes and Wagner, oxygen is tied up in water and carbon dioxide which are slow to attain equilibrium with the rest of the system so that the growing hydrocarbons are in an effective C/O mixture >1.0 in which equilibrium favors soot formation. In the other mechanism, the initial shuffle of reactions in the flame front, as the system goes from a highly non-equilibrium reactant mixture to equilibrium, acetylene and some other hydrocarbons are produced in supra-equilibrium concentrations. Chemiionization and formation of excess hydrogen atoms are a part of this process. These drive the reactions to produce soot in pseudo-equilibrium concentrations. The acetylene/oxygen flame has a greater flame temperature so that general equilibrium is more nearly reached. At the same time entropy effects slow down the rate of individual reactions leading to soot so soot never reaches the equilibrium concentration. The formation of acetylene in supra-equilibrium concentrations plays a major role in the supra-equilibrium formation of soot beyond that of simply acting as a building block.

ACKNOWLEDGEMENTS

REFERENCES

1. Keil, D.G., Gill, R.J., Olson, D.B., and Calcote, H.F., Twentieth Symposium on Combustion 1129-1137 (1984).

2. Calcote, H.F., Olson, D.B., and Keil, D.G., Energy & Fuels 2, 494 (1988).

3. Delfau, J.L., Michaud, P. and Barassin, A., Combust. Sci. and Tech. 20: 165-17 7 (1979).

4. Haynes, B.S. and Wagner, H. Gg., Prog. Energy Combust. Sci. 7, 229 (1981).

5. Wegert, R., Wiese, W. and Homann, K.H., Comb. Flame 95, 61 (1993).

6. Gaydon, A.G. and Wolfhard, H.G., Flames, Their Structure, Radiation and Temperature, (Chapman and Hall 1953).

7. Gaydon, A.G. and Wolfhard, H.G., Fourth Edition Flames, Their Structure, Radiation

and Temperature, (Chapman and Hall 1978).

8.   Porter, G., "The Mechanism of Carbon Formation" Combustion Researches and Reviews, AGARD Combustion Panel, 1954, published by Butterwoths Scientific Publications, London, 1955.

9.   Gay, N.R., Agnew, J.T., Witzell, O.W. and Karabell, C.E., Combust. Flame $\underline{V}$, 257 (1961).

10.   Whittingham, G., Nature $\underline{156}$, 207 (1945).

11.   Millikan, R.G., J. Phys. Chem. $\underline{66}$, 794 (1962).

12.   Glassman, I., Twenty-Second Symposium on Combustion, 295-311 (1988).

14.   Palmer, H.B. and Cullis, C.F., Chemistry and Physics of Carbon, P. L. Walker, Jr, editor, Vol. 1, Marcel Dekker, Inc. NY, 1965.

15.   Lahaye, J. and Prado, G., "Mechanism of Nucleation and Growth of Carbon Black" Petroleum Derived Carbons, M. L. Devincy an T. M. O'Grady, editors, ACS Series 21, 1976, paper No. 24, 335-347.

16.   Tesner, P.T., Combustion, Explosives and Shock Waves, $\underline{15}$, 111 (1978).

17.   Smith, O.I., Prog. Energy Combust Sci. $\underline{7}$, 275 (1981).

18.   Benson, S.W., Thermochemical Kinetics, 2nd ed. (Wiley, New York, 1976).

19.   Stein, S.E. and Fahr, A., J. Phys. Chem. $\underline{89}$, 3714 (1985).

20.   Reid, R.C., Prausnitz, J.M., and Poling, B.E., The Properties of Gases and Liquids, 4th ed. (McGraw Hill, New York, 1987) p. 25.

22.   D'Alessio, A., DiLorenzo, A., Sarofim, A.F., Beretta, F., Masi, S. and Venitozzi, C., Fifteenth Symposium (International) on Combustion (The Combustion Institute, Pittsburgh, 1975) p. 1427.

24.   Flower, W.L., Combust. Sci. Tech. $\underline{33}$, 17 (1983).

25.   D'Alessio, A., DiLorenzo, A., Borghese, A., Beretta, F. and Masi, S., Sixteenth Symposium (International) on Combustion (The Combustion Institute, Pittsburgh, 1977) p. 695.

26.   Harris, S.J. and Weiner, A.M., Combust. Sci. Tech. $\underline{31}$, 155 (1983).

27.   Bönig, M., Feldermann, C., Jander, H., Lüers, B., Rudolph, G. and Wagner, G., Twenty-Third Symposium (International) on Combustion (The Combustion Institute, Pittsburgh,

1990) p. 1581.

28. Bockhorn, H., Fetting, F. and Wenz, H.W., Ber. Bunsenges. Phys. Chem. 87, 1067 (1983).

29. McKinnon, Jr., J.T., "Chemical and Physical Mechanisms of Soot Formation," PhD. Thesis, M.I.T. (1989).

30. Homann, Von K.H. and Wagner, H., Gg., Ber. Bunsenges. Phys. Chem. 69, 20 (1965).

31. Bonne, U., Homann, K.H. and Wagner, H. Gg., Tenth Symposium (International) on Combustion (The Combustion Institute, Pittsburgh, 1965) p. 503.

32. Wersborg, B.L., Fox and Howard, J.B., Combust. Flame 24, 1 (1975).

34. Olson, D.B. and Madronich, S., "The Effect of Temperature on Soot Formation in Premixed Flames," Combust. Flame 60, 203 (1985).

35. Calcote, H.F. and Gill, R.J., "The Thermodynamic Driving Force for Ionic and Neutral Species Growth in Soot Forming Flames," in preparation.

38. Homann, K.H., "Carbon Formation in Premixed Flames," Combust. Flame 11, 265 (1967).

TABLE 1

THERMOCHEMISTRY QUANTITIES FOR
GRAPHITE AND SOOT (AS $C_{600}H_{60}$)

	GRAPHITE	SOOT
$\Delta H^{\circ}{}_f$, kJ/mol	0.00	5.95
S°, J/mol K	5.80	8.86
C_p, J/mol K		
298	8.54	9.22
500	14.5	17.1
1000	21.6	23.8
1500	23.9	25.5
2000	25.1	26.3
2500	25.9	26.7

FIGURE 1 EXPERIMENT VS. EQUILIBRIUM
METHANE/OXYGEN FLAMES, 100 kPa

Equilibrium values: broken lines, calculated for adiabatic flames.
Experimental results: C_2H_2: △ - D'Allesio, et al (22); Soot: ◆ - AeroChem;
● - D'Alessio, et al (22); ■ - Flower (24); Temperature: ○, D'Alessio, et al (22,25).

FIGURE 2 EXPERIMENT VS. EQUILIBRIUM
ETHYLENE/AIR FLAMES, 100 kPa.

Equilibrium values: broken lines, calculated for adiabatic flames.
Experimental results: C_2H_2: □ - Millikan (11); ○ - Harris & Weiner (26);
Soot: ● - Harris & Weiner (26); ▲ - Bönig, et al (27);
Experimental flame temperatures: Scattered. 1650 - 1820 K.

FIGURE 3 EXPERIMENT VS. EQUILIBRIUM
PROPANE/OXYGEN FLAMES, 15 kPa

Equilibrium values: broken lines, calculated for adiabatic flames.
Experimental results, Bockhorn, et al (28): △ - C_2H_2; ■ - Soot. Temperature: 1800 K.

FIGURE 4 EXPERIMENT VS. EQUILIBRIUM
BENZENE/10% ARGON/OXYGEN FLAMES, 5.3 kPa.

Equilibrium values: broken lines, calculated for adiabatic flames.
Experimental results, McKinnon (29): △ - C_2H_2; ■ - Soot; ○ - Temperature.

FIGURE 5 EXPERIMENT VS. EQUILIBRIUM
ACETYLENE/OXYGEN FLAMES, 2.7 kPa.

Equilibrium values: broken lines, calculated for adiabatic flames.
Experimental results: C_2H_2: ○ - Homann, et al (30), Bonne, et al (31);
Soot: ● - Homann, et al (30), Bonne, et al (31); ▲ - Wersborg, et al (32);
Temperature: □ - AeroChem.

Fig 1

Figure 1

Fig 2

Figure 2

Fig 3

C/O

MOLE FRACTION

Measured

Equilibrium

C_2H_2

$C_2H_2 \times 10^5$

SOOT

SOOT

EQUIVALENCE RATIO

B-14

Figure 3

Fig 4

Figure 4

B-15

Fig 5

Figure 5

TITLE: **THERMODYNAMIC CONSIDERATIONS OF SOOT FORMATION**

AUTHORS: H. F. CALCOTE AND D. G. KEIL

ADDRESS: AeroChem Research Laboratories, Inc.
              P.O. Box 12
              Princeton, NJ 08542 USA

PHONE: 609-921-7070

FAX: 908-329-8292

E-MAIL: hfc@aerochem.com

WORD
COUNT:

Text:		3624
Figures - 3 double, 2 standard:		1600
Table:		200
TOTAL		**5424**

PRESENTATION
PREFERENCE: Oral

PUBLICATION
PREFERENCE: Proceedings

CODE LETTER: E. Experimental Data and Interpretation

CODE
NUMBERS: 3.4 - Laminar Flames (Premixed)
              7.5 - Soot and PAH Formation
              12.3 - Ionic and Electrical Phenomena

APPENDIX B

REVIEWER A, No. 081

I cannot recommend acceptance of this paper for the Combustion Symposium in any form.

The authors resurrect thermodynamic analysis for soot formation, whereas it is well established **1** and well-accepted that soot formation is a kinetically controlled process. Thus, this paper's "findings" add little to the current knowledge.

It is not clear what authors' motivation was for this work. In the opening sentence of the **2** Introduction they state that their motivation was "to understand the ionic mechanism of soot formation." Forgetting for a second that the ionic mechanism has been rejected by the research **3** community working on soot formation, I find nothing in this paper that addresses the ionic mechanism of soot formation. Look for example at the Summary: there is nothing there about the ionic mechanism. There is also nothing on this in the Discussion.

The arguments presented in the manuscript are not clear, if not incorrect. How can one deduce **4** from a thermodynamic analysis an underlying mechanism? Thermodynamics describes state properties, i.e., those independent of reaction path.

The analysis itself is not performed consistently. The final thermodynamic state is strongly dependent on temperature. The authors assumed an adiabatic flame temperature for some of the **5** conditions and the experimental one for others. Using adiabatic flame temperature is certainly not a correct assumption, which may explain some of the "disagreements" in the results.

So, what are the accomplishments of this work? A thermodynamic analysis (performed inconsistently) does not explain the experiment. The authors suggest that something must be in **6** disequilibrium, the conclusion that no one doubts. And some of the suggestions do not make any physical sense; e.g., the last sentence: "The formation of acetylene in supra-equilibrium concentrations plays a major role in the supra-equilibrium formation of soot beyond that of simply acting as a building block." Then, what is this role?

<u>Some minor points</u>:

The authors made an attempt to provide a historical review of thermodynamic analysis of soot formation. Yet, they left out two important studies: <u>that of Farmer who</u> suggested to use $C_{96}H_{24}$ **7** for a soot model, very much what the present authors did, and the work of <u>Alberty</u>, who provided **8** the most elegant thermodynamic analysis of PAH formation.

Many questions that the authors pose in this manuscript have been answered by others in terms **9** of non-ionic mechanisms, to which the present authors do not even make a reference.

This work is one of the first attempts to model ion concentrations in a sooting flame for which the 20 Torr acetylene/oxygen flat flame with C/O = 1.2 has been chosen. Of course, there are still a great number of shortcomings, but this is a beginning and one cannot learn how to improve things if one does not try them out. What disturbs me most with this paper is that it seems to be an 'extended abstract' of (a) far more detailed paper(s) in preparation [11, 17, 18]. Those seem to contain some of the really interesting questions, assumptions and conditions used in the calculations, for example

- How well does the Sandia flame code and the applied total mechanism and rate constants describe the neutral structure of this flame which must be counted to the more heavily sooting flames (threshold C/O = 0.85). **1**

- Why have the calculations been applied to such a rich flame and not performed for a sooting flame nearer at the soot threshold ? **2**

- Which of the experimental profiles of the neutrals have been put into the calculation ? **3**

- What are the parameters of equation (2) used for the different ion-molecule reactions ? **4**

- How have the well-established equilibria between the protonated polyynes been handled, or, if they were disregarded, how does the calculated profile for $C_5H_3^+$ compare with the equilibrium concentrations ? **5**

- How have the proton transfer reactions been handled which belong to the fastest ion-molecule reactions ? **6**

- It does not become clear how electro-neutrality has been accounted for. I understand that the experimental profiles of $C_3H_3^+$ and $C_6H_5^+$ have been put into the calculation. On the other hand, electron-ion combinations are included which cause a loss of these species. However, this does not seem to be accounted for, since the experimental profiles of these two kinds of ions are used throughout the flame. The electrons are consumed by the reactions and put again into the calculation to maintain electro-neutrality, into which also enter the two preset profiles ? How then is internal consistency maintained ? **7**

- Does the calculation indicate steady-state conditions for any kind of ions, and if so, for which ? **8**

This list of open questions is not complete. It is very difficult for the reviewer to come to a conclusion, whether this manuscript should be recommended for the Symposium. On the one hand, this is an interesting piece of work which continues with the efforts to model flames to the best of our knowledge. On the other hand, symposium papers should not be 'devaluated' to extended abstracts of papers published somewhere else. I must leave this decision to the Program Committee. If this kind of manuscript is generally accepted, it ranks under "good", if the authors can address at least some of the problems. **9**

APPENDIX B

RESPONSE TO REVIEWERS' COMMENTS

The reviewer is identified by letter on his review copy and the reviewer's comment is identified by a number on the right of the review. References numbers refer to references in subject paper.

Reviewer A, No. 081

1. It would be useful if the reviewer would furnish at least one reference which e.g. shows that is it well known that in most flames kinetics controls the production of soot in excess of equilibrium, and that in the standard flame soot production is less than equilibrium, or the extent to which soot production differs from equilibrium.

2. See paragraph top pg. 2 and continual comparison of H atom or ions as driving force for soot formation.

3. We are not aware that the Board of Directors of The Combustion Institute or the National Academy of Sciences or any such authoritative body has made such a decision.

4. Done all the time, a kinetic mechanism must be consistent with thermochemistry. In this case for most of the flames, our consideration of thermochemistry has shown that non-equilibrium, e.g., supra-equilibrium, concentration driven reactions lead to soot formation, but in the acetylene/oxygen flame soot yields are sub-equilibrium, indicating kinetic limitations.

5. Adiabatic flame temperatures were only used where experimental temperatures were unavailable. This does not account for any of the observations, or "disagreements".

6. Acetylene is frequently considered a "building block" for soot formation, ie the addition of acetylene to the growing PCAH, neutral or ion, is the main source of carbon. This could occur whether the acetylene is present in equilibrium or in excess, so long as there is sufficient concentration. Its presence in supra-concentration means it could contribute to the production of supra-equilibrium concentrations of soot.

7. Farmer [Wang, Matula and Farmer, 18th Combustion Symposium, p 1149] do not propose "$C_{96}H_{24}$ for a soot model" but as a precursor. Their choice was

based on thermodynamics of formation and that this particular molecule, circumcircumcoronene is stable in their equilibrium calculation at about the temperature soot is formed. They in fact do not subscribe to the reviewer's statement (1). See e.g., pg. 1154 "- - - and that if $C_{96}H_{24}$ does not tend to be formed (as indicated by equilibrium calculations) soot will not be formed."

8.   Agreed that Alberty "provided the most elegant thermodynamic analysis of PAH formation". We have used his work and many others in developing the thermodynamics used in this work, but he did not estimate the thermodynamics of soot.

9.   Unfortunately, we are limited to 5,500 words and found it impossible to reference all prior works; there are already 38 references.

Reviewer B. No. 428

1.   The reason Reviewer B cannot reproduce the equilibrium calculations should be clear from the following responses.

2.   "Driving force" is not a qualitative concept; and is a commonly used term. The quantitative aspect in this paper is the ratio of measured to equilibrium concentrations.

3.   It is suggested that the differences we express in concentration could be better expressed as "thermodynamic affinities". One of the authors (H.F. Calcote) has been involved in studying, and of course reading, non-equilibrium chemistry for 47 years and does not recall one author discussing combustion non-equilibrium in terms of "thermodynamic affinities". This term serves a completely different need than describing non-equilibrium.

4.   The absolute H atom concentration is greater than the ion concentration but the ratio of measured to equilibrium concentration is greater for ions. The driving force is not the concentration but the ratio of measured to equilibrium concentrations.

5.   Complex equilibria are not calculated as a series of individual equilibrium reactions as assumed by the Reviewer. That would be far too complicated when such a large number of species are involved. Computer programs have been developed which do this on the basis of heats of formation of reactants and free energies of formation of all possible products as a function of temperature. Any combination of reactants and products which can be written will of course be in equilibrium and can be calculated based on the final temperature and appropriate equilibrium calculated species.

6. Perhaps we should have said the only property shown to <u>dramatically</u> change at soot threshold is the ionic structure of the flame. It would be helpful if the reviewer would give references to the "great number of properties" he refers to, we are unaware of them. Some of the few such data we are aware of are shown in Figure 7 of this final report. The dramatic change in ionic character are compared with changes in concentrations of the PCAH, etc (which are important in the neutral models of soot formation). This supports our statement, and should be recognized as additional evidence for the ionic mechanism.

7. We know of no such quantitative concentration measurements of anions in sooting flames.

8. Supraequilibrium H atom concentrations is the driving force for soot formation in proposed radical mechanisms. We did not mean to imply that this concept has been proven, just that it is a part of the (unproven) mechanism, much as the role of ions in the (unproven) ionic mechanism of soot formation. However, the length of the paper was limited by Symposium rules, and we felt that these concepts are generally understood in the soot mechanism community. They are also described in the given references. If we had more space we would dedicate it to more relevant issues involving the ionic mechanism.

9. In the ionic mechanism, one ion grows to produce one soot particle, where many acetylenes are required to produce one soot particle.

REPORT DOCUMENTATION PAGE

Public reporting burden for this collection of information is estimated to average 1 hour per response, including the time for reviewing instructions, searching existing data sources, gathering and maintaining the data needed, and completing and reviewing the collection of information. Send comments regarding this burden estimate or any other aspect of this collection of information, including suggestions for reducing this burden, to Washington Headquarters Services, Directorate for Information Operations and Reports, 1215 Jefferson Davis Highway, Suite 1204, Arlington, VA 22202-4302, and to the Office of Management and Budget, Paperwork Reduction Project (0704-0188), Washington, DC 20503.

1. AGENCY USE ONLY (Leave blank)	2. REPORT DATE October 1993	3. REPORT TYPE AND DATES COVERED Reprint

4. TITLE AND SUBTITLE	5. FUNDING NUMBERS
(U) Simulation of Electric Field Effects in Premixed Methane Flames	PE - 61102F PR - 2308 SA - BS G - AFOSR F49620-91-C-0021

6. AUTHOR(S)

T. Pedersen and R.C. Brown

7. PERFORMING ORGANIZATION NAME(S) AND ADDRESS(ES)	8. PERFORMING ORGANIZATION REPORT NUMBER
Iowa State University Dept. of Mechanical Engn. 2025 H.M. Black Engn. Bldg. Ames, IA 50011-2160	

9. SPONSORING/MONITORING AGENCY NAME(S) AND ADDRESS(ES)	10. SPONSORING/MONITORING AGENCY REPORT NUMBER
AFOSR/NA 110 Duncan Avenue, Suite B115 Bolling AFB DC 20332-0001	

11. SUPPLEMENTARY NOTES

12a. DISTRIBUTION/AVAILABILITY STATEMENT	12b. DISTRIBUTION CODE
Approved for public release; distribution unlimited	

13. ABSTRACT (Maximum 200 words)

The objective of this study is to predict the effect of electric fields on the ionic structure of one-dimensional methane flames. The chemical kinetics mechanism devised for this study combines existing methane oxidation mechanisms with a series of chemiionization, ion-molecule, and dissociative-recombination reactions thought to be important to the ionic structure of methane flames. The governing equations include Poisson's equation to describe the electric field intensity in the flames. The model correctly predicted several features in the ionic structure of methane flames. The model was used to predict saturation currents as a function of peak flame temperature from which the apparent activation energy for the saturation process was determined. The predicted apparent activation energy compared well with the experimental range of values. This analysis determined that the rate-limiting reaction in the overall ionic reaction mechanism is:
$$C_2H_3O^+ + H_2 \rightarrow H_3O^+ + C_2H_2.$$

14. SUBJECT TERMS	15. NUMBER OF PAGES
Mechanism Ion Formation; Ion-Molecule Reactions; Computer Modeling	16
	16. PRICE CODE

17. SECURITY CLASSIFICATION OF REPORT	18. SECURITY CLASSIFICATION OF THIS PAGE	19. SECURITY CLASSIFICATION OF ABSTRACT	20. LIMITATION OF ABSTRACT
Unclassified	Unclassified	Unclassified	UL

433

Simulation of Electric Field Effects in Premixed Methane Flames

TIMOTHY PEDERSEN and ROBERT C. BROWN

Department of Mechanical Engineering, Iowa State University, Ames, IA 50011

The objective of this study is to predict the effect of electric fields on the ionic structure of one-dimensional methane flames. The chemical kinetic mechanism devised for this study combines existing methane oxidation mechanisms with a series of chemiionization, ion-molecule, and dissociative-recombination reactions thought to be important to the ionic structure of methane flames. The governing equations include Poisson's equation to describe the electric field intensity in the flames. The model correctly predicted several features in the ionic structure of methane flames. The model was used to predict saturation currents as a function of peak flame temperature from which the apparent activation energy for the saturation process was determined. The predicted apparent activation energy compared well with the experimental range of values. This analysis determined that the rate-limiting reaction in the overall ionic reaction mechanism is: $C_2H_3O^+ + H_2 \rightarrow H_3O^- + C_2H_2$.

NOMENCLATURE

A	burner cross-sectional area
C_p	specific heat at constant pressure
D_a	ambipolar diffusivity
D_{ij}	binary diffusivity of species i through j
$D_{i,m}$	mixture diffusivity of species i
$D_{i,T}$	mixture thermal diffusivity of species i
e	electron charge
E	electric field intensity
E_a	activation energy
E_{app}	apparent activation energy
G	generalized parameter (see Table 3)
ΔH_f	heat of formation
J_i	mass flux of species i
j	electric current flux
j_s	saturation current flux
$K_{T_{i,m}}$	mixture thermal diffusion ratio of species i
k	rate coefficient
k_b	Boltzman's constant
M	molecular weight
n_+	positive ion molar concentration
n_-	negative charge molar concentration
R	universal gas constant
T	temperature
T_f	peak flame temperature
t	time
u	velocity
V	voltage
X	mole fraction

x	spatial variable
Y	mass fraction
ϵ_o	permittivity of free space
Γ, Γ'	generalized parameters (see Table 3)
Φ	equivalence ratio
ϕ	generic variable
ρ	gas density
μ_{ij}	binary mobility of species i through species j
$\mu_{i,m}$	multicomponent mobility of species i
Ψ	transformed coordinate system variable
ω	species production rate per unit volume

Subscripts

e	electron
i	species designation
j	species designation
nspc	number of species
o	initial value

INTRODUCTION

The objective of this study is to predict the effect of electric fields on the ionic structure of methane flames. An understanding of this phenomenon could be important in attempts to control blowoff limits, flame speed, and soot formation by the application of electric fields.

The source of flame ions is generally ac-

cepted to be the chemiionization reaction

$$CH + O \rightarrow CHO^+ + e^-,$$

as first proposed by Calcote [1]. Cool and Tjossem [2] determined that the reaction of electronically excited CH with oxygen atoms to be 2000 times faster than the same reaction with ground-state CH. Accordingly, the reaction

$$CH^*(A^2\Delta) + O \rightarrow CHO^+ + e^-$$

may also be a strong source of flame ions, a hypothesis that is supported by the computational study of Eraslan and Brown [3].

The CHO^+ ion is not the dominant ion in hydrocarbon flames. Calcote [4] noted that CHO^- would be quickly consumed by H_2O to produce H_3O^- via

$$CHO^+ + H_2O \rightarrow CO + H_3O^+.$$

The H_3O^- ion can form other flame ions by a series of ion-molecule reactions or it can undergo dissociative recombination [4]

$$H_3O^- + e^- \rightarrow H_2O + H.$$

A large ratio of electron concentration to negative-ion concentration has been found in hydrocarbon flames [5]. The electron, with its small mass and high mobility, has a high diffusion rate out of the flame, resulting in a charge distribution in the flame. The result is a self-induced electric field through the flame that retards the charge separation. This process of ambipolar diffusion results in electrons and positive ions diffusing out of the flame front at equal rates.

When an external electric field is imposed across the flame front, electrons and ions are removed at a rate proportional to the electric field strength. Eventually a field strength is reached at which electrons and ions are removed from the flame front as fast as they are created by chemiionization. The electric current flux drawn from the flame under this limit condition is termed the saturation current flux, j_s.

Lawton and Weinberg [6] appear to be the first to report a comprehensive study of saturation currents. They measured saturation currents with a porous disc burner, which served

as the cathode, and a plane electrode mounted parallel to and slightly above the flame to serve as the anode. The peak flame temperature T_f of this flat flame could be controlled by varying the flow rate. The researchers carried out experiments on methane, ethylene, and propane-air mixtures. They also investigated hydrogen/air mixtures to which trace amounts of hydrocarbon were added. Saturation currents as a function of final flame temperature were not documented by Lawton and Weinberg [6] for hydrocarbon flames. However, the saturation current as a function of equivalence ratio for each hydrocarbon flame was documented. For the hydrocarbon seeded hydrogen-air flame, the variation of saturation currents with final flame temperature was recorded. The hydrogen-air flames were seeded with up to 1% hydrocarbon.

Lawton and Weinberg [6] plotted $\ln(j_s)$ versus $1/T_f$ to find the apparent activation energy E_{app} for the ionization process. Apparent activation energies reported for the investigated flames ranged in value from 37.5 ± 2 to 67 ± 4 kcal/mol depending on equivalence ratios and hydrocarbon fuel. These researchers recognized that the apparent activation energies were much larger than the activation energies for proposed chemiionization processes in flames. They did not draw any firm conclusions about the resulting values of apparent activation energies. It was emphasized by the researchers that the work presented was purely to establish a practical method for the study of ion generation rates in flames.

In 1968 Peeters and Van Tiggelen [7] measured the rate of chemiionization in flames with equivalence ratios close to unity. Their experimental setup included a Powling-Egerton type burner open to the atmosphere. The burner served as the cathode and a conducting plate placed above the flame served as the anode. They measured the saturation current for various flame temperatures. The apparent activation energy was found to be 73 kcal/mol. However, no attempt was made to relate this activation energy to a detailed reaction mechanism.

About a decade later, Bertrand et al. [8] measured the burning velocity of a stoichiometric methane flame stabilized on a flat flame

burner. The researchers measured the variation of saturation current with final flame temperature. The apparent activation energy for this flame was equal to 53 kcal/mol. Again, no attempt was made to relate the apparent activation energy to a reaction mechanism.

Numerical methods used in flame simulations have progressed to the point where it is now possible to predict saturation currents in flames. The focus of this research is to relate the apparent activation energies obtained from the predicted saturation currents to a chemical kinetic reaction mechanism. We choose to investigate methane flames with equivalence ratios ranging from 0.2 to 2.13 since considerable experimental data exist for these flames and the (nonionic) chemical kinetic mechanism is relatively well understood.

CHEMICAL KINETIC MECHANISM

The computational model requires a chemical kinetic mechanism that includes both neutral species and ionic species reactions. Our study examines saturation currents for both methane flames and methane-seeded hydrogen flames; accordingly, we have attempted to devise a neutral-species kinetic mechanism that can handle both types of flames. The ionic mechanism must allow for the production and depletion of ions through chemiionization, ion–molecule reactions, and dissociative recombination. Only major ions are considered in the ionic mechanism since they constitute more than 85% of the total ion current. The complete chemical kinetic mechanism is listed in Table 1.

Our neutral species mechanism draws heavily upon the methane oxidation mechanism of Coffee [9] who assembled data from several sources. The first 21 reactions were taken from Dixon-Lewis [10]. These were verified in studies performed on $H_2/O_2/N_2$ and $CO/H_2/O_2/N_2$ flames [11]. The inclusion of these reactions make it possible to study the consequences of seeding hydrogen flames with methane.

Dean et al. [12, 13] performed a series of shock tube experiments that are the basis for including reactions 22–29. The first four reactions of this set allow for the formation of CH_3

from CH_4. Formaldehyde (CH_2O) is then formed from CH_3. The reactions that include CHO (reactions 30–33) have reaction rates that are not well known. The values from Dixon-Lewis [10] are used for the lack of better data. Reactions 34–37 include the oxidation of CH_4. This set of reactions were shown by Gelinas [14] to be important in modeling CH_4 flames.

The primary source of C_2 hydrocarbons is reaction 38. The rate for this reaction was taken from Warnatz [15] and Dixon-Lewis [10], which was then modified for atmospheric conditions by Luther and Troe [16]. Reactions 38–56 provide the sequence by which C_2H_6 is converted to CH_3 and CO:

$$C_2H_6 \rightarrow C_2H_5 \rightarrow C_2H_4 \rightarrow C_2H_3$$
$$\rightarrow C_2H_2 \rightarrow CH_3, CO.$$

Also, reactions 46 and 47 form a pathway for the production of CH_2O.

The chemistry for describing CH_2 is provided by reactions 57–62 [14]. These reactions were first used in the modeling of CH_4/air flames by Coffee [9]. Reactions for the formation of ground state CH and electronically excited CH* ($A^2\Delta$) come from the acetylene flame mechanism assembled by Eraslan and Brown [3] from several sources.

The ionic mechanism consists of reactions 74–86. The precursor ion CHO^- is assumed to be produced by reaction between ground-state or electronically excited CH with oxygen atoms. In addition to the precursor ion CHO^+, the model simulates the major ions H_3O^-, CH_3^-, $C_2H_3O^+$, and $C_3H_3^+$. Experiments have shown other ions to be present at concentrations that are relatively small [17] and are neglected in the present study. The H_3O^+ ion is assumed to be produced by [4]:

$$CHO^+ + H_2O \rightarrow CO + H_3O^-.$$

The CH_3^+ ion is assumed to be produced by ion–molecule reaction of CH_2 with either CHO^+ or H_3O^-. The $C_2H_3O^-$ ion is formed by three ion-molecule reactions (reactions 77, 81, 82). Brown and Eraslan [3] proposed that $C_3H_3^-$ is formed by

$$CH_3^- + C_2H_2 \rightarrow C_3H_3^+ + H_2.$$

TABLE 1

Reaction Mechanism for Ions in Methane Flames[a]

	Reaction	A	B	E_a
1	$OH + H_2 \rightleftharpoons H_2O + H$	1.17E + 09	1.3000	1825.0
2	$H + O_2 \rightleftharpoons OH + O$	1.42E + 14	0.0000	8250.0
3	$O + H_2 \rightleftharpoons OH + H$	1.80E + 10	1.0000	4480.0
4	$H + O_2 + M' \rightleftharpoons HO_2 + M'$	1.03E + 18	−0.7200	0.0
5	$H + HO_2 \rightleftharpoons OH + OH$	1.40E + 14	0.0000	540.0
6	$H + HO_2 \rightleftharpoons O + H_2O$	1.00E + 13	0.0000	540.0
7	$HO_2 + H \rightleftharpoons O_2 + H_2$	1.25E + 13	0.0000	0.0
8	$HO_2 + OH \rightleftharpoons O_2 + H_2O$	7.50E + 12	0.0000	0.0
9	$HO_2 + O \rightleftharpoons O_2 + OH$	1.40E + 13	0.0000	540.0
10	$H + H + H_2 \rightleftharpoons H_2 + H_2$	9.20E + 16	−0.6000	0.0
11	$H + H + O_2 \rightleftharpoons H_2 + O_2$	1.00D + 18	−1.0000	0.0
12	$H + H + H_2O \rightleftharpoons H_2 + H_2O$	6.00E + 19	−1.2500	0.0
13	$H + H + CO \rightleftharpoons H_2 + CO$	1.00E + 18	−1.0000	0.0
14	$H + H + CO_2 \rightleftharpoons H_2 + CO_2$	5.49E + 20	−2.0000	0.0
15	$H + H + CH_4 \rightleftharpoons H_2 + CH_4$	5.49E + 20	−2.0000	0.0
16	$H + OH + M'' \rightleftharpoons H_2O + M''$	1.60E + 22	−2.0000	0.0
17	$H + O + M'' \rightleftharpoons OH + M''$	6.20E + 16	−0.6000	0.0
18	$OH + OH \rightleftharpoons H_2O + O$	5.72E + 12	0.0000	390.0
19	$OH + CO \rightleftharpoons CO_2 + H$	1.57E + 07	1.3000	−385.0
20	$O + CO + M' \rightleftharpoons CO_2 + M'$	5.40E + 15	0.0000	2300.0
21	$H + CO + M' \rightleftharpoons CHO + M'$	5.00E + 14	0.0000	755.0
22	$CH_4 + O \rightleftharpoons CH_3 + OH$	4.07E + 14	0.0000	7040.0
23	$CH_4 + H \rightleftharpoons CH_3 + H_2$	7.24E + 14	0.0000	7590.0
24	$CH_4 + OH \rightleftharpoons CH_3 + H_2O$	1.55E + 06	2.1300	1230.0
25	$CH_4 + M \rightleftharpoons CH_3 + H + M$	4.68E + 17	0.0000	46910.0
26	$CH_3 + O \rightleftharpoons CH_2O + H$	6.02E + 13	0.0000	0.0
27	$CH_2O + O \rightleftharpoons CHO + OH$	1.82E + 13	0.0000	1550.0
28	$CH_2O + H \rightleftharpoons CHO + H_2$	3.31E + 14	0.0000	5290.0
29	$CH_2O + OH \rightleftharpoons CHO + H_2O$	7.58E + 12	0.0000	72.0
30	$CHO + O_2 \rightleftharpoons CO + HO_2$	3.00E + 12	0.0000	0.0
31	$CHO + H \rightleftharpoons CO + H_2$	4.00E + 13	0.0000	0.0
32	$CHO + OH \rightleftharpoons CO + H_2O$	5.00E + 12	0.0000	0.0
33	$CHO + O \rightleftharpoons CO + OH$	1.00E + 13	0.0000	0.0
34	$CH_2O + CH_3 \rightleftharpoons CHO + CH_4$	2.23E + 13	0.0000	2590.0
35	$CH_3 + OH \rightleftharpoons CH_2O + H_2$	3.98E + 12	0.0000	0.0
36	$CH_3 + HO_2 \rightleftharpoons CH_4 + O_2$	1.02E + 12	0.0000	200.0
37	$CO + HO_2 \rightleftharpoons CO_2 + OH$	1.50E + 14	0.0000	11900.0
38	$CH_3 + CH_3 \rightleftharpoons C_2H_6$	4.56E + 17	−7.6500	4250.0
39	$C_2H_6 + O \rightleftharpoons C_2H_5 + OH$	2.51E + 13	0.0000	3200.0
40	$C_2H_6 + H \rightleftharpoons C_2H_5 + H_2$	5.00E + 02	3.5000	2620.0
41	$C_2H_6 + OH \rightleftharpoons C_2H_5 + H_2O$	6.63E + 13	0.0000	675.0
42	$C_2H_5 + H \rightleftharpoons C_2H_6$	7.23E + 13	0.0000	0.0
43	$C_2H_5 + H \rightleftharpoons CH_3 + CH_3$	3.73E + 13	0.0000	0.0
44	$C_2H_5 \rightleftharpoons C_2H_4 + H$	2.29E + 11	0.0000	19120.0
45	$C_2H_5 + O_2 \rightleftharpoons C_2H_4 + HO_2$	1.53E + 12	0.0000	2446.0
46	$C_2H_4 + O \rightleftharpoons CH_2 + CH_2O$	2.53E + 13	0.0000	2516.0
47	$C_2H_4 + OH \rightleftharpoons CH_2O + CH_3$	5.00E + 13	0.0000	3020.0
48	$C_2H_4 + O \rightleftharpoons C_2H_3 + OH$	2.53E + 13	0.0000	2516.0
49	$C_2H_4 + O_2 \rightleftharpoons C_2H_3 + HO_2$	1.33E + 15	0.0000	27680.0
50	$C_2H_4 + H \rightleftharpoons C_2H_3 + H_2$	2.00E + 15	0.0000	10000.0
51	$C_2H_4 + OH \rightleftharpoons C_2H_3 + H_2O$	4.40E + 14	0.0000	3270.0
52	$C_2H_3 + M \rightleftharpoons C_2H_2 + H + M$	3.01E + 16	0.0000	20380.0
53	$C_2H_3 + O_2 \rightleftharpoons C_2H_2 + HO_2$	1.57E + 13	0.0000	5030.0
54	$C_2H_3 + H \rightleftharpoons C_2H_2 + H_2$	7.53E + 13	0.0000	0.0
55	$C_2H_3 + OH \rightleftharpoons C_2H_2 + H_2O$	1.00E + 13	0.0000	0.0
56	$C_2H_2 + OH \rightleftharpoons CH_3 + CO$	5.48E + 13	0.0000	6890.0

TABLE 1—Continued

	Reaction	A	B	E_a
57	$CH_3 + H \rightleftharpoons CH_2 + H_2$	2.00E + 11	0.7000	−1500.0
58	$CH_3 + OH \rightleftharpoons CH_2 + H_2O$	6.00E + 10	0.7000	1010.0
59	$CH_2 + O_2 \rightleftharpoons CHO + OH$	1.00E + 14	0.0000	1860.0
60	$CH_2 + O_2 \rightleftharpoons CH_2O + O$	1.00E + 14	0.0000	1860.0
61	$CH_2 + O_2 \rightleftharpoons CO_2 + H_2$	1.00E + 14	0.0000	1860.0
62	$CH_2 + H \rightleftharpoons CH + H_2$	4.00E + 13	0.0000	0.0
63	$CH + O \rightleftharpoons CO + H$	4.00E + 13	0.0000	0.0
64	$CH + O_2 \rightleftharpoons CO + OH$	2.00E + 13	0.0000	0.0
65	$C_2H + O \rightleftharpoons CO + CH$	1.00E + 13	0.0000	0.0
66	$CH^* + M \rightleftharpoons CH + M$	4.00E + 10	0.5000	0.0
67	$CH^* + O_2 \rightleftharpoons CH + O_2$	2.40E + 12	0.5000	0.0
68	$CH^* \rightleftharpoons CH$	1.90E + 06	0.0000	0.0
69	$C_2H + O_2 \rightleftharpoons CH^* + CO_2$	4.50E + 15	0.0000	25000.0
70	$C_2H + O \rightleftharpoons CH^* + CO$	7.10E + 11	0.0000	0.0
71	$C_2H_2 + H \rightleftharpoons C_2H + H_2$	6.00E + 13	0.0000	23651.0
72	$C_2H_2 + OH \rightleftharpoons C_2H − H_2O$	1.0E + 13	0.0000	7000.0
73	$C_2H + O_2 \rightleftharpoons CO + CHO$	5.00E + 13	0.0000	1505.0
74	$CH + O \rightleftharpoons CHO^+ + e^-$	2.52E + 11	0.0000	1700.0
75	$CH^* + O \rightleftharpoons CHO^+ + e^-$	5.04E + 14	0.0000	1700.0
76	$CHO^+ + H_2O \rightleftharpoons H_3O^+ + CO$	1.00E + 16	−0.0897	0.0
77	$H_3O^+ + C_2H_2 \rightleftharpoons C_2H_3O^+ + H_2$	8.39E + 15	0.0000	0.0
78	$CHO^- + CH_2 \rightleftharpoons CH_3^- + CO$	5.62E + 14	−0.0060	0.0
79	$H_3O^- + CH_2 \rightleftharpoons CH_3^- + H_2O$	6.17E − 14	−0.0060	0.0
80	$CH_3^- + C_2H_2 \rightleftharpoons C_3H_3^- + H_2$	7.24E + 14	0.0000	0.0
81	$C_3H_3^- + H_2O \rightleftharpoons C_2H_3O^- + CH_2$	7.24E + 14	0.0000	0.0
82	$CH_3^- + CO_2 \rightleftharpoons C_2H_3O^- + O$	7.24E + 14	0.0000	0.0
83	$H_3O^- + e^- \rightleftharpoons H_2O + H$	2.29E − 18	−0.5000	0.0
84	$C_3H_3^- + e^- \rightleftharpoons products$	1.50E − 19	−0.5000	0.0
85	$CH_3^- + e^- \rightleftharpoons CH_2 + H$	2.29E + 18	−0.5000	0.0
86	$C_2H_3O^- + e^- \rightleftharpoons M + H$	2.29E + 18	−0.5000	0.0

[a] Reaction rates are in the form $k = AT^B \exp(-E_a/RT)$ and have units of cm^3/mol-s.

There are four possible mechanisms for the recombination of ions in flames. Three of these mechanisms, three-body, radiative, and mutual neutralization recombination, have been ruled out by previous research [4] as unimportant pathways for ionic recombination. The fourth and most widely accepted mechanism is dissociative recombination represented by reactions 83–86 in Table 1.

Reaction rate coefficients have been measured for only a limited number of ion−molecule reactions. Accordingly, coefficients have been estimated from the average dipole orientation (ADO) theory [18–20] for reactions for which experimental data do not exist. The ADO theory predicts a temperature-dependent rate coefficient that is correlated to the parametric rate expression

$$k = AT^{-n}.$$

The values of n range from 0.006 to 0.09.

The heats of formation for ions have proved very important in predicting ionic structure of flames [3]. The values used in the present simulation are given in Table 2.

MODEL FORMULATION

The flame simulated in this work is a one-dimensional, laminar, premixed flame. The equations describing the structure of this flame in the presence of an electric field include the

TABLE 2

Heats of Formation for Ions

Species	ΔH_f^o (kcal/mol)	Ref.
H_3O^+	139.0	21
CH_3^+	256.0	22
CHO^-	199.1	21
$C_3H_3^+$	255.0	23
$C_2H_3O^-$	151.0	23

mass and species conservation equations and Poisson's equation to describe the electric field intensity.

Mass conservation:

$$\frac{\partial \rho}{\partial t} + \frac{\partial (\rho u)}{\partial x} = 0. \tag{1}$$

Species conservation:

$$\rho \frac{\partial Y_i}{\partial t} + \rho u \frac{\partial Y_i}{\partial x} = -\frac{1}{A} \frac{\partial (A J_i)}{\partial x} + \omega_i. \tag{2}$$

The neutral and ionic species are assumed to obey the boundary conditions [3]:

$$Y = Y_0 \qquad \text{at } x = 0 \tag{3}$$

and

$$\frac{\partial Y}{\partial x} = \text{constant at } x = \infty. \tag{4}$$

The unsteady terms in the conservation equations are retained as a computational device only. Their inclusion allows steady-state solutions to be solved by time marching, an approach proposed by Spalding and Stephenson [25].

Poisson's Equation:

$$\frac{d^2 V}{dx^2} = -\frac{1}{\epsilon_o}(n_+ - n_-)e \tag{5}$$

The boundary conditions for Poisson's Equation applied to the flame are

$$V = 0 \qquad \text{at } x = 0 \tag{6}$$

and

$$V = V_0 \qquad \text{at } x = L, \tag{7}$$

where $x = 0$ and L are the positions of the two electrodes in the one-dimensional flame.

The pressure across a flame is usually taken to be constant. Accordingly, the momentum equation is usually not solved in laminar flame simulations. However, the imposed electric field across the flame gives rise to a force on charge carriers. The neglect of the momentum equation must be justified in our simulations.

The net force per unit volume, F, produced by the electric field is (17)

$$F = Ee(n_+ - n_-). \tag{8}$$

Substituting the current flux

$$j = j_\pm = Een_\pm \mu_\pm \tag{9}$$

into Eq. 8 gives an expression for the force per unit volume in terms of mobility and current:

$$F = j\left(\frac{1}{\mu_+} - \frac{1}{\mu_-}\right). \tag{10}$$

Multiplying Eq. 10 by the distance from the flame to an electrode will give an expression for the pressure drop across the flame:

$$\Delta p = jx\left(\frac{1}{\mu_-} - \frac{1}{\mu_-}\right). \tag{11}$$

Lawton and Weinberg [17] predict the maximum ΔP, from Eq. 11, to be on the order of 0.0004 atm. Accordingly, ionic wind effects can be neglected in the flame.

The temperature field, in principle, can be solved from an energy equation applied to the flame. In practice, however, unaccountable heat loss from the flame can greatly influence the temperature field, making prediction difficult in some circumstances. We have chosen to use experimental temperature profiles in place of the energy equation in our simulations.

Mass flux, J_i, is obtained from a simplified expression proposed by Warnatz [26] that we have modified to include electric mobility effects:

$$J_i = -\rho D_{i,m} \frac{\partial Y_i}{\partial x} - D_{i,T} \frac{\partial \ln T}{\partial x} + \mu_{i,m} \rho Y_i E, \tag{12}$$

where the mixture diffusivity of species i, $D_{i,m}$, is calculated from binary diffusivities, D_{ij}:

$$D_{i,m} = \frac{1 - Y_i}{\sum\limits_{\substack{j=1 \\ j \neq i}}^{nspc} \frac{X_j}{D_{i,j}}}, \tag{13}$$

and the thermal diffusivity of species i, $D_{i,T}$, is calculated from

$$D_{i,T} = K_{T_{i,m}} \rho Y_i \frac{1 - Y_i}{\left(X_i \sum\limits_{\substack{j=1 \\ j \neq i}}^{nspc} \frac{X_j}{D_{ij}}\right)}. \tag{14}$$

Warnatz [26] has shown that the first two terms in Eq. 12 are accurate to within a few percent

of the exact solution of the Stefan–Maxwell equations. In this study, thermal diffusion is calculated only for H and H_2 because these small species are the only two with significant thermal diffusion rates.

The binary mobilities, μ_{ij}, can be related to binary diffusivities by the Einstein relationship [27]:

$$\frac{D_{ij}}{\mu_{ij}} = \frac{k_b T}{e} = T \times 8.617 \times 10^{-5}. \quad (15)$$

Little experimental data are available on the diffusion of ions. It is assumed that the diffusivity of ions is equal to that of the corresponding neutral species. From these assumed ion diffusion coefficients, the mixture mobility, $\mu_{i,m}$, can be determined [27]:

$$\mu_{i,m} = \left(\sum_{\substack{j=1 \\ j \neq i}}^{nspc} \frac{X_i}{\mu_{ij}} \right)^{-1} cm^{-1} V^{-1} s^{-1}. \quad (16)$$

The mobility of electrons in nitrogen at 1000 K is approximately [27]

$$\mu_e \approx \frac{2.0 \times 10^{22}}{n_-} cm^{-1} V^{-1} s^{-1}, \quad (17)$$

where n_- is the electron density. The diffusion coefficient for electrons can then be determined by rearranging the Einstein relationship:

$$D_e = 8.93 \times 10^3 \, cm^2/s. \quad (18)$$

The diffusivity is assumed to scale with temperature to the 3/2 power [17]. Thus, electron diffusivity as a function of temperature is

$$D_e = 0.2824 \times T^{1.5} \, cm^2/s. \quad (19)$$

In the absence of more complete data, this relationship is used to estimate electron diffusion in this work.

Calculation of ion diffusion currents is complicated by the self-induced electric field that develops among the charge carriers due to the diffusion of electrons and positive ions away from each other [17]. This electric field impedes the further diffusion of charge carriers, with the result that all charge carriers can be described by a common diffusion coefficient called the ambipolar diffusion coefficient, D_a [17]:

$$D_a = \frac{D_+ \mu_+ + D_- \mu_-}{\mu_+ + \mu_-}, \quad (20)$$

where the + and − subscripts denote properties of positive and negative charge carriers, respectively. However, this description of ion diffusion is approximate and inconvenient when treating a large number of different charge carriers. We prefer, instead, to explicitly calculate the self-induced electric field arising from charge separation. In this approach, ion diffusion and ion mobility are distinct processes.

This calculation procedure consists of solving Poisson's equation (Eq. 5) to find the electric field intensity generated by the distribution of charge carriers at a given instance in time. The resulting electric field intensity E is used to calculate the contributions of ion currents to the overall mass flux of individual ions as given by Eq. 12. The mass fluxes J_i of individual ions is substituted into Eq. 2 and solved for the distribution of charge carriers during the next time step. Poisson's equation is again solved to find the electric field intensity corresponding to the new charge distribution. Like chemical species, the electric field intensity settles down to a steady-state profile after a sufficient number of time steps.

Solution of the continuity and species conservation equations is greatly simplified by the coordinate transformation [28]:

$$\frac{\partial \psi}{\partial x} = \rho \quad \text{and} \quad \frac{\partial \psi}{\partial t} = -\rho u. \quad (21)$$

Overall continuity is automatically satisfied and the neutral species conservation equation becomes

$$\rho \frac{\partial \phi}{\partial t} = \rho \frac{\partial}{\partial \psi} \left(\rho \Gamma \frac{\partial \phi}{\partial \psi} \right) + G, \quad (22)$$

where ϕ is a generic variable representing mass fractions Y_i. Γ and G for neutral species are defined in Table 3 [28]. The transformed equation for ionic species conservation is

$$\rho \frac{\partial \phi}{\partial t} = \rho \frac{\partial}{\partial \psi} \left(\rho \Gamma \frac{\partial \phi}{\partial \psi} \right) + \rho \frac{\partial}{\partial \psi} (\rho \Gamma') + G, \quad (23)$$

where the expressions corresponding to Γ, Γ', and G for ions are also given in Table 3. The appropriate boundary conditions for the transformed coordinates are

$$\phi = \phi_0 \qquad \text{at } \psi = 0 \qquad (24)$$

and

$$\frac{\partial \phi}{\partial \psi} = \text{constant at } \psi = \infty \qquad (25)$$

Solving Eqs. 22 and 23 using the above boundary conditions gives the solution in the Ψ coordinate system. A simple transformation back to the x coordinate system is obtained from

$$x = \int_{\psi=0}^{\psi} \frac{d\psi}{\rho}. \qquad (26)$$

The resulting system of stiff partial differential equations is solved by split operator techniques [29, 30] and a specialized method of lines algorithm described in detail in Ref. 28.

Poissons equation (Eq. 5) must be solved periodically as the electron and ionic species profiles evolve in time. After one complete iteration on all species conservation equations, Poisson's equation is solved. The numerical solution of Poisson's equation is simplified by transforming it into a pair of first order ordinary differential equations. This is done by replacing voltage with electric field intensity:

$$\frac{dE}{dx} = \frac{1}{\epsilon_0}(n_+ - n_-)e, \qquad (27)$$

$$\frac{dV}{dx} = -E, \qquad (28)$$

with $V(x = 0)$ and $V(x = L)$ as prescribed boundary conditions. These boundary values are zero when no external electric field is applied to the flame. The resulting boundary

TABLE 3

Values of Γ, Γ', and G for the Species Conservation Equations

Equation	Γ	Γ'	G
Neutral model	$\rho D_{i,m}$	—	ω_i
Ionic model	$\rho D_{i,m}$	$-\mu_{i,m}\,\rho Y_i E$	ω_i

value problem is solved using a shooting method.

Flow simulations are performed on a HDS AS/9160. The number of grid points used for the simulations range from 50 to 70. The average CPU time required to reach steady state was 20 min for a single run.

RESULTS AND DISCUSSIONS

The focus of this study is simulation of ionic species profiles and saturation currents in methane flames. However, the importance of accurate neutral species profiles for the prediction of ion profiles in flames cannot be overstated. Unfortunately, most flame studies have concentrated on measurement of either ion or neutral profiles to the exclusion of the other. We have been careful to select methane flames for which experimental data exists on both neutral and ionic species concentration profiles. We found experimental data at three different equivalence ratios, ϕ, representing lean, stoichiometric, and rich methane flames that are complete enough to compare with our model predictions. We also found limited data on a hydrogen flame seeded with 1.8% methane. For each flame, we compare model predictions to experimental data for both neutral and ionic species concentration profiles to validate our kinetic mechanisms. These validation comparisons are made in the absence of externally applied electric fields. After validating the ionic mechanism of our model, we performed simulations with externally applied electric fields to investigate the phenomenon of saturation currents.

Lean Flame ($p = 40$ torr, $\phi = 0.2$)

The experimental data for the neutral species profile comes from the work of Peeters and Mahnen [31]. The CH_4, O_2, H_2O, CO, and CO_2 shown in Fig. 1a and 1b are in good agreement with the experimental data. The concentration profiles of the minor neutral species H, H_2, O, HO_2, and CH_2O, shown in Figs. 1c and 1d, are within the uncertainty of experimental data. The model tends to overpredict the experimental data in the post flame region, but ionic structure is most strongly
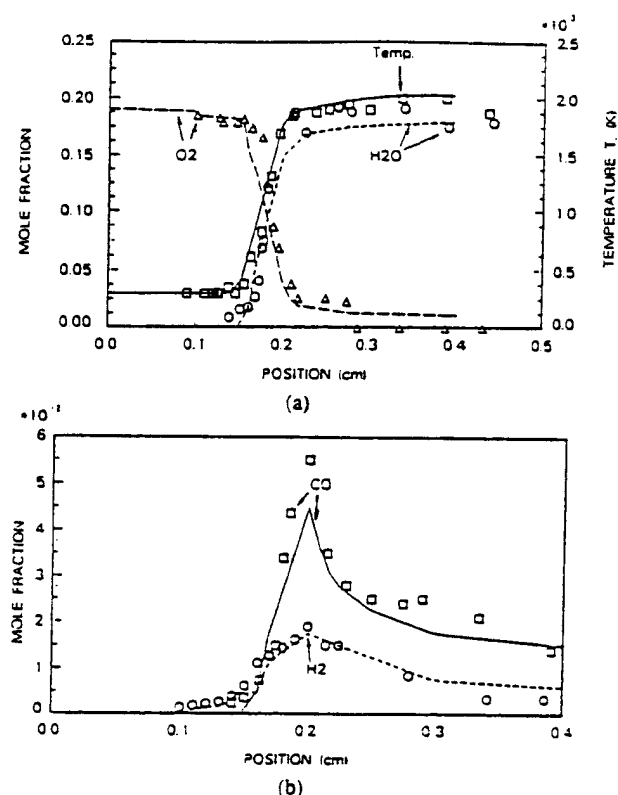

Fig. 1. Predicted and experimental neutral species profiles for a 40 torr, $\phi = 0.2$ methane flame (lines are model predictions, symbols are experimental data from Peeters and Mahnen [31]). (a) CH_4, CO, and CO_2. (b) H_2O and O_2. (c) H, H_2, O, and OH. (d) HO_2 and CH_2O.

influenced by conditions in the flame front where model predictions are good.

The results of Olsson and Andersson's [32] sensitivity study on a lean ($\Phi = 0.2$), low pressure (40 torr) methane–oxygen flame is relevant to our attempts to simulate neutral species profiles. Their study indicated that small perturbations in the reaction rates for reactions that produce CO from CHO could result in variations of up to 50% in some species concentrations. The concentration profiles for CH_3, H, H_2, O, and HO_2 were found to be sensitive to changes in the reaction rate for

$$CHO + M \rightarrow H + CO + M.$$

The reaction rate for this particular reaction has a high degree of uncertainty associated with it [33]. Olsson and Andersson [32] showed that increasing the reaction rate by a factor of five, well within its range of uncertainty, produced changes in the concentrations of the aforementioned species in excess of 50%. Con-

sidering the sensitivity of the species profiles to the rate of this reaction, it can be concluded that the predicted concentration profiles are within the uncertainty of experimental data.

Goodings et al. [34] used a mass spectrometer to determine ion currents of several ionic species as a function of position in the flame front of methane/oxygen flames at 40 torr and an equivalence ratio of 0.2. The experimental profiles are shown in Fig. 2a. The ion concentration profiles predicted by the model for this flame are shown in Fig. 2b. Although direct comparison between ion currents and ion concentrations cannot be made, several qualitative observations are possible from the figures.

The model predicts H_3O^+ to be the dominant ion with an ion density of $5 \times 10^{10}/cm^3$. The peak value of this ion occurs slightly downstream of the peak concentrations for the other ions. The slower decay of H_3O^+ is attributed to the reaction

$$CHO^+ + H_2O \rightarrow H_3O^+ + CO,$$
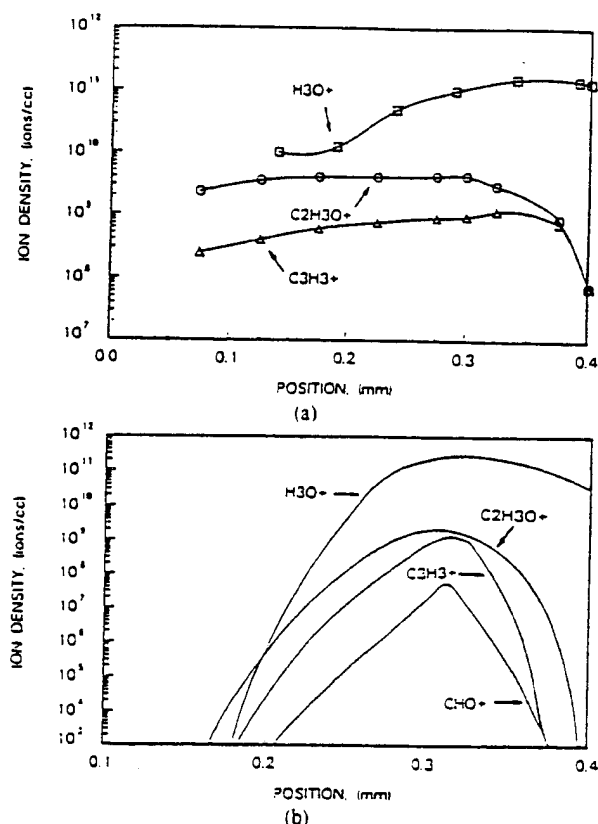
T. PEDERSEN AND R. C. BROWN

Fig. 2. Predicted and experimental ionic species profiles for a 40 torr, $\phi = 0.2$ methane flame. (a) Experimental data from Goodings et al. [34]. (b) Model predictions.

TABLE 4

Relative Peak Ion Concentrations for a CH_4/O_2 Flame ($p = 760$ torr, $\phi = 1.0$)

Species	Experimental Ratio[a]	Predicted Ratio[a]
H_3O^+	0.804	0.770
$C_2H_3O^+$	0.158	0.182
CH_3^-	0.023	0.011
CHO^+	0.004	0.036
$C_3H_3^+$	—	0.0001

[a] Referenced to total ion concentration.

to appear at concentrations only 1/1000 of that of the predominant ion, $C_2H_3O^-$. The major discrepancy in the model was overprediction of CHO^- by a factor of ten. Very likely this overprediction is the result of our exclusion of minor ionic species in the model, which, taken together, could significantly deplete CHO^-, the precursor of larger ions.

Stoichiometric Flame ($p = 760$ torr, $\phi = 1.0$)

The experimental data for neutral species are taken from Bechtel et al. [36] for a flame at atmospheric pressure and an unburned gas temperature of 298 K. The predicted and experimental profiles for O_2, H_2O, and temperature are shown in Fig. 3a. The model accurately predicts the measured O_2 and H_2O profiles. Figure 3b shows that the H_2 and CO concentrations are correctly predicted to peak in the flame front. The general trend of the predicted profiles agree with the experimental data. However, the predicted peak concentration of CO falls short of the experimental value. Bechtel et al. [36] indicate that the error associated with the peak value of CO is $\pm 10\%$. Therefore, the discrepancy between predictions and experiments is within experimental uncertainty.

The experimental ionic profiles for the stoichiometric, atmospheric methane-oxygen flame come from the work of Peeters et al. [37]. Figure 4a contains the experimental ion concentration profiles while Figure 4b contains the predicted ion concentration profiles. Similar to the lean flame results, the H_3O^+ ion, in both model predictions and experimental data, peaks late and decays slowly compared with other

which produces the majority of the H_3O^- ions in a region where there is a rapid increase in the production of H_2O. The other major ions decay more rapidly at rates that appear to be comparable for all ions. This rapid decay occurs because the reaction intermediates that form these ions by ion-molecule reactions are depleted very rapidly in the flame. This general behavior is observed in the experimental data of Goodings et al. [34] shown in Fig. 2a. Calcote [35] has noted that this slow decay of H_3O^+ and rapid decay of the other major ions characterizes all hydrocarbon flames.

Since ion currents measured by mass spectrometry cannot be easily converted into ion concentrations, we tabulate relative ion concentrations in Table 4 for a more quantitative comparison between model predictions and experiment. The peak fractional concentrations predicted for H_3O^+, $C_2H_3O^-$, and CH_3^- compare reasonably well with the corresponding experimental values. The $C_3H_3^-$ ion, which was not detected experimentally, was predicted
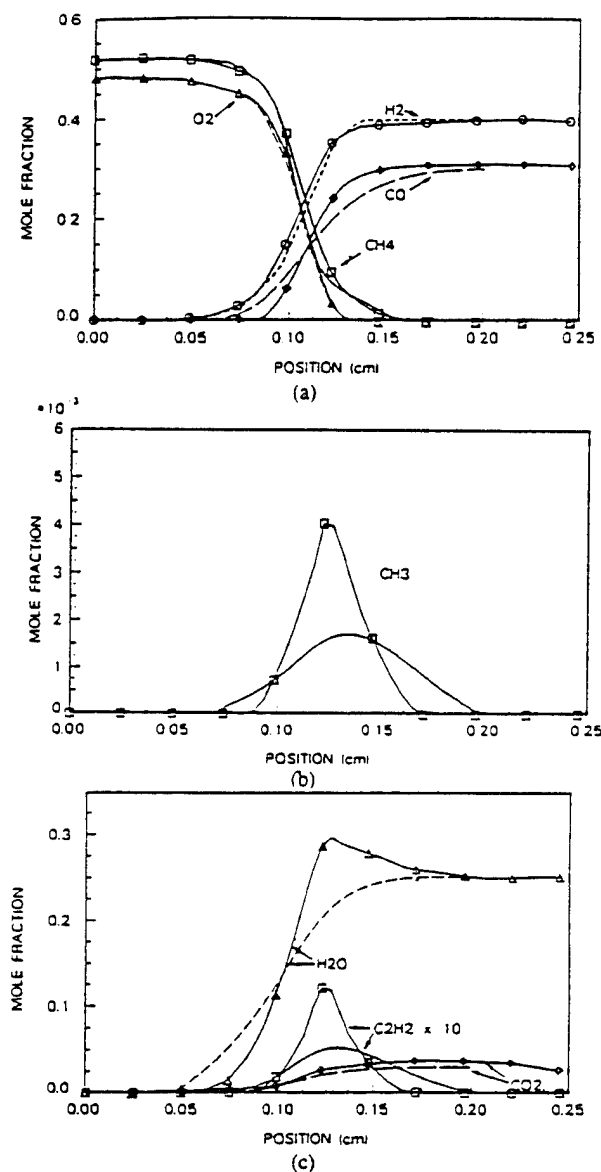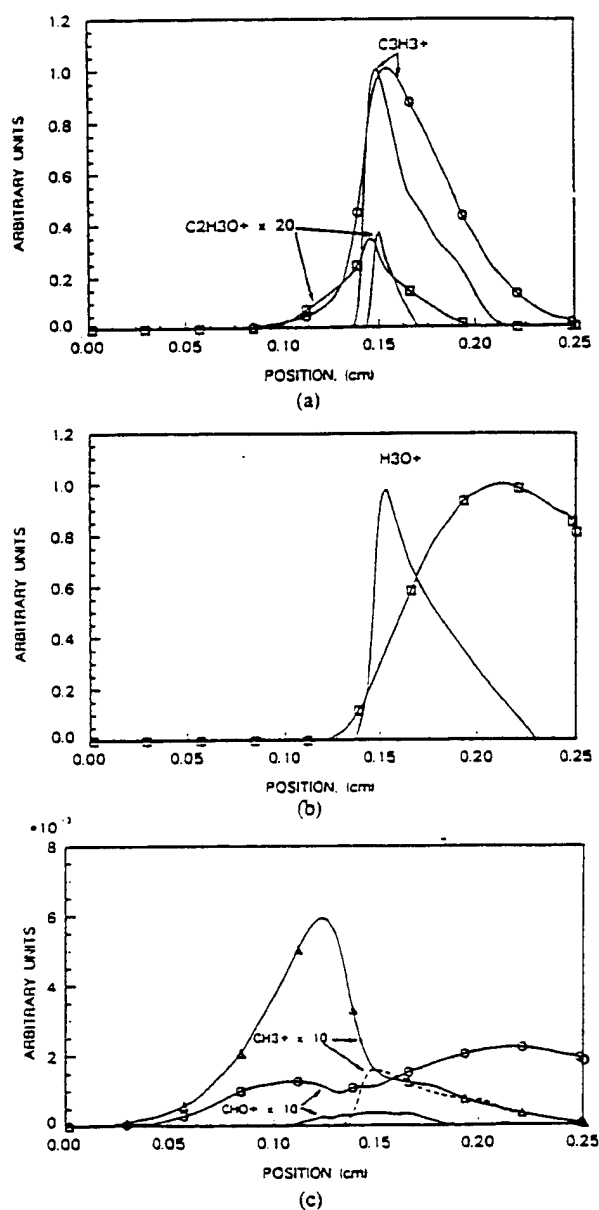
(a)

(b)

Fig. 3. Predicted and experimental neutral species profiles for a 760 torr, $\phi = 1.0$ methane flame (lines are model predictions, symbols are experimental data from Bechtel et al. [36]). (a) H_2O, O_2, and flame temperature. (b) CO and H_2.

(a)

(b)

Fig. 4. Predicted and experimental ionic species profiles for a 760 torr, $\phi = 1.0$ methane flame. (a) Experimental data from Peeters et al. [37]. (b) Model predictions.

flame ions. The experimental ion profiles are notably broader than the predicted profiles, but in the narrow flame front of an atmospheric flame this discrepancy may well represent experimental difficulties in spatial resolution.

More revealing are comparisons of the peak concentrations for the various ions, shown in Table 5. The model correctly predicts the relative ordering of ions by abundance. Furthermore, predicted peak concentrations for the four major ions H_3O^+, CHO^+, $C_3H_3^+$ and $C_2H_3O^+$ are within a factor of four of their experimental counterparts. The final flame temperature used in the simulation is 2240 K, which comes from the measured temperature profile of Bechtel et al. [36]. Peeters et al. [37] document a range of final flame temperatures varying from 1830 to 2084 K. In the same paper, Peeters et al. [37] show the ion yield to increase approximately 20% per 75 K increase in temperature. Therefore, differences in flame

temperatures between simulation and experiment can account for much of the discrepancies in the ion concentrations.

Rich Flame ($p = 760$ torr, $\phi = 2.13$)

The rich flame experiments of Goodings et al. [23] are notable in that data for both ionic and neutral species were collected. The predicted and experimental neutral species profiles for CH_4, O_2, H_2, and CO are illustrated in Fig. 5a. The predicted O_2 and CH_4 profiles show

TABLE 5

Peak Ion Concentrations for a Stoichiometric CH_4/O_2 Flame ($p = 760$ torr, $\phi = 1.0$)

Species	Experimental Concentration (mol/cm³)	Predicted Concentration (mol/cm³)
H_3O^+	1.5×10^{11}	3.1×10^{11}
$C_2H_3O^+$	4.3×10^9	2.0×10^9
$C_3H_3^+$	1.2×10^9	1.5×10^9
CHO^+	1.9×10^7	6.1×10^7

Fig. 5. Predicted and experimental neutral species profiles for a 760 torr, $\phi = 2.13$ methane flame (lines are model predictions, symbols are experimental data from Goodings et al. [23]). (a) CH_4, CO, H_2, and O_2. (b) CH_3. (c) CO_2, C_2H_2, and H_2O.

good agreement with the experimental data. The post flame concentrations of major stable products, H_2, H_2O, and CO are well predicted, although CO, in particular, plateaus earlier than predicted. We attribute some discrepancies in the preheat zone of the flame to apparent errors in the temperature profile reported by Goodings et al. [25].

The model predicts CH_3 concentration, shown in Fig. 5b, that is a factor of two lower than the data from Goodings et al. [23]. This

underprediction of CH_3 for rich flames arises from its rapid conversion to C_2H_6. This same trend was observed in the rich flame simulation performed by Coffee et al. [9]. They reported an underprediction in the CH_3 profile by a factor of three compared with the experimental data for a rich flame. However, the actual equivalence ratio used by Coffee et al. [9] was not documented.

The predicted value of C_2H_2, shown in Fig. 5c, is also a factor of two lower than the experimental data. CH_3 is directly responsible for the production of C_2H_2, thereby causing the factor of two discrepancy in the data. These differences can be attributed to an incomplete understanding of the intermediate reactions responsible for the oxidation of CH_4.

The predicted and experimental ionic profiles for this rich flame are compared in Fig. 6. The relative concentrations of H_3O^+, $C_2H_3O^-$, and $C_3H_3^-$ are correctly predicted, with H_3O^- and $C_3H_3^-$ being the dominant ions in the flames. Figure 6a illustrates that the location of peak concentrations are correctly predicted for $C_2H_3O^-$ and $C_3H_3^-$ although the experimental profiles are broader than predicted. The H_3O^+ ion, illustrated in Fig. 6b, does not peak downstream of the other positive ions, as is expected from the experimental data.

The CHO^- and CH_3^+ ions, illustrated in Fig. 6c, are poorly predicted in terms of both peak concentrations and profile shapes. Van Tiggelen [38] reports that for rich methane flames, concentrations of CH_3^+ and CHO^+ are about one tenth that of H_3O^+. Peeters et al. [65] report that concentrations of CH_3^+ and CHO^+ are a factor of 100 smaller than that of H_3O^+. Goodings et al. [32] show the ion concentration of CH_3^+ to be a factor of 400 smaller and the concentration of CHO^+ to be a factor of 600 smaller than H_3O^+. The prediction by this model show CH_3^+ and CHO^+ concentrations to be three orders of magnitude smaller than the concentrations of H_3O^+. The underprediction of these two ions can be traced to the neutral species model, which underpredicts CH_3 and CH_2 by a factor of two. These two species participate in reactions to produce CH and CH_2, the precursors of CHO^- and CH_3^-. Although Goodings et al.

Fig. 6. Predicted and experimental ionic species profiles for a 760 torr, $\phi = 2.13$ methane flame (lines without symbols are model predictions, lines with symbols are experimental data from Goodings et al. [23]. (a) $C_2H_3O^+$ and $C_3H_3^+$. (b) H_3O^+. (c) CHO^+ and CH_3^+.

throughout the post-flame region. The experimental CHO^+ profile exhibits two peaks, one before and one after the flame front. These discrepancies may be the result of expansion cooling in the sampling nozzle during the experiment.

Methane-Seeded Hydrogen Flame

The model was used to simulate a stoichiometric, atmospheric hydrogen flame seeded with 1.8% methane reported by Peeters et al. [37]. The major ion, H_3O^+, is predicted to peak just after the flame front and exhibits a slow decay in the post-flame region. The predicted ion density of $1.0 \times 10^{11}/cm^3$ for H_3O^+ agrees well with the value of $1.8 \times 10^{11}/cm^3$ reported by Peeters et al. [37]. The experimental profile also shows a slow decay in the postflame region.

The model predicts an ion density on the order of $10^9/cm^3$ for the $C_2H_3O^-$ ion, which agrees well with the value of $10^9/cm^3$ reported by Peeters et al. [37]. The model predicts all other ions to have ion densities less than $10^9/cm^3$. The CHO^-, CH_3^-, and $C_3H_3^-$ ions did not appear in measurable quantities in the flame of Peeters et al. [37].

In their experiments, Peeters et al. [37] measure a large concentration of CH_5O^- in the flame. It is reported to have an ion density of $2.5 \times 10^{10}/cm^3$. The reaction mechanism used in the present research does not take into account the formation of this ion, which has not been reported as a major flame ion by other researchers.

Saturation Currents

Saturation currents were determined from the simulations in a manner similar to that which would be employed in actual experiments. A series of flame simulations with specified initial conditions and temperature profile were run in which the electric field voltage V_0 applied to the electrodes was increased from one run to the next until the electric current flux, j, through the flame became constant. This current was recorded as the saturation current flux, j_s, for the specified flame conditions. The apparent activation energy, E_{app}, for the satu-

[34] did not report concentrations for CH and CH_2, their origin suggests that our model underpredicts them, giving rise to underpredicted CH_3^+ and CHO^+.

The experimental profiles for CH_3^+ and CHO^+ reported by Goodings et al. [34] show trends that are not in accord with observations of most other researchers. The experimental data shows the CH_3^- ion to peak before the flame front with a slow decay that extends

ration current was determined from the slope of the line produced by plotting $\log(j_s)$ versus $1/T_f$. In actual experiments, the peak flame temperature T_f would be controlled by varying the flow rate of gas mixture to the burner. However, as previously noted, predicting heat transfer from a laboratory burner flame is problematic unless more information is provided about burner operation than is typical in the literature. In the absence of detailed temperature profiles for the experimental flames in which saturation currents were measured, we simply applied a scaling factor to known temperature profiles of comparable flames to achieve desired peak flame temperatures in our simulations.

Simulations were performed for the lean, stoichiometric, and rich flames described previously as well as for a stoichiometric hydrogen flame seeded with 1% methane. Apparent activation energies are given in Table 6.

The saturation current is predicted to peak at an equivalence ratio close to unity. Although we do not have experimental data for methane flames with which to compare this prediction, it is supported by experimental observations by Peeters et al. [37] for other hydrocarbon flames. This behavior reflects the existence of a maximum in ion generation rate at stoichiometric conditions.

The apparent activation energy for the saturation current in methane flames is predicted to range between 41.4 and 46.8 kcal/mol. Although the variance in the experimental data is rather large, it agrees reasonably well with model predictions.

Lawton and Weinberg [6, 17], whose value of activation energy agrees within a few percent of our values, were unable to identify the rate-limiting process responsible for this apparent activation energy. They hypothesized that free-radical reactions might play a role. However, we think ion–molecule reactions are a better explanation.

We employed sensitivity analysis to trace the origin of the apparent activation energy in the simulations. A simple but effective sensitivity analysis systematically changes rate constants to evaluate the importance of individual chemical reactions on some overall system parameter. Preexponential factors are customarily altered to affect changes in rate constants; we chose to vary rate constants through changes in activation energies of individual ion–molecule reactions. This modified approach to sensitivity analysis gave us a direct test as to whether a single reaction was responsible for the apparent activation energy of ion saturation current. We determined that the origin of the apparent activation energy is

$$C_2H_3O^+ + H_2 \rightarrow H_3O^+ + C_2H_2,$$

which has an activation energy of 42.19 kcal/mol. To understand the surprising rate-limiting action of this reaction, the major pathways for charge transfer from chemiionizaton to dissociative recombination were traced. Figure 7 summarizes this analysis for stoichiometric methane flames, showing major reaction pathways between ions by bold arrows and minor pathways by thin arrows. The rate limiting action of the reaction appears to arise from the channeling of a large fraction of positive

TABLE 6

Activation Energies Obtained from Saturation Currents for Atmospheric, Methane Flames and a 1% Methane-Seeded Hydrogen Flame

Flame	Equivalence Ratio	Experimental E_a (kcal/mol)	Predicted E_a (kcal/mol)
CH_4/O_2	0.2	—	41.36
CH_4/O_2	1.0	46.0	46.8
CH_4/O_2	2.13	—	42.5
$H_2/O_2/1\%CH_4$	1.0	28.1	42.6

Fig. 7. Positive ion pathways in a $\phi = 1.0$ methane flame (heavy arrows denote primary pathways).

charges through $C_2H_2O^+$ on their way to dissociative recombination by the reaction

$$H_3O^+ + e^- \rightarrow H_2O + H.$$

This pathway was prominent for all equivalent ratios examined in this study.

Simulations of the methane-seeded hydrogen flame produced an apparent activation energy comparable to the methane flames. This prediction is in accordance with the fact that chemiionization arises from the hydrocarbons in the flame and, hence, should closely follow the methane reaction mechanism. However, the activation energy obtained experimentally by Lawton and Weinberg was only half that predicted by the simulation, although the saturation current was of the right order of magnitude. We see no plausible explanation for such a small activation energy in methane-seeded hydrogen flames; further experimental verification of this activation energy would appear to be in order.

CONCLUSIONS

A simple ionic reaction mechanism is proposed that predicts the general features of ions in lean to stoichiometric methane flames. The proposed reaction mechanism provides a means for the production and recombination of major ions thought to exist in methane flames. The largest discrepancy between predictions and experiments occurred for rich flame simulations in which the model underpredicted concentrations for CHO^+ and CH_3^- ions. This discrepancy is attributed to neutral species reaction mechanisms associated with reaction intermediates.

Using this ionic reaction mechanism, the saturation currents for lean, stoichiometric, and rich methane flames were calculated. The limited literature on saturation currents rarely reports saturation currents as functions of temperature. This deficiency does not allow for a direct comparison between the experimental and the predicted saturation currents. However, the literature does report apparent activation energies for saturation currents, which we compared to values obtained from simula-

tions. The predicted values range from 41.36 kcal/mol for the lean flame to 46.81 kcal/mol for the stoichiometric flame. These values fall within the range of values reported in the literature for methane flames.

The predicted apparent activation energies were used to determine the rate limiting reaction in the ionic reaction mechanism. We have traced the activation process for all equivalence ratios to the ion–molecule reaction:

$$C_2H_3O^+ + H_2 \rightarrow H_3O^+ + C_2H_2.$$

This reaction is responsible for channeling a large fraction of positive charge to dissociative-recombination reaction.

REFERENCES

1. Calcote. H. F. Dissertation. Princeton University, 1947.
2. Cool, A. T., and Tjossem. J. H., in *Gas-Phase Chemiluminescence and Chemiionization* (A. Fontijn. Ed.), Elsevier. Amsterdam. 1985.
3. Eraslan. Ahmet N., and Brown, Robert C., *Combust. Flame* 74:19–37 (1988).
4. Calcote, H. F., *Eighth Symposium (International) on Combustion*, The Combustion Institute, Pittsburgh, 1960, pp. 184–199.
5. Calcote. H. F., Kurzius, S. C., and Miller, W. J., *Tenth Symposium (International) on Combustion*. The Combustion Institute, Pittsburgh, 1965, pp. 605–619.
6. Lawton. F., and Weinberg, F. J., *Proc. R. Soc. A* 277:468–497 (1964).
7. Peeters. J., and Van Tiggelen. A., *Twelfth Symposium (International) on Combustion*. The Combustion Institute, Pittsburgh, 1968, pp. 437–446.
8. Bertrand. C., Dussart, B., and Van Tiggelen. P. J., *Seventeenth Symposium (International) on Combustion*, The Combustion Institute, Pittsburgh, 1978, pp. 967–973.
9. Coffee. Terence P., *Combust. Flame* 55:161–170 (1984).
10. Dixon-Lewis, G., in First Specialist Meeting (International) on Combustion. The Combustion Institute, France, 284–289.
11. Dixon-Lewis, G., *Philos. Trans. R. Soc. (Lond.) A* 292:45–99 (1979).
12. Dean. A. M., Johnson. R. L., and Steiner, D. C., *Combust. Flame* 37:41–62 (1980).

T. PEDERSEN AND R. C. BROWN

13. Dean, A. M., and Johnson, R. L., *Combust. Flame* 38:109–123 (1980).

14. Gelinas, R. J., *Science Applications*, Preprint No. SAI/PL/C297, 1979.

15. Warnatz, J., *Eighteenth Symposium (International) on Combustion*, The Combustion Institute, 1981, pp. 369–384.

16. Luther, K., and Troe, J., *Seventeenth Symposium (International) on Combustion*, The Combustion Institute, Pittsburgh, 1979, pp. 535–542.

17. Lawton, J., and Weinberg, F., *Electrical Aspects of Combustion*, Clarendon Press, Oxford, 1969.

18. Su, T., and Bowers, M. T., *J. Chem. Phys.* 58:3027–3037 (1973).

19. Su, T., and Bowers, M. T., *Int. J. Mass Spectrosc. Ion Phys.* 12:347–356 (1973).

20. Su, T., Su, C. F. E., and Bowers, M. T., *J. Chem. Phys.* 69:2243–2250 (1978).

21. Stull, D. R., and Prophet, H., *JANAF Thermochemical Tables*, 2nd ed., National Standard Reference Data Series, U.S. National Bureau of Standards, Washington, D.C., 1971.

22. Anicich, V. G., Huntress, Jr., W. T., and McEwan, M. J., Jet Propulsion Laboratory Report, California Technical Institute, 1985.

23. Goodings, J. M., Bohme, K. D., and Sugden, T. M., *Sixteenth Symposium (International) on Combustion*, The Combustion Institute, Pittsburgh, 1977, pp. 891–902.

24. Delfau, J. L., and Barassin, A., *Eighteenth Symposium (International) on Combustion*, The Combustion Institute, Pittsburgh, 1980, pp. 443–450.

25. Spalding, D. B., and Stephenson, P. L., *Proc. R. Soc. A* 324:315–337 (1971).

26. Warnatz, J., *Ber. Bunsenges. Physical Chem.* 82:193–200 (1978).

27. Hunter, S. R., and Christophorou, L. G., in *Electron-Molecule Interactions and Their Applications* (L. G. Christophorou, Ed.), American Press, New York, 1984, pp. 89–220.

28. Eraslan, Ahmet N., and Brown, Robert C., *Computer Meth. Appl. Mech. Eng.* 64:61–77 (1987).

29. Hindmarsh, A. C., in *Scientific Computing* (R. S. Stepleman, Ed.), North-Holland, Amsterdam, 1983.

30. Goyal, G., Paul, P. J., Mukunda, H. S., and Deshpande, S. M., *Combust. Sci. Technol.* 60:167–189 (1988).

31. Peeters, Jozef, and Mahnen, Gilbert, *Fourteenth Symposium (International) on Combustion*, The Combustion Institute, Pittsburgh, 1972, pp. 133–146.

32. Olsson, Jim O., and Andersson, Lars L., *Combust. Flame* 67:99–109 (1987).

33. Westbrook, C. K., and Dryer, F. L., *Eighteenth Symposium (International) on Combustion*, The Combustion Institute, Pittsburgh, 1980, pp. 749–767.

34. Goodings, J. M., Bohme, K. D., Chun-Wai, Ng, *Combust. Flame* 36:27–43 (1979).

35. Calcote, H. F., in *Ion-Molecule Reactions*, Plenum Press, New York, 1972.

36. Bechtel, J.H., Blint, Richard J., Dasch, Cameron J., and Weinberger, Doreen A., *Combust. Flame* 42:197–213 (1981).

37. Peeters, J., Vinkier, C., and Van Tiggelen, A., *Oxidat. Combust. Rev.* 4:93–132 (1969).

38. Van Tiggelen, A., in *Ionization in High Temperature Gases*, Academic, London, 1963.